



FEDERAL UNIVERSITY OF CEARÁ
DEPARTMENT OF TELEINFORMATICS ENGINEERING
POSTGRADUATE PROGRAM IN TELEINFORMATICS ENGINEERING

Radio Resource Allocation for Coordinated Multi-Point Systems

Master of Science Thesis

Author

Rodrigo Lopes Batista

Advisor

Prof. Dr. Tarcisio Ferreira Maciel

Co-Advisor

Prof. Dr. Francisco Rodrigo Porto Cavalcanti

FORTALEZA – CEARÁ
AUGUST 2011

This page was intentionally left blank



UNIVERSIDADE FEDERAL DO CEARÁ
DEPARTAMENTO DE ENGENHARIA DE TELEINFORMÁTICA
PROGRAMA DE PÓS-GRADUAÇÃO EM ENGENHARIA DE TELEINFORMÁTICA

Alocação de Recursos de Rádio para Sistemas Multi-Ponto Coordenados

Autor

Rodrigo Lopes Batista

Orientador

Prof. Dr. Tarcisio Ferreira Maciel

Co-orientador

Prof. Dr. Francisco Rodrigo Porto Cavalcanti

*Dissertação apresentada à Coordenação do Programa de Pós-graduação em Engenharia de Teleinformática da Universidade Federal do Ceará como parte dos requisitos para obtenção do grau de **Mestre em Engenharia de Teleinformática**.*

FORTALEZA – CEARÁ
AGOSTO 2011

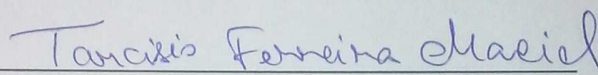
RODRIGO LOPES BATISTA

**RADIO RESOURCE ALLOCATION FOR COORDINATED MULTI-
POINT SYSTEMS**

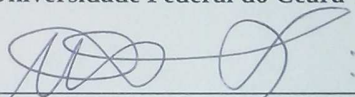
Dissertação submetida à Coordenação do Programa de Pós-Graduação em Engenharia de Teleinformática, da Universidade Federal do Ceará, como requisito parcial para a obtenção do grau de Mestre em Engenharia de Teleinformática.
Área de concentração: Sinais e Sistemas.

Aprovada em 05/08/2011.

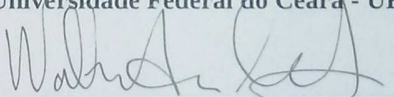
BANCA EXAMINADORA



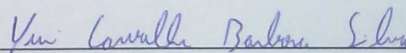
Prof. Dr. Tarcisio Ferreira Maciel (Orientador)
Universidade Federal do Ceará - UFC



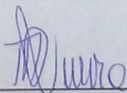
Prof. Dr. Francisco Rodrigo Porto Cavalcanti
Universidade Federal do Ceará - UFC



Prof. Dr. Walter da Cruz Freitas Jr.
Universidade Federal do Ceará - UFC



Prof. Dr. Yuri Cavalho Barbosa Silva
Universidade Federal do Ceará - UFC



Prof. Dr. Robson Domingos Vieira
Instituto Nokia de Tecnologia - INdT

Dedications

I dedicate this work to scientific progress. I hope have collaborated for developing this too promising topic that is the radio resource allocation under cooperative transmission. I also hope this work will serve to motive future works and that technological improvements can be achieved from this research to good of society.

Acknowledgements

I would like to express my sincere gratitude to all those who contributed to this work.

First, I am very grateful for the expertise, guidance, suggestions, dedication, friendship, patience, understanding, encouragement and time the advisor of this dissertation, Prof. Dr. Tarcisio Maciel Ferreira provided me throughout the entire research and writing processes.

I am also indebted to my committee members, whose insight and knowledge were invaluable to achieve this dissertation.

My sincere thanks to my colleagues doctorate students Brauner and Elvis, for the discussions which greatly contributed for my growth as a researcher in the field of wireless communications.

I would like to express my acknowledgment to project managers with whom I had the opportunity to work and obtain knowledge: Prof. Dr. Walter da Cruz Freitas Júnior and Prof. Dr. Yuri Carvalho Barbosa Silva.

I thank Prof. Dr. Francisco Rodrigo Porto Cavalcanti for believing in my professionalism, responsibility and collaboration.

I would like to thank my friend Deborah Fernandes and once again Prof. Dr. Tarcisio Ferreira Maciel for reviewing the text.

Thanks to the Research and Development Center, Ericsson Telecomunicações S.A., Brazil, for giving me financial support under EDB/UFC.22 and UFC.32 Technical Cooperation contracts.

I can not express my appreciation to all faculty and staff of the GTEL, laboratory with excellent infrastructure where I found a warm and homely atmosphere.

I would like to thank the Profs. from UFES: Dr. Alvaro Cesar Pereira Barbosa, Dr. Anilton Salles Garcia and Dr. Magno Martinello, for friendship, guidance during undergraduate studies and supporting my application to the master's degree.

My family and friends, even though many miles away, remained present in their expressions of support.

Though he does not know how much help he provided me, I'd like to thank Jesuíno, who inspired me calm in times of stress.

Also, I would like to especially thank my friend Manuel, an example of person for me.

Special thanks to my parents Liesse and Maria, truly the greatest masters I ever had.

To my wife Fernanda, who helped me giving understanding when preparing this dissertation. Her coffee kept me writing.

And finally, though not less important, I thank to God, for his friendship and guidance.

Abstract

The International Telecommunications Union (ITU) established through the International Mobile Telecommunications (IMT)-Advanced a set of requirements for high performance of 4th Generation (4G) communication systems and, with the aim of meeting such requirements, 3rd Generation Partnership Project (3GPP) Long Term Evolution (LTE) is considering a set of enhancements, referred to as LTE-Advanced. In the LTE-Advanced context, Coordinated Multi-Point (CoMP) communication appears as a promising technology to boost system throughput and to allow for an efficient Radio Resource Allocation (RRA). CoMP systems promise very high performance in terms of spectral efficiency and coverage benefits when perfect Channel State Information (CSI) is available at the transmitter. However, perfect CSI is difficult to obtain in CoMP systems due to an increased number of channel parameters to be estimated at the receiver and to be fed back to the transmitter. So, the performance of such systems is compromised when the CSI is not perfectly known during CoMP processing, which is an important problem to be addressed. Space Division Multiple Access (SDMA) grouping algorithms are usually employed in order to find a suitable set of users for spatial multiplexing. The largest SDMA group is not always the best group in a given data transmission such that higher gains might be achieved by dynamically adjusting the SDMA group size. Besides, algorithms that balance the Signal to Interference-plus-Noise Ratio (SINR) among different links might ensure a certain level of link quality and so provide a more reliable communication for the scheduled users.

This master thesis provides system-level analyses for RRA algorithms that exploit coordination in the downlink of CoMP systems to implement adaptive resource reuse and so improve system throughput. Herein, RRA strategies which consider dynamic SDMA grouping, joint precoding and power allocation for SINR balancing are studied in CoMP systems assuming imperfect CSI in order to obtain a better approximation with regard to the real-world implementations. It is shown through system-level analyses that quite high throughput gains are achieved through intelligent RRA. In conclusion, the results show that Sequential Removal Algorithms (SRAs) and SINR balancing provide system spectral efficiency gains. However, a critical degradation on the performance of these RRA strategies due to imperfect CSI is also shown.

Keywords: CoMP, imperfect CSI, SDMA grouping, SINR balancing.

Resumo

A União Internacional para Telecomunicações (ITU) estabeleceu através da iniciativa para o Sistema Avançado Internacional de Telecomunicações Móveis (IMT-Advanced), um conjunto de requisitos de alto desempenho para os sistemas de comunicação de quarta geração (4G) e, com o objetivo de atender tais requisitos, a Evolução de Longo Prazo (LTE) do Projeto de Parceria para a Terceira Geração (3GPP) está considerando um conjunto de melhorias, referidas como LTE-Avançado. No contexto do LTE-Avançado, a comunicação multi-ponto coordenada (CoMP) aparece como uma tecnologia promissora para aumentar a vazão do sistema e permitir uma Alocação de Recursos de Rádio (RRA) eficiente. Os sistemas CoMP prometem alto desempenho em termos de eficiência espectral e benefícios de cobertura quando a Informação do Estado do Canal (CSI) perfeita está disponível no transmissor. No entanto, CSI perfeita é difícil de se obter em sistemas CoMP devido a um alto número de parâmetros de canal a serem estimados no receptor e enviados para o transmissor. Assim, o desempenho de tais sistemas é comprometido quando a CSI não é perfeitamente conhecida durante o processamento CoMP tal que esse é um problema importante a ser abordado. Algoritmos de agrupamento para Múltiplo Acesso por Divisão no Espaço (SDMA) geralmente são utilizados a fim de encontrar um conjunto adequado de usuários para multiplexação espacial. O maior grupo SDMA nem sempre é o melhor grupo em uma transmissão de dados tal que maiores ganhos podem ser obtidos ajustando dinamicamente o tamanho do grupo SDMA. Além disso, os algoritmos que balanceiam a Razão Sinal-Interferência mais Ruído (SINR) entre diferentes canais podem garantir um certo nível de qualidade de canal e assim proporcionar uma comunicação mais confiável para os usuários agrupados.

Esta dissertação de mestrado fornece análises em nível sistêmico para algoritmos de RRA que exploram a coordenação no enlace direto de sistemas CoMP para implementar reuso adaptativo de recursos e assim melhorar o desempenho do sistema. São estudadas aqui estratégias de RRA em sistemas CoMP que consideram agrupamento SDMA dinâmico, precodificação e alocação de potência conjuntas para balanceamento de SINR, sendo assumida CSI imperfeita a fim de conseguir maior aproximação com relação às implementações em cenários reais. É mostrado através de análises em nível sistêmico que ganhos de vazão bastante altos são alcançados através de RRA inteligente. Em conclusão, os resultados mostram que Algoritmos de Remoção Sequencial (SRAs) e de balanceamento de SINR proporcionam ganhos de eficiência espectral do sistema. No entanto, é também mostrada uma degradação crítica no desempenho dessas estratégias de RRA devido à CSI imperfeita.

Palavras-chave: CoMP, CSI imperfeita, agrupamento SDMA, balanceamento de SINR.

Contents

Abstract	iii
Resumo	iv
List of Figures	vii
List of Tables	ix
List of Algorithms	x
Notation	x
<hr/>	
1 Introduction	1
1.1 4G communication systems	1
1.2 Coordinated Multi-Point systems	2
1.2.1 Downlink CoMP transmission	3
1.2.2 CSI feedback on downlink CoMP	5
1.2.3 Radio resource allocation in CoMP systems	6
1.3 State-of-the-art	7
1.4 Open problems	11
1.5 Contents	12
1.5.1 Contributions	12
1.5.2 Scientific production	13
1.5.3 Outline	14
2 System model	15
2.1 Introduction	15
2.2 Downlink physical resource	16
2.3 Multi-cell system	17
2.4 Wireless channel model	18
2.5 Downlink CoMP transmission model	20
2.6 CSI modeling	21
2.7 Radio resource allocation	22
2.8 Inter-cluster interference estimation	24
2.9 Link-to-system interface	24
2.10 System-level simulation	26

2.10.1 Simulation parameters and performance metrics	27
3 UE spatial grouping	29
3.1 Introduction	29
3.2 Problem statement	29
3.3 Coordinated scheduling approach	31
3.3.1 Individual single-cell scheduling	32
3.3.2 Joint multi-cell scheduling	34
3.3.3 Performance in the conventional scenario	35
3.3.4 Performance with coordinated scheduling	37
3.4 Joint processing approach	39
3.4.1 Grouping algorithm	40
3.4.2 Grouping metric	41
3.4.3 Dynamic SDMA group size	44
3.4.4 Spatial precoding	45
3.4.5 Power allocation	46
3.4.6 Performance with SDMA grouping	47
3.5 Summary	52
4 SINR balancing	54
4.1 Introduction	54
4.2 Problem statement	55
4.3 SINR balancing under sum-power constraint	56
4.3.1 Power assignment	56
4.3.2 Beamforming	57
4.4 Target SINR feasibility and SRAs	57
4.5 Power minimization under SINR constraints	59
4.6 Results	59
4.6.1 SINR balancing strategies definition	59
4.6.2 Performance metrics	60
4.6.3 Performance with SINR balancing	60
4.6.4 Impact of imperfect CSI on the CoMP performance	64
4.7 Summary	65
5 Conclusions	67
5.1 Summary of the dissertation	67
5.2 Conclusions about RRA for CoMP systems	68
5.3 Perspectives of future works	69
Bibliography	71

List of Figures

1.1	Downlink CoMP architectures.	4
1.2	Downlink CoMP transmission approaches.	4
2.1	OFDMA frame structure.	17
2.2	3-sector cell.	17
2.3	Coverage area of the system	18
2.4	Curves of link-level used for link adaptation.	25
3.1	CDF of BLER varying the parameter α of the exponential filter.	35
3.2	System spectral efficiency achieved by single-cell scheduling algorithms in the conventional scenario.	36
3.3	CDF of BLER and PDF of the usage of the MCSs presented by single-cell scheduling algorithms in the conventional scenario.	37
3.4	System spectral efficiency and CDF of BLER presented by single-cell scheduling algorithms in the both conventional and CoMP scenarios.	38
3.5	System spectral efficiency and PDF of the usage of the MCSs achieved by the joint multi-cell scheduling algorithm considered for the CoMP scenario.	38
3.6	Average inter-cluster interference power and CDF of the BLER achieved by the joint multi-cell scheduling algorithm considered for the CoMP scenario.	39
3.7	System spectral efficiency and PDF of the group size achieved by the CAP grouping algorithm.	47
3.8	CDF of BLER and PDF of the usage of the MCSs presented by the CAP grouping algorithm.	48
3.9	System spectral efficiency achieved by the RND, CC, CAP and SP grouping algorithms.	49
3.10	PDF of the usage of the MCSs and CDF of BLER presented by the SP and Capacity (CAP) grouping algorithms with fixed group size.	50
3.11	System spectral efficiency achieved by the SP grouping algorithm regarding several fixed group sizes.	50
3.12	System spectral efficiency achieved by several SRAs.	51
3.13	PDFs of the usage of the MCSs and group sizes achieved by the SP grouping algorithm combined with SRA MinGain.	52

4.1	System spectral efficiency achieved by the SINR balancing with and without inter-cluster interference knowledge and CDF of the BLER presented by the SINR balancing algorithm.	61
4.2	CDFs of the SINR and balanced SINR presented by the SINR balancing algorithm.	61
4.3	System spectral efficiency achieved by SRAs for several SINR gaps $\Delta_{\gamma_j^t}$	62
4.4	System spectral efficiency achieved by the power minimization algorithm for several SINR gaps $\Delta_{\gamma_j^t}$ [dB].	62
4.5	CDFs of the balanced SINR and BLER presented by the power minimization algorithm.	63
4.6	System spectral efficiency and power economy achieved by the power minimization algorithm.	64
4.7	Effect of channel estimation errors, partial CSI feedback and feedback delay on the system spectral efficiency.	65

List of Tables

1.1	State-of-the-art references for CoMP.	7
1.2	State-of-the-art references for RRA.	9
2.1	SINR thresholds for link adaptation.	26
2.2	Simulation parameters.	27
4.1	Signal to Interference-plus-Noise Ratio (SINR) balancing strategies definition. . .	60

List of Algorithms

3.1 RND scheduler for CS.	33
3.2 MaxGain scheduler for CS.	33
3.3 MaxSINR scheduler for CS.	34
3.4 BRA scheduler for CS.	35
3.5 RND grouping-based algorithm under TGS criterion.	41
3.6 BF grouping algorithm using the CAP metric under MGM stop criterion.	42
3.7 BF grouping algorithm using the CC metric under TGS criterion.	43
3.8 BF grouping algorithm using the SP metric under TGS criterion.	44
3.9 SRA with a given removal criterion.	44
4.1 SINR balancing algorithm.	58

Notation

Acronyms

3G	3 rd Generation
3GPP	3 rd Generation Partnership Project
4G	4 th Generation
AoA	Angle of Arrival
AoD	Angle of Departure
AP	Antenna Port
AWGN	Additive White Gaussian Noise
BER	Bit Error Rate
BF	Best Fit
BLER	Block Error Rate
BRA	Best Rate Allocation
CAP	Capacity
CC	Convex Combination
CDF	Cumulative Distribution Function
CDI	Channel Direction Information
CoMP	Coordinated Multi-Point
CQI	Channel Quality Indicator
CB	Coordinated Beamforming
CS	Coordinated Scheduling
CSI	Channel State Information
eNB	Evolved Node B
EPA	Equal Power Allocation
FDD	Frequency Division Duplexing
FFT	Fast Fourier Transform
FTP	File Transfer Protocol
JP	Joint Processing
JT	Joint Transmission
ICT	Information and Communication Technology
IEEE	Institute of Electrical and Electronics Engineers
IMT	International Mobile Telecommunications
ITU	International Telecommunications Union
LTE	Long Term Evolution
MCS	Modulation and Coding Scheme

MaxGain	Maximum Gain
MinGain	Minimum Gain
MGM	Maximum Grouping Metric
MIMO	Multiple Input Multiple Output
ML	Maximum Likelihood
MMSE	Minimum Mean Square Error
MaxSINR	Maximum SINR
MinSINR	Minimum SINR
MR	Maximum Rate
MU	Multi-User
NLOS	Non Line of Sight
OFDMA	Orthogonal Frequency Division Multiple Access
OFDM	Orthogonal Frequency Division Multiplexing
PDF	Probability Distribution Function
PF	Proportional Fair
PMI	Precoding Matrix Indicator
PRB	Physical Resource Block
QAM	Quadrature Amplitude Modulation
QoS	Quality of Service
RAN	Radio Access Network
RD	Research and Development
RI	Rank Indicator
RND	Random
RR	Round Robin
RRA	Radio Resource Allocation
SCM	Spatial Channel Model
SDM	Space Division Multiplexing
SDMA	Space Division Multiple Access
SNR	Signal to Noise Ratio
SINR	Signal to Interference-plus-Noise Ratio
SP	Successive Projection
SOCP	Second-Order Cone Program
SRA	Sequential Removal Algorithm
TDD	Time Division Duplexing
TGS	Target Group Size
TTI	Transmission Time Interval
UE	User Equipment
UTRA	Universal Terrestrial Radio Access
VoIP	Voice over Internet Protocol
WF	Water Filling
WiMAX	Worldwide Interoperability for Microwave Access
ZF	Zero-Forcing
ZMCSCG	Zero-Mean Circular Symmetric Complex Gaussian

Symbols

Some notational conventions are adopted:

- ▶ Italic letters are used for scalars, lowercase boldface letters for vectors and uppercase boldface letters for matrices;
- ▶ Calligraphic letters are used to represent sets;
- ▶ \mathbb{E} denotes the expectation of a random variable;
- ▶ $\eta(0, \sigma^2)$ denotes a zero-mean Gaussian distribution with variance σ^2 ;
- ▶ p_j denotes the j^{th} component of a vector \mathbf{p} ;
- ▶ $|\cdot|$ denotes set cardinality;
- ▶ $\|\cdot\|_1$, $\|\cdot\|_2$ and $\|\cdot\|_{\text{FRO}}$ denote 1-, 2- and Frobenius-norms, respectively;
- ▶ $\mathbf{1} = [1 \ 1 \ \dots \ 1]^T$ denotes a vector of ones;
- ▶ $\text{diag}\{\mathbf{p}\}$ denotes a diagonal matrix, where the elements of the main diagonal are given by the vector \mathbf{p} ;
- ▶ Finally, $(\cdot)^T$ and $(\cdot)^H$ denote transpose and conjugate transpose, respectively.

Introduction

1.1 4G communication systems

The evolution of Radio Access Networks (RANs) has enabled the users of portable devices connectivity to multimedia services anytime and anywhere, which will demand high spectral efficiency of upcoming wireless cellular systems. The technology to support the offer and supply the demand of these services must improve the performance of the 3rd Generation (3G) wireless cellular systems. The International Telecommunications Union (ITU) is the leading united nation's agency for Information and Communication Technology (ICT) issues and it is committed to connecting the world, ensuring interoperability of radio access technologies and convergence of heterogeneous services. ITU established through the International Mobile Telecommunications (IMT)-Advanced a set of requirements for high performance 4th Generation (4G) communication systems [1].

These key requirements include high quality multimedia applications within a wide range of services and platforms, high instantaneous peak data transmission rates, high average user throughput, low latency packet data transmission, flexible frequency allocation, multibeam transmission, among others [1]. With the aim of meeting the requirements of IMT-Advanced as defined by ITU, the Institute of Electrical and Electronics Engineers (IEEE) has specified a technology known as Worldwide Interoperability for Microwave Access (WiMAX) while the 3rd Generation Partnership Project (3GPP) has specified an Evolved Universal Terrestrial Radio Access (UTRA) technology known as Long Term Evolution (LTE)-Advanced [2].

3GPP continues to study further advancements for the Evolved UTRA networks with the objective of developing a framework for the evolution of the 3GPP radio access technology towards a high data rate, low latency and packet optimized radio access technology. These targets/requirements are documented in 3GPP TR 36.913 [2]. These requirements will include further significant enhancements in terms of performance and capability compared to the 3G wireless cellular systems [3].

LTE-Advanced should fulfill and even surpass all the IMT-Advanced requirements in terms of capacity, data rates and low-cost deployment [3]. The data rates targeted by LTE-Advanced require a significant improvement in the link quality at the User Equipment (UE). But the link capacity of current cellular systems such as LTE is already quite close to the Shannon limit [3]. Although some link improvements are possible, e.g. using additional bandwidth as a means to improve the coding/modulation efficiency, it is necessary to find methods for improving the link quality. Already in current networks, multiple, geographically dispersed antennas connected to a central baseband processing unit are used as a cost-efficient way

of building networks. Such structures open up for new Radio Resource Allocation (RRA) strategies.

Recently, advanced antenna architectures have been attracting a lot of interest as an efficient means to improve the performance of conventional cellular networks. Alike Multiple Input Multiple Output (MIMO) systems, multi-cell cooperative transmission was recently raised in the LTE-Advanced context as a promising solution to improve levels of link quality and, consequently, the system performance compared to the conventional cellular networks [4]. In the context of LTE-Advanced, multiple transmission points responsible for Coordinated Multi-Point (CoMP) transmission are arranged in a distributed way and each cell can be equipped with co-located multiple antennas. The use of multiple antennas at both the transmitter and receiver sides has attracted attention in wireless communications, because MIMO technology offers significant improvement to the radio link and, consequently, to the system throughput without requiring additional bandwidth or increased transmit power. Indeed, LTE-Advanced has regarded the CoMP technology as an efficient means of meeting the IMT-Advanced requirements [5]. In addition, efficient RRA strategies are necessary to explore the available spatial degrees of freedom, coordinate the resources usage, and manage the intra-CoMP-cell interference [6].

In current systems, geographically distributed multiple transmission points over the coverage area play the role of transmit antennas to the UE. In LTE-Advanced systems, CoMP transmission implies dynamic coordination among multiple geographically separated transmission points. From a radio interface perspective, there is no difference from the user perspective if the transmission points belong to the same Evolved Node B (eNB) or different eNBs [5].

The actual number and placement of transmission points depend on several factors, such as the geographical user and service densities, planned coverage, Quality of Service (QoS) requirements, propagation environment, among others. For example, for the upgrade of an existing system the current position of the existing sites might be considered to place the transmission points. In this way, investments made on the already deployed cellular system are protected and new RRA strategies can be employed to enhance the link quality and evolve networks in a cost-efficient manner [3].

CoMP transmission is considered as a promising candidate in future 4G wireless networks (LTE-Advanced) to combat the inter-cell interference that degrades the cell-edge throughput performance, to enhance link quality and consequently boost the capacity of cellular systems [3–5, 7, 8].

1.2 Coordinated Multi-Point systems

In the following, a brief introduction to essential background on downlink CoMP is given. CoMP systems allow to decrease the average access distances between eNBs and UEs. Moreover, CoMP provides coverage handling, decreasing transmit powers, and/or increasing system capacity. CoMP transmission has been proposed as an efficient way to suppress the inter-cell interference and appears as a promising architecture to increase the downlink capacity of cellular systems [9].

CoMP systems can be seen as multiple transmission points geographically distributed over the system's coverage area performing cooperative transmission for several UEs. Multiple transmission points constitute a set of geographically separated transmit antennas participating in the cooperative transmission, which in the 3GPP context are installed at eNBs. For cooperative transmission it is necessary that data be shared among the

multiple transmission points. The manner by which the data is made available at the multiple transmission points and is transmitted from the participating points defines a CoMP transmission approach.

In fact, CoMP transmission techniques take advantage of characteristics of the CoMP network architecture to implement efficient RRA strategies. One key challenge inherent to cooperation among multiple transmission points in the downlink is to improve the system spectral efficiency and, more importantly, the throughput of cell-edge users, since they are strongly influenced by the inter-cell interference [10]. Thus, the CoMP processing is compromised in establishing cooperative transmission as well as in managing intra-cell interference. By allowing full coordination among multiple transmission points the intra-cell interference can be reduced or even completely eliminated depending on the transmission approach and on the availability and quality of Channel State Information (CSI).

In the LTE downlink, the UEs measure the perceived CSI and report it to a set of transmission points. As the CSI is typically made available through feedback channels, it is subject to feedback delays and/or errors and so presents inaccuracies. Although the CoMP technology has potentially significant capacity and coverage benefits, it naturally increases system complexity. Indeed, CoMP systems promise very high performance in terms of spectral efficiency and coverage benefits when perfect CSI knowledge is available at the transmitter [11]. However, in a real-world implementation of cooperative techniques, a substantial amount of signaling is required to ensure reliable CSI to be available wherever necessary. Moreover, the performance of such systems is compromised when the CSI is not perfectly known during CoMP processing so that this is an important issue to be investigated. In this context, prediction schemes for the inter-cell interference could be used to reduce the high demand for link quality estimates in CoMP systems [12].

In the following, important aspects for the performance evaluation of RRA strategies in CoMP systems are addressed. In Section 1.2.1, the downlink CoMP transmission is treated in terms of network architectures and transmission approaches. CSI feedback in CoMP systems also needs to be addressed since its benefits are strongly constrained to practical aspects. In Section 1.2.2, considerations about CSI feedback in the downlink of CoMP systems are detailed. Finally, the RRA problem in CoMP systems is investigated in Section 1.2.3.

1.2.1 Downlink CoMP transmission

In downlink CoMP systems, data transmission is performed across several geographically distributed antennas, which requires a network architecture for the available CoMP transmission approaches. While the network architecture deals with the availability of CSI and UEs data among the multiple transmission points, the downlink CoMP transmission approach limits the degree of coordination available to transmission strategies.

In the literature [9, 13], two basic architectures for enabling the CoMP transmission are found: centralized and decentralized architectures. In downlink CoMP, the main design choice is whether signal processing is to be done in a centralized or decentralized way. Figure 1.1 illustrates these two principal downlink CoMP architectures.

As it can be seen in Figure 1.1, the CoMP cooperating sets are organized by two network architectures where the difference between them is in the manner on how the CSI as well as the UE data are shared. Both architectures require the knowledge of the overall or global CSI relating to all UEs served by the CoMP cooperating set. These two network architectures are briefly explained in the sequel.

► **Centralized:** As shown in Figure 1.1(a), all eNBs in a CoMP set are connected to a central

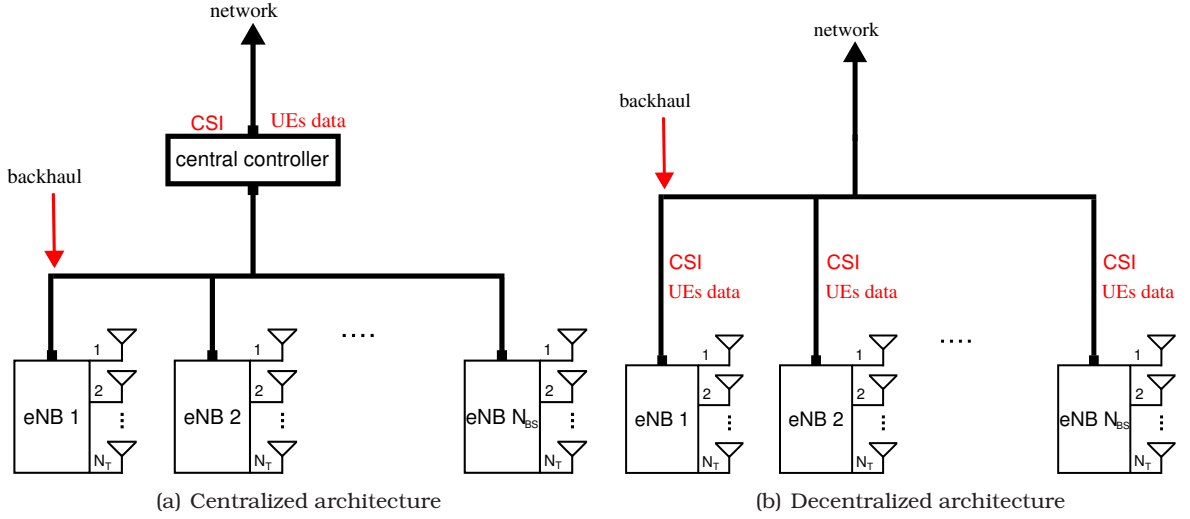


Figure 1.1: Downlink CoMP architectures.

controller for coordinated processing through the backhaul network. In this model, the CSI of a given UE with respect to all transmission points is reported to its serving cell. Afterwards, the local CSI in each eNB is reported to the central controller via backhaul in order to form the overall CSI [9, 13];

- **Decentralized:** As shown in Figure 1.1(b), there is not a central controller connecting all eNBs such that it is necessary to perform individual processing in each eNB. Thus, each eNB of the network needs to have the global CSI with regard to all UEs served by the CoMP cooperating set, which can be shared via fast backhaul links [9, 13].

Indeed, CoMP systems are able to exchange data, control information and CSI with all eNBs and, consequently, coordinate interference. In CoMP systems, the availability of CSI allows the coordination by transmission strategies, such as power allocation, beamforming and time-frequency scheduling. In the following, different downlink CoMP transmission approaches that can be used in order to implement spatial reuse of radio resources are discussed.

In the downlink of CoMP systems, 3GPP distinguishes the Coordinated Scheduling (CS)/Coordinated Beamforming (CB) and the Joint Processing (JP)/Joint Transmission (JT) transmission approaches [5] and they are illustrated in Figure 1.2.

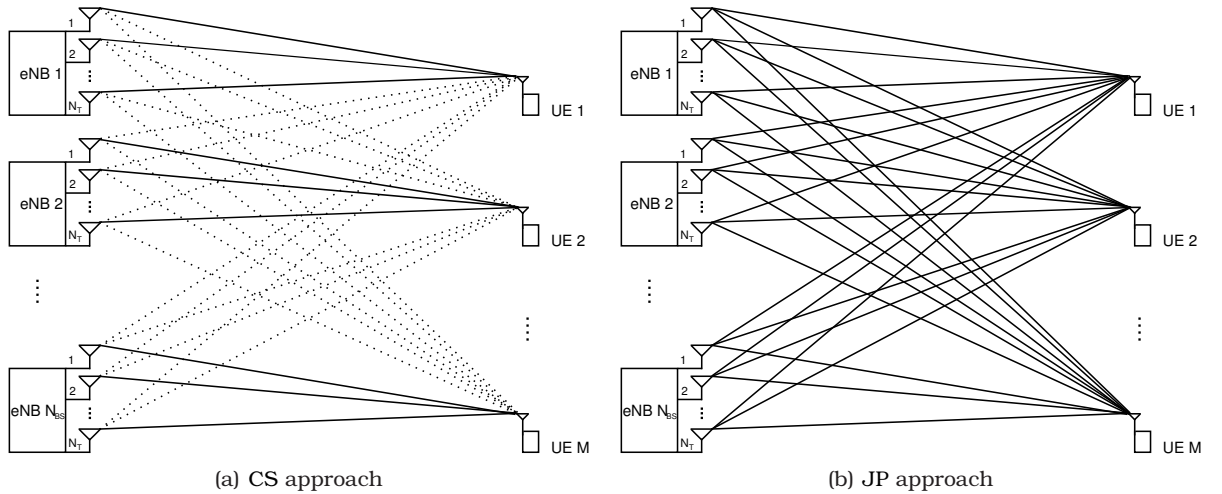


Figure 1.2: Downlink CoMP transmission approaches.

These approaches are detailed in the sequel.

- ▶ **Coordinated Scheduling (CS):** As shown in Figure 1.2(a), UE data is only available in one eNB, i.e., a transmission to a scheduled UE is performed by a unique transmission point, which is termed serving cell. No sharing of UE data or signal-level synchronization between eNBs is necessary since they only acquire and exchange CSI [5, 7, 9, 13];
- ▶ **Joint Processing (JP):** As shown in Figure 1.2(b), data to a single UE is simultaneously transmitted from multiple transmission points, being possible that a single or even multiple UEs be served. In this approach, the eNBs acquire and exchange both CSI and UEs data. Note that the concept of an individual serving cell for one UE disappears [5, 7, 9, 13].

Depending on the CoMP transmission approach considered, the downlink CoMP transmissions intended to multiple UEs can be mutually orthogonal or not in the spatial domain. When observing the CS approach, transmissions to different UEs are not mutually orthogonal in the spatial domain. Although the interference inside a CoMP cooperating set can not be “perfectly” canceled, the CSI available at the eNB can be used by efficient RRA strategies in order to, at least, reduce/manage the interference inside the CoMP cooperating set. When observing the JP approach, the spatial orthogonality is achieved from joint transmission through the use of spatial multiplexing techniques, which is sometimes referred to as Space Division Multiplexing (SDM), and interference-free transmissions become possible.

1.2.2 CSI feedback on downlink CoMP

In the LTE downlink, the CSI is obtained by measurement and feedback mechanisms from the UE, in which the reporting of CSI between the UEs and the multiple transmission points occurs in order to facilitate scheduling decisions. It is almost impossible for the CSI to perfectly reflect the actual channel conditions at the instant of CoMP transmission because it is subject to several sources of imperfections in real-world situations. In the following, these causes of imperfections are presented.

Firstly, there can be errors when measuring the channel perceived by each UE. Also, there is limitation on the number of channel measurements that can be reported through feedback channels. In addition to this, the reporting period is usually much higher than once every Transmission Time Interval (TTI) due to the overhead for measuring and reporting on the feedback channel. Finally, there is an inevitable time delay from the time the channel measurement is taken until the actual CoMP transmission takes place, due to processing and reporting delays. During this time, the channel conditions may change considerably and unpredictably due to fast fading, making the CSI outdated at the time it is being used.

Regarding those uncertainties in the measurements of CSI as well as limited feedback, imperfections can be introduced into the CSI available for CoMP processing. In a realistic CoMP scenario, channel estimation errors, periodicity on measurement of the CSI, partial CSI feedback and outdated CSI shall be assumed in an imperfect CSI model.

The two main categories of imperfect CSI model have been identified to be [5]:

- ▶ **Explicit CSI feedback:** The explicit feedback mechanism in support of downlink CoMP is characterized by having a channel part and an interference part. In the former, the channel as observed by each UE relating to CoMP transmission points is reported to the eNB, without assuming any transmission or receiver processing. In the latter, interference outside the CoMP transmission points is reported to the eNB [5];
- ▶ **Implicit CSI feedback:** Considering ways to reduce reporting overhead, it considers hypotheses of different transmission and/or reception processing, e.g., Channel Quality

Indicator (CQI)/Precoding Matrix Indicator (PMI)/Rank Indicator (RI). CQI is a measure of prevailing channel conditions. In [14] the CQI is a quantized value of the measured Signal to Interference-plus-Noise Ratio (SINR) at the UE. PMI is an index of a selected precoding matrix and RI is the number of spatial transmission layers [5].

The uplink feedback overhead versus downlink performance trade-off should be assessed with the goal of achieving minimum overhead for a given performance.

1.2.3 Radio resource allocation in CoMP systems

Orthogonal Frequency Division Multiple Access (OFDMA)-based systems provide a high flexibility for the RRA that can be exploited by efficient strategies. Indeed, RRA in OFDMA-based systems allows each UE to be assigned resources that are orthogonal in time and frequency by design. Thus, the RRA is simplified because signals sent to UEs on orthogonal resources do not interfere with each other. Furthermore, the time-frequency diversity in an OFDMA-based system allows to dynamically allocate resources for different UEs, and to adapt the Modulation and Coding Scheme (MCS) and power for each time-frequency resource according to the current channel conditions. In this way, efficient RRA strategies can significantly improve the performance of OFDMA-based systems, achieving a higher resource utilization and system capacity.

Together with the inherent resource granularity of OFDMA, advanced RRA algorithms can be developed for CoMP systems. However, RRA in such systems is a very complex task due to the inclusion of the space dimension. Herein, space resources result from the spatial reuse of the same frequency-time resource and signals transmitted by the eNB to a group of UEs on the resource essentially interfere with each other. Thus, the CoMP transmission for different UEs on a same resource is inherently coupled by the co-channel interference. Herein, frequency-time resources are shared among UEs using Space Division Multiple Access (SDMA) [6].

The general RRA problem in an OFDMA-based CoMP system can be viewed as implementing spatial reuse of radio resources among multiple geographically separated transmission points. However, because there is a large number of resources to be managed and a large number of possible assignments, the RRA in such systems has many degrees of freedom and becomes therefore a very complex task.

In the following, the RRA is introduced for each CoMP transmission approach detailed in Section 1.2.1:

- ▶ **Coordinated Scheduling (CS):** As stated before, a transmission to a scheduled UE is performed by a unique transmission point. However, decisions with respect to RRA are made with coordination among the cells by the eNB in order to control interference among cells;
- ▶ **Joint Processing (JP):** In this approach, multiple transmission points work as a distributed antenna array under coordination of the eNB in order to serve a single or even multiple UEs, forming a *macroscopic* MIMO system, such that spatial multiplexing techniques can be used for joint data transmission to multiple UEs [9]. Thus, SDMA and precoding techniques can be used for RRA in order to obtain throughput gains by exploiting the spatial degrees of freedom [6, 15].

Both RRA strategies introduced above have in common the ability of CoMP processing with the CSI among all UEs and transmission points involved on the downlink CoMP transmission.

By exploiting the available CSI, the possibilities for allocating radio resources are increased in CoMP.

However, the good performance of RRA strategies in both CoMP approaches requires that the UEs participating in the CoMP transmission be spatially compatible. In the CS approach, UEs spatially compatible are those that share the same resource in space while the levels of inter-cell interference are under control. In JP approach, these UEs are those whose channels are favorable for spatial separation [6].

Once the set of UEs able to efficiently share the same spatial resource is defined, it is necessary to perform an adequate power allocation among the grouped UEs in order to achieve high spectral efficiency on the usage of the considered resource. The power allocation shall enhance link quality and consequently boost the capacity of cellular systems.

From the exposition, three main topics for RRA can be highlighted:

- ▶ Spatial grouping of UEs that are able to efficiently share the same resource in the spatial domain;
- ▶ Spatial separation of signals intended to different UEs by SDM techniques when considering JP approaches;
- ▶ Power allocation among the used resources and UEs grouped on each CoMP transmission.

Indeed, by combining the inherent resource granularity of OFDMA with the flexibility of the CoMP architecture, advanced RRA algorithms can be developed to control the UE spatial grouping, spatial separation of signals and the power allocation. On the other hand, imperfections on the CSI and inter-cell interference might hinder finding the optimal RRA solutions.

1.3 State-of-the-art

In this section, a literature review on RRA strategies for CoMP systems is provided. Initially, the degrees of freedom on downlink CoMP transmission with respect to CoMP network architecture, transmission approaches and imperfect CSI are addressed.

Table 1.1 gives a set of works related to network architectures and transmission approaches introduced in Section 1.2.1 and imperfect CSI feedback introduced in Section 1.2.2.

Table 1.1: State-of-the-art references for CoMP.

Parameter		References
CoMP architecture	Centralized	[9, 13]
	Decentralized	[9, 13]
CoMP transmission approach	CS	[5, 7, 9, 13]
	JP	[5, 7, 9, 13]
Imperfect CSI	Channel estimation	[16–19]
	Quantization	[16, 17, 19, 20]
	Partial feedback	[9, 20, 21]
	Time delay	[17, 19, 22]

In the following, the state-of-the-art references for CoMP presented in Table 1.1 are discussed.

The authors in [13] and in [9] agree in the manner on how the CSI is shared among the multiple points in a centralized CoMP architecture. However, the model presented by [9] for the decentralized CoMP architecture differs from the model of [13]. In [9], eNBs are connected to other eNBs in a same CoMP cooperating set through backhaul links. Hence, each UE reports its CSI only to its serving cell. This model requires less feedback channel resources

for sharing of CSI, since the sharing of CSI among eNBs can be carried out via fast backhaul links. In [4], each UE reports its CSI to all eNBs. Therefore, there is no need for a backhaul network because each eNB has its own version of the CSI of all UEs. However, the feedback link must support the sharing of the CSI of all UEs involved in CoMP transmission.

In CoMP systems, the optimal number of eNBs within the clusters depends on the reliability of CSI, as well as on the overhead that can be supported [9]. In fact, a substantial amount of signaling is required to ensure reliable knowledge of the complete CSI, which requires a large bandwidth for the feedback channel and an enhanced backhaul network connecting the eNBs. Indeed, there is a trade-off between the potential performance gains of cooperation versus the increased signaling overhead [5].

As stated in Section 1.2.2, in real-world implementations of cooperative techniques, practical aspects of the system such as channel estimation, outdated CSI and limited feedback channel bandwidth need to be addressed. In the following, the previous works listed in Table 1.1 about imperfect CSI feedback introduced in Section 1.2.2 are shortly discussed.

Usually, CSI at the UE is obtained through channel estimation, which is in general inaccurate and thus the measured CSI is only an imperfect estimate of the actual CSI [16, 18]. The UE can generate a meaningful estimate of the CSI, for example, by Maximum Likelihood (ML) and linear Minimum Mean Square Error (MMSE) estimation. In practice, CSI is often obtained by sending known training symbols to the UE [11].

Due to quantization at the UE, the CSI available at the eNB is usually assumed to be imperfect, which leads to a partial interference cancellation. In order to reduce feedback signal overhead achieved by JP transmissions, the precoding is codebook-based in [7]. In principle, the best precoding matrices for interference coordination within a CoMP cooperating set are selected in addition to the individual selection of the best precoding matrix at each cell so that the received SINR is maximized at a UE [7]. In [17], two models for imperfect CSI are presented: noisy/outdated CSI and quantized CSI. In the first one, two sources of error are considered: channel estimation error and feedback delay; while in the second one, the feedback is digitized before transmission. It is shown that these sources of errors cause a degradation in performance of Multi-User (MU)-MIMO systems [17, 19]. In [16], because of limitation in the backhaul bandwidth, the channel estimates are quantized and fed back in the form of codebooks indices. In this work, a limited feedback model was considered, where each UE feeds back quantized Channel Direction Information (CDI) as well as unquantized CQI, being it a channel magnitude or SINR information. In [20], the authors point out a channel quantization model in which the quantization is chosen from a codebook of channel vectors with unit norm.

Since each UE has performed channel estimation, the UE should inform its CSI to the eNB by using the uplink feedback channel. But there is always a time delay between the instant of CSI measurement and the actual instant of transmission of the data. From this, it follows that the CSI available at the eNB is outdated [17]. In [16], feedback delay is modeled through a correlation coefficient between the CSI at the eNB and the CSI at the UE, which is known to both receiver and transmitter. Then, the authors additionally incorporated the opposite effect of time delay to the estimated channel in order to suppress it. Clearly, CoMP processing under an outdated CSI may harm the performance of the system when the feedback delay is a significant measure.

Other limitation with respect to the limited CSI concerns the number of channels that can be reported to the eNB via feedback channel [9]. In general, the channel estimation is also limited, since each UE is not able to estimate their channels for all the eNBs in the CoMP

system [16, 18], but instead it performs estimation only for the strongest channels [23]. In general, scheduling and space-domain precoding require a lot of CSI, such that this subject has been considered in a number of papers. In [21], a two-phase feedback strategy is proposed, in which all the UEs feed back part of the channel information for scheduling – in the first phase –, and only the selected UEs feed back the rest of channel information for precoding – in the second phase. In [20], the authors showed that in the downlink of coherent CoMP systems, UEs located in different cells have small spatial correlation and so they can be selected based only on their channel norms, since in this case the orthogonality depends more on the larger-scale fading than on small-scale fading. From this observation the authors propose a low feedback UE scheduler based on UEs' locations and channel norms. In [22], CSI was considered to be the instantaneous Signal to Noise Ratio (SNR) of the different subcarriers and its report was assumed to be outdated.

In the following, a literature review on RRA strategies is provided. Table 1.2 shows the set of RRA strategies discussed in Section 1.2.3.

Table 1.2: State-of-the-art references for RRA.

Parameter		References
UEs scheduling	Classical schedulers	[7, 8, 24–28]
	Power allocation	[29–32]
	SDMA in MU-MIMO	[6, 15, 33–36]
	UE spatial grouping in CoMP	[10, 37, 38]
SINR balancing	Power allocation	[19, 37, 39–41]

In the following, the state-of-the-art references for RRA presented in Table 1.2 are discussed.

In recent works found in literature [7, 8, 24–26, 28], it has been shown that MU-MIMO transmission schemes applied to the downlink of CoMP systems can bring significant gains in the average cell throughput, cell-edge user throughput and fairness. Classical RRA strategies, such as Proportional Fair (PF) and Round Robin (RR), show different performances regarding the three aforementioned aspects [7, 25, 26]. In [7], the UEs are selected independently of channel quality. In [24, 25], the scheduler of UEs uses an RR policy and, in [8, 26, 28, 42], the scheduler of UEs uses a PF policy.

Indeed, average cell throughput, cell-edge user throughput and fairness are crucial aspects for RRA in CoMP systems [27]. As it is known, spectral efficiency is maximized by efficient RRA strategies based on a Maximum Rate (MR) policy [27]. It is well-known that, when no interference is considered, the system throughput is maximized by assigning each subcarrier on each transmission point to the UE with the highest channel gain and by allocating afterwards power to the Physical Resource Blocks (PRBs) according to the Water Filling (WF) algorithm [32]. Equal Power Allocation (EPA) is simpler and performs only marginally worse than WF, especially for high SNRs [29–31]. When interference from multiple transmission points is considered, this solution should still provide high system throughput by selecting UEs close to the transmission points [27].

All these works focus on the CoMP transmission using simple strategies of UEs scheduling. However, as introduced in Section 1.2.3, the good performance of RRA strategies in both CoMP approaches requires that the UEs participating in the CoMP transmission be spatially compatible. Thus, dynamic RRA strategies should try to exploit the spatial degrees of freedom of downlink CoMP transmission.

For the CS transmission approach, in [10], a dynamic RRA algorithm for the downlink of CoMP systems that exploits the CSI in order to improve the system spectral efficiency implements spatial reuse of radio resources among multiple geographically separated transmission points as well as controls the inter-cell interference. In [24], a dynamic grouping

algorithm of cooperating eNBs for the uplink of CoMP systems significantly improves fairness amongst the UEs of the network. These approaches effectively make use of coordinated spatial grouping.

For MU-MIMO systems, in [6, 15, 33–36], UE spatial grouping algorithms are considered, which avoid placing UEs with highly correlated channels on the same transmission. Among them, the Successive Projection (SP) algorithm [15, 34, 35] can be highlighted, in which the channels of a set of UEs are successively projected onto the null space of the channels of previously selected UEs. In general, the higher the channel gains are, the higher the achievable throughput is. However, considering null space projections, the effective gains of the channels of the UEs are conditioned to the degree of spatial correlation among the channels. Due to the null space SPs keeping a significant similarity with the projection performed by linear spatial precoding, the SP algorithm effectively captures the spatial compatibility among the UEs [6, 15, 34, 35].

Given the above, it is important to highlight that the UE spatial grouping problem in the CoMP scenario has been only partially investigated and that there is a great motivation for applying SDMA techniques in CoMP systems. In [9], the JP transmission approach is exploited by mimicking the benefits of a large virtual MIMO array, i.e., allowing the UE data to be jointly processed by several interfering eNBs. Indeed, the use of SDMA in CoMP systems, as in MU-MIMO wireless systems that are affected by the inter-cell interference, can provide a substantial gain in the system throughput [15]. This is possible by exploiting the available spatial degrees of freedom and using spatial processing techniques to best separate the signals intended for different UEs. Such techniques are widely known from the classical array processing literature (see, e.g., [15, 34, 43] for an overview).

The CSI can be used to mitigate the interference and efficiently separate streams intended to different UEs through spatial precoding and adaptive UE spatial grouping. For example, it is possible to guarantee that the data streams sent to different UEs will not interfere with each other [34]. This is a spatial scheduling task and an UE spatial grouping algorithm is usually employed in order to find a suitable set of UEs for spatial multiplexing. In [10], an UE's grouping algorithm for CoMP systems selects a set of spatially compatible UEs that can efficiently share the same resource in space while the spatial multiplexing of signals conveyed through them is done by using Zero-Forcing (ZF) precoding. This algorithm deals with user orthogonalization in an MU-CoMP system based on successive projections onto null space. However, the system throughput might be improved in [10] with an adaptive size of the UEs set, such that it can be dynamically adapted according to the channel conditions and the load of UEs [37].

The throughput of the scheduled UEs can still be improved regarding a transmitter optimization problem where each one is subject to a SINR constraint. The SINR balancing problem with joint beamforming and power control has the objective of providing a minimum quality to the scheduled UEs. In [19] and [40], the optimal power allocation problem for downlink MU-MIMO systems was solved, respectively, under per-eNB and per-antenna power constraints. In [41], an alternative solution via Second-Order Cone Program (SOCP) is proposed in considering both per-eNB and per-antenna power constraints. Nevertheless, it is difficult to obtain an efficient solution for the optimization problem and so it is desirable to obtain more efficient algorithms. It was shown in [19] that the sub-optimal power allocation based on the scaled water-filling algorithm provides near-optimal performance. An iterative algorithm to maximize the minimum SINR of a set of co-channel links is proposed in [39] such that data streams are transmitted from multiple antennas to several single-antenna

UEs under a sum power constraint. The referred algorithm considers both precoding and power allocation optimization problems, which are both formulated as eigenvalue problems. The precoding problem and the power allocation problem are solved alternately in an iterative way and it is shown in [39] that the algorithm converges after a few iterations. However, this solution has some limitations in the CoMP scenario, in which UEs are subject to a strong inter-cell interference and there is a power limitation per antenna [37]. This solution is not optimal when per-antenna power constraints are considered [39]. While the authors in [39] have studied a single cell scenario, the solution can easily be extended to the joint optimization of several cells [39].

Different CoMP transmission approaches as well as the several RRA strategies presented above have impacts on performance and signaling requirements. For CoMP transmission approaches, any imperfect estimation of channel, delay and feedback error assumptions should also be indicated [5]. 3GPP also defines that performance evaluations should include a high-level description of the RRA strategies simulated [5].

1.4 Open problems

The general problem of RRA in a CoMP system to maximize the throughput is a complex optimization problem. It involves subproblems like resource reuse, UE spatial grouping, antenna selection, resource assignment, precoding and power allocation, among others [6]. The study of grouping UEs along with the JP transmission approach is a crucial problem, since it has been considered the main CoMP transmission approach adopted in the literature [5, 7, 8, 24–26, 28]. Besides, it allows the usage of SDM techniques which can provide throughput gains by exploiting the spatial degrees of freedom [15, 34, 43]. Thus, the focus in this dissertation is on the JP transmission approach, but the CS transmission approach has also been investigated within this dissertation.

Initially, it is focused more specifically on the RRA subproblem of determining a suitable set of UEs to spatially reuse a given radio resource among multiple geographically separated transmission points, having as objective the maximization of the total system throughput. After that, for the JP approach, the SINR balancing problem, which has the objective of providing a minimum quality to the downlink CoMP transmissions of the UEs grouped, is discussed. In the following, the considered RRAs subproblems for both CoMP transmission approaches are stated.

- **UE spatial grouping problem:** In the CS approach, the CSI is used to coordinate the decisions of scheduling and to control the inter-cell interference perceived by each UE. The UE spatial grouping problem for this transmission approach corresponds to determining which UEs can simultaneously use the same resource on different transmission points. In the JP approach, the multiple transmission points are treated as a distributed antenna array to perform MU-MIMO canceling the interference between UEs participating of the CoMP transmission. For example, it is possible to guarantee that the data streams sent to different UEs will not interfere with each other. Thus, RRA strategies can be used for joint data transmission to multiple UEs by the antenna array of the CoMP system. The problem to be solved here is to choose a set of UEs that can efficiently share the same resource in space, which is termed SDMA group.
- **SINR balancing problem:** In the JP approach, in order to provide a more reliable communication for the UEs of the SDMA group, it is desirable to support a certain level of link quality, which mainly depends on the SINR. In the SINR balancing problem, each

UE is subject to an SINR constraint. Hence, the quality of UEs' links might be assured if individual target SINR values are met [39].

The 3GPP offers only guidelines to follow, but does not specify how to implement RRA strategies for the problems considered above as well as to ensure the requirements for high performance 4G communication systems previously introduced in Section 1.1. That is, the standard proposes what to do and does not specify how, leaving several open issues and opportunities for Research and Development (RD).

1.5 Contents

This section explains what this dissertation aims to contribute with, namely with the proposal and study of RRA strategies for the subproblems treated in Section 1.4. As mentioned before, in this dissertation, the focus is on the RRA subproblem of spatially reusing PRBs among multiple transmission points to maximize the system throughput. The RRA in an OFDMA-based CoMP system consists basically in determining a suitable set of UEs to spatially use the radio resources available among the multiple transmission points.

In the CS approach, because dynamic resource reuse and interference coordination became major concerns for the sub-problem considered, it is moved from a single-cell to a multi-cell system model in order to capture the effects of inter-cell interference and of intra-cell interference coordination in both conventional and CoMP scenarios. In the JP approach, the UE spatial grouping is employed in order to find a suitable set of UEs for spatial multiplexing. Next, the SINR balancing problem is solved efficiently in the CoMP scenario by an iterative beamformer and power update algorithm [39].

It is well-known that the optimum solution of these subproblems may also be quite complex. It is difficult to obtain an efficient solution for the optimization problem, which motivates the use of efficient and low-complexity algorithms. Therefore, the focus is on simple and effective algorithms for solving the involved RRA subproblems, avoiding excessive and/or non-linear operations.

The RRA strategies in this dissertation were considered for the downlink of CoMP systems mainly based on LTE characteristics, which has been chosen as representative of 4G communication systems. Initially, it is assumed perfect CSI in studies about RRA strategies. But, the influence of several error sources on the CSI is also investigated.

In the following, Section 1.5.1 lists the main contributions and Section 1.5.2 lists the scientific production of this master's work. Section 1.5.3 presents the organization of the rest of this dissertation.

1.5.1 Contributions

This dissertation provides system-level analyses for the performance gains achieved with different degrees of coordination using different RRA strategies in CoMP systems. In the following, the main contributions of this master thesis aligned to this objective are described.

- ▶ In the **conventional system**, each cell performs scheduling independently, so that no information about other eNBs and transmissions is used and no coordination is possible. Its performance is observed when an estimate of the inter-cell interference perceived by each UE is available or not.
- ▶ Since the information about the interference can be accurately determined by processing the CSI between all UEs and transmission points involved on the downlink CoMP transmission, a **better choice of the modulation** can be done.

- ▶ The use of the CSI can be done to schedule a certain number of UEs while coordinating interference among eNB-UE links, and therefore implement a dynamic RRA, which corresponds to the **CS approach**.
- ▶ The **JP approach** transmits from multiple points to a given set of UEs using spatial precoding. This precoding may be employed to reduce the interference levels or to increase the received power perceived by each UE and so enhance the UE link quality. The evaluation of JP performance is a main topic in this master thesis.
- ▶ In the JP approach, the objective of the UE spatial grouping is to find a suitable set of UEs for spatial multiplexing [10]. Improvements on the UE spatial grouping might be achieved when the **SDMA group size is dynamically adjusted** [37].
- ▶ The **SINR balancing** aims to ensure a certain level of link quality and thus provide a more reliable communication for the grouped UEs in an SDMA group [39]. The SINR balancing algorithm [39] with small modifications is investigated in a multiuser CoMP scenario, in which UEs are subject to an SINR constraint and strong inter-cell interference, and there is a power limitation per antenna [37]. SINR balancing with scaled power allocation is performed for SDMA group [19, 39]. The considered solution in this dissertation extends the algorithm in [39] which is based on the single cell scenario and a sum power constraint.
- ▶ **Power minimization** is performed after the SINR balancing in order to reduce the power used in excess and so the inter-cell interference [39].
- ▶ The performance gains achieved with the RRA strategies and the **impact of imperfect CSI** on the performance of the RRA strategies is also investigated [38].

1.5.2 Scientific production

Throughout the master's course this dissertation has contributed with the following publications. A list with three conference papers follows below:

- i. Rodrigo L. Batista, Tarcisio F. Maciel, Yuri C. B. Silva and Francisco Rodrigo P. Cavalcanti, "Impact Evaluation of Imperfect Channel State Information on the Performance of Downlink CoMP Systems", 28th Brazilian Symposium on Telecommunications (SBrT'11), Curitiba, Paraná, Brazil, Sept 2011.
- ii. Rodrigo L. Batista, Tarcisio F. Maciel, Yuri C. B. Silva and Francisco Rodrigo P. Cavalcanti, "SINR balancing combined with SDMA grouping for CoMP systems", 74th Vehicular Technology Conference (VTC2011-Fall), San Francisco, USA, Sept 2011.
- iii. Rodrigo L. Batista, R. B. dos Santos, Tarcisio F. Maciel, Walter C. Freitas Jr., and Francisco Rodrigo P. Cavalcanti, "Performance evaluation for Radio Resource Allocation algorithms in CoMP systems", 72nd Vehicular Technology Conference (VTC2010-Fall), Ottawa, Canada, Sept 2010.

This master thesis has been conceived in the context of UFC.22 and UFC.32 research projects, that belong to a cooperation between GTEL and Ericsson Research. Five technical reports have been produced during the period of the master's course and one is in the process of writing. The list follows below:

- i. Elvis M. G. Stancanelli, Rodrigo L. Batista, Yuri C. B. Silva, Tarcisio F. Maciel and Francisco Rodrigo P. Cavalcanti, "Initial studies on dynamic UE spatial grouping for CoMP systems", Second Technical Report of UFC.32 Project, July 2011.
- ii. Elvis M. G. Stancanelli, Rodrigo L. Batista, Yuri C. B. Silva, Tarcisio F. Maciel and Francisco Rodrigo P. Cavalcanti, "Initial studies on dynamic UE spatial grouping for CoMP systems", First Technical Report of UFC.32 Project, December 2010.
- iii. Ricardo B. dos Santos, Rodrigo L. Batista, Tarcisio F. Maciel, Elvis M. G. Stancanelli, Walter C. Freitas Jr. and Francisco Rodrigo P. Cavalcanti, "RRA for Rate Maximization in CoMP Systems", Final Technical Report of UFC.22 Project, July 2010.
- iv. Ricardo B. dos Santos, Rodrigo L. Batista, Tarcisio F. Maciel, Elvis M. G. Stancanelli, Walter C. Freitas Jr. and Francisco Rodrigo P. Cavalcanti, "RRA for Rate Maximization in CoMP Systems", Third Technical Report of UFC.22 Project, February 2010.
- v. Ricardo B. dos Santos, Elvis M. G. Stancanelli, João César M. Feitosa, Rodrigo L. Batista, Tarcisio F. Maciel, Walter C. Freitas Jr. and Francisco Rodrigo P. Cavalcanti, "RRA in Coordinated Multi-Point Systems", Second Technical Report of UFC.22 Project, August 2009.

1.5.3 Outline

This chapter provided some background required to the good understanding of RRA problems in CoMP systems. It started with a review on the evolution of RANs. After that, some concepts with respect to the CoMP transmission are provided as well as some relevant works related to CoMP systems and RRA are referred. The remainder of this document is organized as follows:

- ▶ **Chapter 2:** In this chapter, the system model is addressed. Herein, the models adopted for CoMP systems and the needs for CoMP processing are presented. Aspects such as frame structure, multi-cell network deployment, wireless channel model, downlink CoMP transmission model, imperfect CSI model, RRA and link-to-system level interface are discussed. All models presented in this chapter relate to definitions made in Section 1.2 concerning RRA in CoMP systems.
- ▶ **Chapter 3:** In this chapter, RRA strategies for the UE spatial grouping problem are presented. Initially, the UE spatial grouping problem, which was introduced in Section 1.4, is formulated. After that, several RRA strategies for the UE spatial grouping problem observing both CS and JP transmission approaches are presented. Finally, the results are presented and discussed, being summarized at the end of the chapter.
- ▶ **Chapter 4:** In this chapter, the formulation for the SINR balancing problem in the CoMP scenario is discussed, which was also introduced in Section 1.4. After that, a well-known solution for the SINR balancing problem is considered by doing some particular considerations for its application in CoMP systems. Next, power minimization is performed while the SINR constraints are maintained feasible. General discussions and conclusions are also given at the end of the chapter.
- ▶ **Chapter 5:** This chapter draws the main conclusions regarding the RRA problems in CoMP systems studied in this work.

System model

2.1 Introduction

This dissertation focuses on communication in the downlink of a centralized Coordinated Multi-Point (CoMP) network whose architecture has been shortly presented in Section 1.2.1. The Evolved Node Bs (eNBs) available in the network are grouped into disjoint clusters (or CoMP cooperating sets) so that a given eNB cannot belong to more than one cluster operating at the same time-frequency resource. It is assumed perfect synchronization and that eNBs in a cluster are connected via a fast backhaul link to a central controller. Thus, eNB antennas act as inputs of a generalized Multi-User (MU)-Multiple Input Multiple Output (MIMO) system, while User Equipment (UE) antennas from multiple UEs are considered as the outputs.

Physical modeling of wireless channels requires knowledge of the electromagnetic field between transmitter and receiver. In principle, one could study the system performance based on field equations and taking into account the influence of obstructions and other elements of the environment (as ground, buildings and vehicles in the vicinity between the eNBs UEs) onto this electromagnetic field. However, a performance evaluation of a CoMP system (or other wireless systems as well) considering real electromagnetic propagation presents very high complexity, mainly due to the large physical dimension of the system and large number of variables involved in electromagnetic propagation. Thus, it is adopted a system model based on statistical characterization of the system and of the involved radio channels, which require only channel parameters [43, 44].

In CoMP systems, multiple transmission points belonging to adjacent eNBs apply transmission strategies in order to coordinate resources usage and manage intra-cluster interference. By allowing full coordination among the eNBs within a cluster, the intra-cluster interference can be managed or even completely eliminated depending on the selected transmission schemes and on the available Channel State Information (CSI) [5]. For the Long Term Evolution (LTE)-like system model considered in this dissertation, one has that CSI is periodically measured and reported by UEs and used for CoMP processing in the system, a feature that is supported by LTE [5]. Using the available CSI, Coordinated Scheduling (CS) and Joint Processing (JP) techniques may be used to coordinate the intra-cluster interference, as introduced in Section 1.2.1. This dissertation gives more attention to JP techniques and focus on CoMP processing considering that CSI is available at the time of transmission. Nevertheless, CS approaches are also considered.

In general, imperfect CSI limits the regimes in which downlink CoMP is beneficial [9] such that the success of CoMP transmissions depends on the reliability of CSI. In general, perfect

CSI is difficult to obtain in CoMP systems due to an increased number of channel parameters to estimate and feed back to the transmitter. In fact, a substantial amount of signaling would be required to ensure a reliable CSI. Consequently, in practical cases, CSI is usually inaccurate. Inaccuracies originate, for example, from measurement errors, quantization of the reported values, feedback delays, etc., as mentioned in Section 1.2.2. In this dissertation, some types of imperfections of CSI due to measurement delays, partial CSI feedback and imprecise estimation of the CoMP channels are addressed.

The performance of the considered CoMP system is evaluated by means of system-level simulations, in which the impact of different Radio Resource Allocation (RRA) strategies on the performance of CoMP systems is investigated. Semi-static simulations composed by a high number of system snapshots with fixed time duration are adopted. The system modeling and notation is highly LTE-oriented and, consequently, most of the notation and terms correspond to those adopted by 3rd Generation Partnership Project (3GPP) LTE.

In the following, the models adopted to evaluate the system performance are presented. The rest of this chapter is organized as follows. In Section 2.2, the considered frame structure is discussed. The CoMP scenario is addressed in Section 2.3. The main features of the models employed for the radio channel are presented in Section 2.4. In Section 2.5, the downlink CoMP transmission model used in this dissertation is detailed. In Section 2.6, the transmission model from Section 2.5 is extended to consider imperfect CSI. Section 2.7 introduces the main considerations for the RRA problem modeling. Section 2.8 contains a simple mechanism for inter-cluster interference estimation. The link-to-system interface is described in Section 2.9. Finally, in Section 2.10, simulation details are presented.

2.2 Downlink physical resource

In order to achieve high data transmission rates, 3GPP decided to use Orthogonal Frequency Division Multiplexing (OFDM) as basis for its signal bearer, which is a transmission form that uses a large number of closely spaced carriers and that can be efficiently modulated with low rate each. OFDM has many advantages including its robustness to multipath fading and interference [43].

In 3GPP, downlink transmission using OFDM is designed to work in both Frequency Division Duplexing (FDD) and Time Division Duplexing (TDD) modes of operation [43]. FDD is suitable for bi-directional voice service since it occupies a symmetric downlink and uplink channel pair. However, FDD is inefficient for handling asymmetric data services since data traffic may only occupy a small portion of a channel bandwidth at any given time. On the other hand, TDD can flexibly handle both symmetric and asymmetric broadband traffic. It requires only one channel for transmitting downlink and uplink sub-frames at two distinct time slots. Here, only the downlink FDD mode is discussed.

For downlink, 3GPP specifies the Orthogonal Frequency Division Multiple Access (OFDMA) technology (which is based on OFDM) as radio access technique. It allows each UE to be assigned resources that are orthogonal in frequency. OFDMA also has the advantage of enabling the baseband transmission on a single frequency-flat sub-carrier. In the downlink, an OFDM frame structure takes the form of a frequency-time resource grid as shown in Figure 2.1.

As it can be seen in Figure 2.1, each radio frame has a bandwidth BW and the duration of one Transmission Time Interval (TTI). Usually, due to signaling constraints, subcarriers are not allocated individually, but in blocks of adjacent subcarriers, which represent the Physical Resource Blocks (PRBs) [45]. Channel coherence bandwidth is assumed larger than

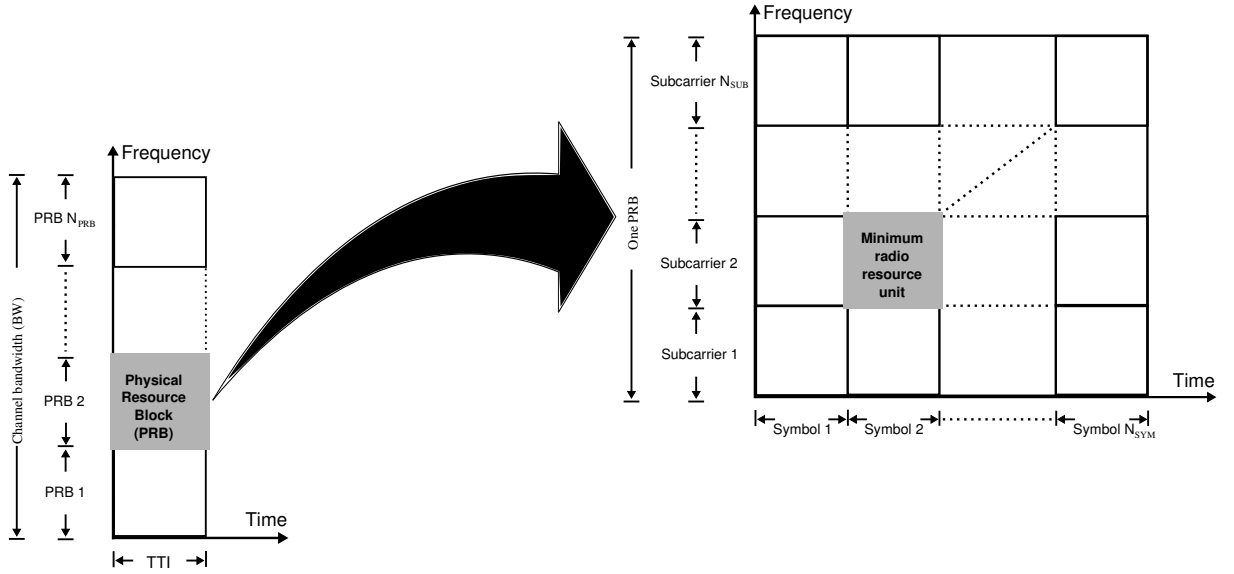


Figure 2.1: OFDMA frame structure.

the bandwidth of a PRB leading to flat fading over each PRB. The PRB is defined as one TTI in time domain, which is divided into N_{SYM} symbols, and N_{SUB} contiguous OFDM sub-carriers spaced of Δ_f Hz.

While the minimum physical resource in OFDMA can be seen as a unit comprising one OFDM symbol in time domain and one OFDM sub-carrier in frequency domain, the minimum allocable resource in real LTE systems is the PRB. This unit corresponds to the available resource that can be assigned to UEs by an RRA function of the system. Since the number of UEs is typically larger than the number of available resources, UEs have to be scheduled by the RRA algorithm. As shown in Figure 2.1, there exist N_{PRB} PRBs in the system, indicated by $n = 1, 2, \dots, N_{PRB}$, and each of them might be assigned to one or more UEs in each cluster.

2.3 Multi-cell system

This dissertation focuses on the downlink of a multi-cell system under dynamic coordination among multiple geographically separated transmission points over the system's coverage area.

Let us assume that each eNB is placed on the corner shared by the sectors of the 3-sector cell and each sector is represented by a regular hexagon, whose maximal diameter is given by R . The 3-sector model of cell adopted in this dissertation is shown in Figure 2.2.

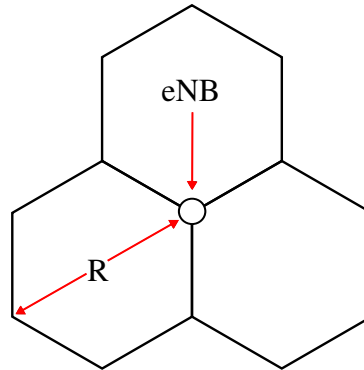


Figure 2.2: 3-sector cell.

The scenario considered in this dissertation corresponds to a cell network with eNBs uniformly distributed over the coverage area. In the considered notation, it is assumed that the multi-cell system is composed of C clusters, indicated by $c = 1, 2, \dots, C$. It is considered that a cluster comprises a number of N_{eNB} eNBs under its control and the number

of sectors/cluster is denoted by $N_{\text{SEC}} = 3N_{\text{eNB}}$.

Graphically, the considered conventional and CoMP scenarios are shown in Figure 2.3.

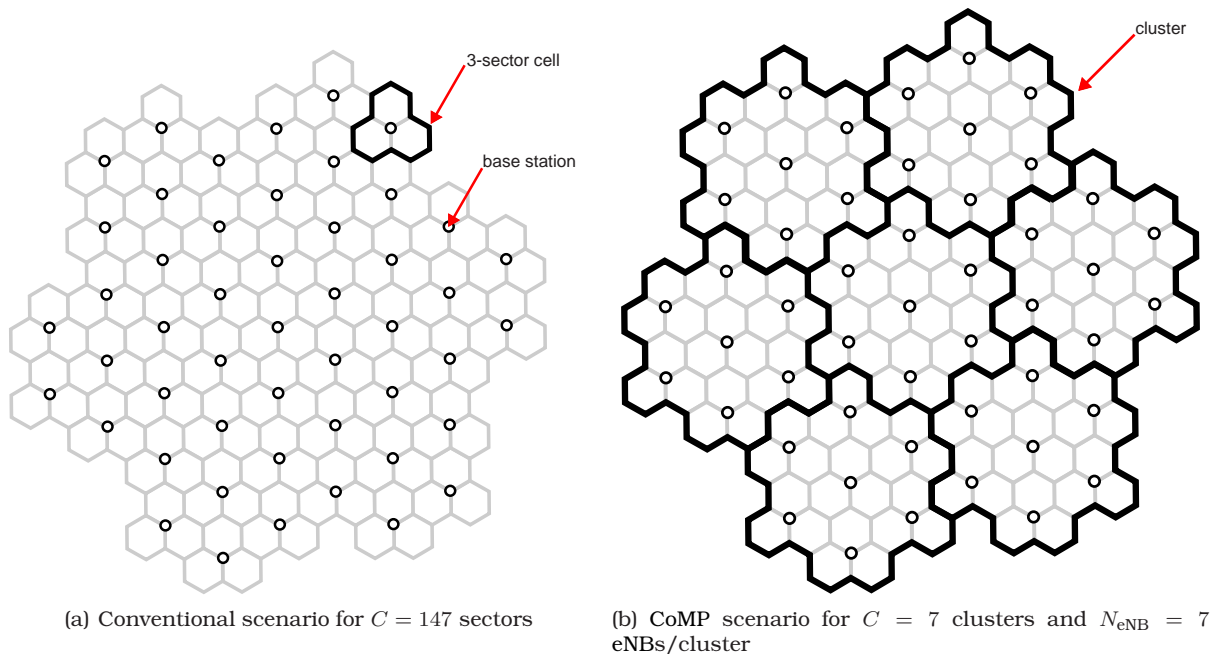


Figure 2.3: Coverage area of the system for $N_{\text{eNB}} = 49$ eNBs.

Figure 2.3(b) presents the coverage area of the CoMP system for $C = 7$ clusters and $N_{\text{eNB}} = 7$ eNBs/cluster where a center cluster is surrounded by one tier of clusters. The inter-cell interference perceived by a given UE within its cluster is managed. However, the UEs at the cluster-edge perceive a strong inter-cell interference from other clusters. From Figure 2.3(a), the conventional scenario is analogous to the CoMP scenario when each sector is similar to a cluster and it has its own isolated central controller. The central controller is not shown in Figure 2.3, but it can be co-located in some eNB or placed at any point in the coverage area of the multi-cell system connecting eNBs belonging to a given cluster through a fast backhaul.

It is possible to note in Figure 2.3 that UEs belonging to sectors placed on the system edge experience less interference than those UEs placed on the central sector, making the Signal to Interference-plus-Noise Ratio (SINR) values of these UEs more optimistic. The wrap-around technique aims to eliminate these unwanted border effects and generally use the cell replication or a virtual geometric model. The wrap-around model described in [26] is considered here. The multi-cell layout that is folded like a torus consists of a mapping between the plane and toroidal models.

Let us assume that each sector is equipped with N_{ANT} directional transmit antennas and serves N_{UE} UEs uniformly distributed over its coverage area. It is assumed that frequency resources can be fully reused in all sectors. In the CoMP scenario, it is also assumed that a cluster comprises $M = N_{\text{SEC}}N_{\text{ANT}}$ transmission points, indicated by $m = 1, 2, \dots, M$, whose resource usage and transmission strategies are coordinated. The cluster serves a number $J = N_{\text{SEC}}N_{\text{UE}}$ of single-antenna UEs, indicated by $j = 1, 2, \dots, J$, which are uniformly distributed over its coverage area. In the conventional scenario the sector is equipped with $M = N_{\text{ANT}}$ transmit antennas and serves $J = N_{\text{UE}}$ UEs. In the considered notation, the antennas of each sector at the eNB will be referred as Antenna Ports (APs).

2.4 Wireless channel model

The 3GPP defines the following three fading environments: suburban macrocell, urban macrocell and urban microcell [44]. In the macrocell environment, it is usually assumed

that the eNB antennas are above rooftop height and the scatterers surrounding the UE are about the same height as or are higher than the UE, while in the microcell environment the surrounding objects are usually at the same height as the eNB antennas [46]. This implies that the multipath richness is higher in microcell environment. In this dissertation, the urban microcell environment was chosen due to higher throughput, which is an important characteristic to be evaluated by RRA strategies for the rate maximization, as mentioned in Section 1.4.

The modeling of wireless channels adopted herein considers variations of the channel strength over time and frequency. The variations can be roughly divided into two types: large-scale fading and short-scale fading. The former originates due to path loss of signal, as a function of distance, and shadowing, due to large objects such as buildings and hills obstructing the communication path. Large-scale fading changes occur as the UE moves through distances of the order of the cell size and is typically frequency independent. Short-scale fading originates from constructive and destructive interference of signal replicas coming through multiple signal paths between transmitter and receiver. Short-scale fading changes occur at the spatial scale of the order of the carrier wavelength and is often frequency dependent. Shadowing and distance dependent path loss will also affect the average received signal strength significantly. Frequency-selective fading will result in rapid and random variations in the channel attenuation.

The distance dependent path loss is based on the COST 231 Walfish-Ikegami Non Line of Sight (NLOS) model. Particular aspects of path loss modeling for the urban microcell environment are described in [44]. Low channel variations due to shadowing are modeled by a lognormal distribution of mean zero and standard deviation σ .

In order to incorporate physical concepts about short-scale fading into the wireless channel model, the Spatial Channel Model (SCM) is adopted which is a stochastic channel model developed by 3GPP for evaluating MIMO system performance. It incorporates important parameters such as phases, delays, Doppler shifts, Angle of Departure (AoD), Angle of Arrival (AoA) and angle spread models to provide a description of MIMO channels [44].

The details of the generation of relevant parameters for the SCM as well as the values of such parameters are specified by 3GPP and can be found in [44]. This dissertation uses the SCM implementation available in [47] in order to obtain values for short-scale fading.

In this dissertation, the complex channel coefficient denotes the sampled frequency response of the channel in the frequency domain, including path loss, shadowing and short-scale fading effects. The frequency response of the channel is obtained by applying the Fast Fourier Transform (FFT) to the channel responses obtained with help of the SCM.

For a given PRB, the complex channel coefficient corresponds to the middle subcarrier of the considered PRB. Let $h_{j,m,c,n}$ denote the complex channel coefficient between the transmit antenna m of cluster c and the UE j on the PRB n . Let $\mathbf{h}_{j,c,n} \in \mathbb{C}^{1 \times M}$ denote the complex channel vector that models the link between the UE j and all M transmit antennas of cluster c on the PRB n . The channel vector $\mathbf{h}_{j,c,n}$ is given by

$$\mathbf{h}_{j,c,n} = \left[h_{j,1,c,n} \ h_{j,2,c,n} \ \cdots \ h_{j,M,c,n} \right], \quad (2.1)$$

where:

- ▶ $j = 1, 2, \dots, J$, and J is the number of UEs in a cluster;
- ▶ $c = 1, 2, \dots, C$, and C is the number of clusters in the multi-cell scenario;

- $n = 1, 2, \dots, N_{PRB}$, and N_{PRB} is the number of PRBs in the CoMP system.

2.5 Downlink CoMP transmission model

In the following, the discussion is restricted to one PRB n , such that the index n will be omitted for simplicity of notation. When considering the transmission on a single PRB of a given cluster of the multi-cell system, a cellular network consisting of M transmit antennas and J UEs is typically observed. Assuming that UE j is served and scheduled by the RRA algorithm in cluster c , the downlink signal $y_{j,c}$ received by UE j on a given PRB from all M transmit antennas in cluster c is given by

$$y_{j,c} = \mathbf{h}_{j,c} \mathbf{x}_{j,c} + \underbrace{\sum_{j' \neq j}^J \mathbf{h}_{j,c} \mathbf{x}_{j',c}}_{z_{j,c}^{intra}} + \underbrace{\sum_{c' \neq c}^C \sum_{j'}^J \mathbf{h}_{j,c'} \mathbf{x}_{j',c'}}_{z_{j,c}^{inter}} + \eta_{j,c}, \quad (2.2)$$

where:

- $\mathbf{x}_{j,c} \in \mathbb{C}^{M \times 1}$ is the symbol vector transmitted by the M antennas of cluster c to the j^{th} UE;
- $\eta_{j,c} \in \mathbb{R}$ is the Additive White Gaussian Noise (AWGN), with zero mean and variance σ_η^2 , perceived by the j^{th} UE in the cluster c ;
- $z_{j,c}^{intra}$ is the intra-cluster interference. This is the interference originated from antennas of a same cluster and it is known to the eNB, since it is assumed perfect channel knowledge inside the cluster;
- and $z_{j,c}^{inter}$ is the inter-cluster interference. This is the interference originated from antennas of other clusters. Even though it is unknown to the eNBs it can be estimated by the UE j and reported via feedback channels.

For each PRB and cluster c , whose index is also omitted in the sequel for simplicity of notation, the transmitted signal \mathbf{x}_j for the UE j is given by

$$\mathbf{x}_j = \underbrace{\mathbf{w}_j \sqrt{p_j}}_{\mathbf{u}_j} d_j = \mathbf{u}_j d_j, \quad (2.3)$$

where:

- $\mathbf{w}_j \in \mathbb{C}^{M \times 1}$ is the unitary-norm precoding vector for the link between UE j and all antennas of the cluster;
- $p_j \in \mathbb{R}$ is the transmit power allocated for the UE j ;
- $\mathbf{u}_j \in \mathbb{C}^{M \times 1}$ is the precoding vector including the transmit power p_j allocated for the UE j ;
- and $d_j \in \mathbb{C}$ is the unit-variance data symbol to be sent to UE j .

As stated in Section 1.2.1, downlink CoMP transmissions can be or not mutually orthogonal between UEs within a same cluster depending on the considered CoMP transmission approach. In the CS transmission approach, data is only available at the serving sector such that there is intra-cluster interference between transmissions to different UEs within a same cluster. In the JP transmission approach, transmissions to different UEs

within a same cluster will be typically mutually orthogonal herein, implying that there is no interference between the transmissions, i.e., no intra-cluster interference.

In both approaches, RRA decisions are made with coordination among eNBs corresponding to the cluster such that the intra-cluster interference can be managed by different CoMP transmission strategies. However, CoMP transmission strategies are only allowed between eNBs belonging to the same cluster, whereas eNBs belonging to different clusters are not coordinated and thus they are potential inter-cluster interference sources.

In the following, the SINR is modeled as a measure of link quality perceived by a UE j receiving data in a cluster on a given PRB. Using \mathbf{h}_j of (2.1), let us define the approximate spatial matrices \mathbf{R}_j for the UE j as

$$\mathbf{R}_j = \mathbf{h}_j^H \mathbf{h}_j. \quad (2.4)$$

Then, using (2.4), the SINR γ_j perceived by the UE j can be given by

$$\gamma_j = \frac{p_j \mathbf{w}_j^H \mathbf{R}_j \mathbf{w}_j}{\underbrace{\sum_{j' \neq j}^G p_{j'} \mathbf{w}_{j'}^H \mathbf{R}_j \mathbf{w}_{j'}}_{z_j^{intra}} + z_j^{inter} + \sigma_\eta^2}. \quad (2.5)$$

where:

- ▶ $\sigma_\eta^2 \in \mathbb{R}$ is the noise power;

2.6 CSI modeling

This section lists the form of explicit CSI considered in the dissertation. Imperfect CSI feedback is addressed and modeled by considering CSI estimation errors, partial CSI feedback and outdated CSI knowledge.

In the following, CSI estimation errors are modeled. Usually, CSI at the receiver is obtained through estimation, which is in general inaccurate and thus the measured CSI is only an erroneous estimate of the actual CSI [16]. The receiver can generate a meaningful estimate of the CSI, for example, by Maximum Likelihood (ML) and linear Minimum Mean Square Error (MMSE) estimates [11]. Here is assumed MMSE estimation, so that the channel estimate $\hat{\mathbf{h}}_j$ can be modeled as [48]

$$\hat{\mathbf{h}}_j = \mathbf{h}_j^\rho = \sqrt{1-\rho} \mathbf{h}_j + \sqrt{\rho} \mathbf{e}_j, \quad (2.6)$$

where:

- ▶ $\mathbf{e}_j \in \mathbb{C}^{1 \times M}$ is the complex channel estimation error vector whose entries are Zero-Mean Circular Symmetric Complex Gaussian (ZMCSCG) random variables with variance σ_e^2 ;
- ▶ and ρ is a parameter that captures the quality of the channel estimation.

By the property of MMSE estimation [11], the channel estimate $\hat{\mathbf{h}}_j$, whose entries are i.i.d. ZMCSCG variables with variance σ_h^2 , is uncorrelated with \mathbf{e}_j . Assuming $\sigma_e^2 = \sigma_h^2$, the estimated channel variance is given by $\sigma_h^2 = (1-\rho)\sigma_h^2 + \rho\sigma_e^2 = \sigma_h^2$ and so the channel energy is preserved. Note that the parameter ρ models exactly the percent of channel error \mathbf{e}_j in comparison to the estimated channel $\hat{\mathbf{h}}_j$ and it is given by

$$\frac{\mathbb{E} \left\{ \left[\sqrt{\rho} \mathbf{e}_j \right]^2 \right\}}{\mathbb{E} \left\{ \left[\hat{\mathbf{h}}_j \right]^2 \right\}} = \rho \frac{\sigma_e^2}{\sigma_h^2} = \rho. \quad (2.7)$$

Now, the partial CSI due to the limitation on number of reported channels is introduced. In the considered model, the UE j is able to generate a meaningful estimate for the channels with the $l \leq M$ highest channel gains $\|\mathbf{h}_{j,m}\|_1^2$ among a number M of antennas in all the cluster. Each link among the UE j and the M antennas of its cluster c that can not be estimated and so can not be reported to the eNB, is filled with zero in the resulting channel vector, which is denoted by $\hat{\mathbf{h}}_j = \mathbf{h}_j^{\rho,l}$.

The CSI after estimation is reported to the transmitter via feedback channel in which time delays can occur. For the sake of simplicity, it is assumed that all UEs in the CoMP system experience the same time delay, which is denoted by an integer number $\Delta\tau$ of TTIs. Finally, the outdated CSI is given in $\Delta\tau$ TTIs, i.e., $\hat{\mathbf{h}}_j = \mathbf{h}_j^{\rho,l,\Delta\tau}$. This is the CSI effectively used as CSI of UE j during the CoMP processing.

In this dissertation, the imperfect CSI issue is addressed in order to illustrate conditions closer to real-world implementations of CoMP transmission techniques. It is also investigated the performance achieved by RRA strategies in CoMP systems for perfect CSI, which occurs for $\rho = 0$, $l = M$, and $\Delta\tau = 0$. In the rest of this work, the indexes ρ , l and $\Delta\tau$ will be omitted for simplicity of notation, using such indexes only when each is the parameter being varied in analyses. In this way, both perfect and imperfect CSI for each UE j are denoted in the form of channel vectors $\hat{\mathbf{h}}_j$.

2.7 Radio resource allocation

In order to control the allocation of the shared resources among the UEs at each instant of time, the RRA tries to exploit the channel variations through appropriate CoMP processing using the CSI available at the time of the data transmission. In this way, the RRA in a CoMP system will choose a set of UEs within a cluster that can efficiently share the same PRB in space and will try to improve the received signal quality and/or cancel intra-cluster interference. The RRA strategies considered in this dissertation consider two main steps: scheduling and power allocation.

The scheduling is the process of dynamically allocating the available PRBs among the UEs based on some set of rules that characterize the scheduling algorithm. In particular, the scheduling algorithm in the conventional scenario performs individual allocation of PRBs in each sector without knowledge of RRA decisions in other sectors. The scheduling algorithm in an OFDMA-based CoMP system implements spatial reuse of radio resources among multiple geographically separated transmission points. Here, the assignment decisions are taken independently for each PRB. For each PRB and cluster, the scheduling algorithm will select a set $\mathcal{G} \subset \{1, 2, \dots, J\}$ of UEs to receive data, where the number of UEs it contains will be denoted by $G = |\mathcal{G}| \leq M$. Then, considering a group \mathcal{G} , a channel matrix $\hat{\mathbf{H}} \in \mathbb{C}^{G \times M}$ can be defined as follows

$$\hat{\mathbf{H}} = \begin{bmatrix} \hat{\mathbf{h}}_1^T & \hat{\mathbf{h}}_2^T & \dots & \hat{\mathbf{h}}_G^T \end{bmatrix}^T. \quad (2.8)$$

In the JP transmission approach, data to a single UE is simultaneously transmitted from multiple transmission points belonging to a cluster through spatial precoding. Then, considering a group \mathcal{G} , a precoding matrix $\mathbf{W} \in \mathbb{C}^{M \times G}$ can be defined as follows

$$\mathbf{W} = \begin{bmatrix} \mathbf{w}_1 & \mathbf{w}_2 & \dots & \mathbf{w}_G \end{bmatrix}, \quad (2.9)$$

where each $\mathbf{w}_j \in \mathbb{C}^{M \times 1}$ is defined over all M transmit antennas such that the precoding vector

\mathbf{w}_j for each UE j belonging to the group \mathcal{G} can be written as follows

$$\mathbf{w}_j = [w_{1,j} \ w_{2,j} \ \dots \ w_{M,j}]^T. \quad (2.10)$$

When considering the CS approach, the scheduling algorithm consists in determining which sectors will transmit and which UEs will receive on each PRB of the cluster. In this approach, while the scheduling decisions are made with coordination among all sectors belonging to the same cluster, the data intended to each UE is only available at the serving sector of this UE. This scenario provides flexibility to decide if all sectors associated to a cluster will be used or if some of them will be turned off to avoid the intra-cluster interference and reduce the error probabilities. In this approach, the precoding vector \mathbf{w}_j of the UE j , defined in (2.10), becomes a sector selection vector, whose entries $w_{m,j}$, $\forall 1 \leq m \leq M$, are binary variables indicating whether sector m sends data to the UE j , as defined in

$$w_{m,j} = \begin{cases} 1 & \text{If the UE } j \text{ is allocated in sector } m, \\ 0 & \text{Otherwise,} \end{cases} \quad (2.11a)$$

subject to

$$\sum_{1 \leq m \leq M} w_{m,j} \leq 1, \forall j. \quad (2.11b)$$

where constraint (2.11b) limits the number of sectors selected for transmission to a given UE to be one.

In the sequel, the power allocation is described. In this dissertation, it has been assumed per-sector power constraints, which are motivated by the fact that each sector has a separate power amplifier with a limited linear range. Although optimal, Water Filling (WF) is not considered in this dissertation, but Equal Power Allocation (EPA) is performed among the subcarriers. While the EPA approach is not optimal, references in the literature [29–31] show that the difference in performance is minimal. Let the total transmit power available on each sector be defined herein as P_{TOT} . Thus, P_{TOT} is equally divided among the N_{PRB} PRBs and the maximum transmit power allocated to each PRB is given by

$$P_{\text{PRB}} = \frac{P_{\text{TOT}}}{N_{\text{PRB}}}. \quad (2.12)$$

It is worth mentioning that in the JP transmission approach the maximum per-PRB transmit power P_{PRB} will draw only an upper bound on the per-PRB transmit power of a given sector, since each sector is shared among several UEs. On the other hand, in the CS transmission approach, the transmission power p_j is totally allocated for the UE j , i.e., $p_j = P_{\text{PRB}}$, in a given sector m when the UE j is allocated on that sector, i.e., $w_{m,j} = 1$.

When observing the JP approach, the RRA strategies consider the downlink of a cluster with M transmission antennas and also a total power constraint on all antennas together expressed as $P_{\text{SUM}} = M P_{\text{PRB}}$, besides per-sector power constraints. The power assignment can achieve different power allocations p_j for each UE j , such that a power allocation vector is defined as follows

$$\mathbf{p} = [p_1 \ p_2 \ \dots \ p_G]^T, \quad (2.13a)$$

subject to

$$\|\mathbf{p}\|_1 \leq P_{\text{SUM}}. \quad (2.13b)$$

For the JP approach, the modeling of a power allocation vector \mathbf{p} is motivated due to use of a total power constraint P_{SUM} by RRA strategies.

Considering the previous definitions, the matrix $\mathbf{U} \in \mathbb{C}^{M \times G}$ comprised by the precoding matrix \mathbf{W} and by the power allocation vector \mathbf{p} , see Section 2.5, can be written as

$$\mathbf{U} = [\mathbf{U}_1^T \ \mathbf{U}_2^T \ \dots \ \mathbf{U}_{N_{\text{SEC}}}^T]^T = \mathbf{W} \sqrt{\text{diag}\{\mathbf{p}\}}, \quad (2.14)$$

where $\mathbf{U}_i \in \mathbb{C}^{N_{\text{ANT}} \times G}$ is the part of the matrix \mathbf{U} relating to the sector i and all G UEs.

2.8 Inter-cluster interference estimation

CoMP transmission strategies are only allowed between eNBs belonging to the same cluster, whereas eNBs belonging to different clusters are not coordinated and thus are potential interference sources. Hence, while a given transmission point can enhance the communication within a given cluster, this same transmission point probably will harm another cluster depending on the leakage.

In the CoMP processing, the intra-cluster interference z_j^{intra} can be perfectly controlled. On the other hand, the inter-cluster interference z_j^{inter} is hard to be perfectly known, but it can be estimated. It is known that each UE is able to generate an estimate for the inter-cluster interference z_j^{inter} . According to the 3GPP [5] an interference measure received by the eNB should be used in order to perform link adaptation. Hence the accuracy of inter-cluster interference estimation directly affects the system throughput. This mechanism seeks to explore whether it is possible to further improve the inter-cluster interference estimation and to improve system throughput. However, no definition of this measure is provided in 3GPP [5].

Here, an approach for inter-cluster interference estimation is considered in which the link adaptation can be significantly improved. In the following, it is defined a simple interference estimation mechanism, taking the interference measurement capability of the UE into account. Since the information necessary to calculate the inter-cluster interference z_j^{inter} is available, it is employed an approximation based on exponential filtering. Thus, the inter-cluster interference estimate $\hat{z}_j^{\text{inter}}(t)$ of UE j at TTI t is modeled by [10, 37, 38]

$$\hat{z}_j^{\text{inter}}(t) = \alpha \cdot z_j^{\text{inter}}(t-1) + (1-\alpha) \cdot z_j^{\text{inter}}(t-1), \quad (2.15)$$

where:

- ▶ $\hat{z}_j^{\text{inter}}(t-1)$ is the last interference estimate;
- ▶ $z_j^{\text{inter}}(t-1)$ is the interference obtained from the last TTI $t-1$;
- ▶ and α is a factor that controls the oblivion of the exponential filter.

Please note that such an inter-cell interference estimate \hat{z}_j^{inter} should be more precise for schedulers that select the same UEs on the same PRBs for several consecutive TTIs.

2.9 Link-to-system interface

In the following, the link-to-system interface is addressed, which is used to map the system-level metrics, such as SINR into link-level performance figures, such as Block Error

Rate (BLER). First, the RRA schedules a set \mathcal{G} of UEs to receive data. Then, based on the available CSI, the link adaptation will set the data transmission rate of each radio link in order to provide the best possible quality through the use of a suitable Modulation and Coding Scheme (MCS). A high order modulation scheme transports more bits per symbol and allows higher throughputs at the cost of correspondingly higher SINR values at the UE. The throughput in a transmission is determined by the chosen MCS and the BLER associated to a transmission depends on the instantaneous channel quality. Hence, the link adaptation technique will try to adapt the Modulation and Coding Scheme in order to maximize the throughput or reduce the BLER for each transmission, handling variations in the instantaneous radio link quality [49].

For the sake of simplicity, the MCS for each PRB is adapted independently, likewise the RRA strategies work. The SINR measured for a given link using (2.5) is employed to determine the BLER for the block of data sent on each PRB. The BLER is used instead of the Bit Error Rate (BER), since the PRB is composed by several OFDMA symbols.

The curves of BLER are obtained from [49], which plots the $\text{BLER}(\gamma, \text{MCS})$ as a function of the Signal to Noise Ratio (SNR) γ perceived by a given UE and the MCS employed on the link. On their turn, the curves of average throughput are derived from the BLER function for each MCS, as follows

$$\bar{r}(\gamma, \text{MCS}) = (1 - \text{BLER}(\gamma, \text{MCS})) \cdot r(\text{MCS})L. \quad (2.16)$$

where:

- ▶ $r(\text{MCS})$ is the number of bits/symbol supported for a given MCS;
- ▶ and $L = N_{SYM}N_{SUB}$ is the total number of symbols per block of the PRB.

Aligned with LTE, a set of fifteen MCSs are available for link adaptation. Figure 2.9 shows the BLER and the average throughput curves available for link adaptation, from MCS-1 (leftmost) to MCS-15 (rightmost).

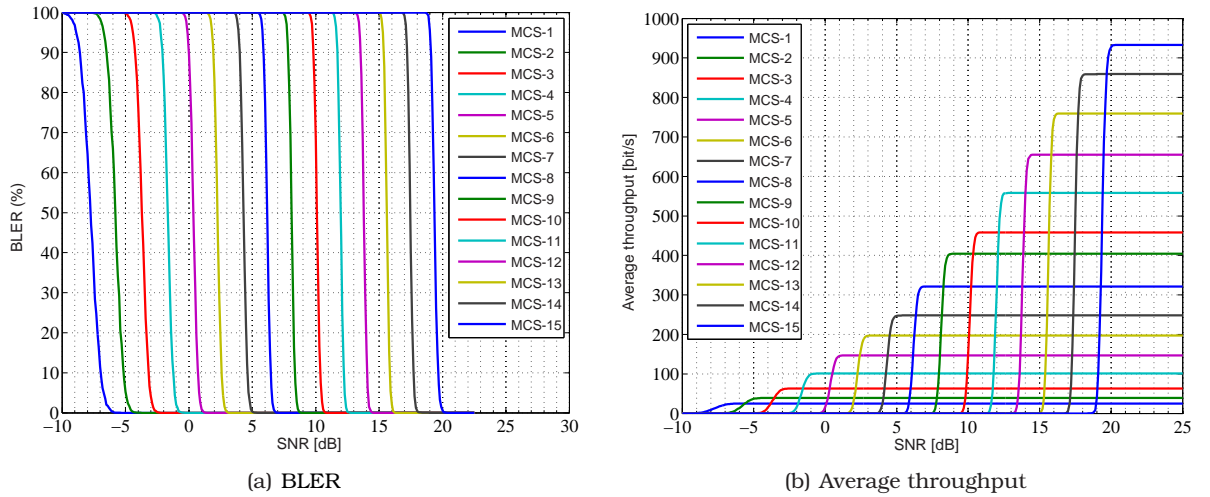


Figure 2.4: Curves of link-level used for link adaptation.

In each transmission, the link adaptation is determined such that the MCS that yields the maximum average throughput $\bar{r}(\text{MCS})$ is selected according to

$$\text{MCS}^* = \arg \max_{\text{MCS}} \{\bar{r}(\gamma, \text{MCS})\}. \quad (2.17)$$

By (2.17), SINR thresholds can be found for each MCS, i.e., minimal SINR values required to use each MCS. Regarding the available modulation schemes in 3GPP described in [23],

which take into account 4-, 16- and 64-Quadrature Amplitude Modulation (QAM), as well as the code rate also defined in [23], which is between 1/13 and 1, the MCSs considered in this dissertation and its respective SINR thresholds are summarized in Table 2.1.

Table 2.1: SINR thresholds for link adaptation.

MCS	Modulation	Code rate [*1024]	Rate [Bits/symbol]	SINR threshold [dB]
MCS-1	4-QAM	78	0.1523	-6.2
MCS-2	4-QAM	120	0.2344	-5.6
MCS-3	4-QAM	193	0.3770	-3.5
MCS-4	4-QAM	308	0.6016	-1.5
MCS-5	4-QAM	449	0.8770	0.5
MCS-6	4-QAM	602	1.1758	2.5
MCS-7	16-QAM	378	1.4766	4.6
MCS-8	16-QAM	490	1.9141	6.4
MCS-9	16-QAM	616	2.4062	8.3
MCS-10	64-QAM	466	2.7305	10.4
MCS-11	64-QAM	567	3.3223	12.2
MCS-12	64-QAM	666	3.9023	14.1
MCS-13	64-QAM	772	4.5234	15.9
MCS-14	64-QAM	873	5.1152	17.7
MCS-15	64-QAM	948	5.5547	19.7

Note that UEs with an SINR value below -6.2 dB do not receive data because the BLER would be too high and the resource probably wasted. This value was determined in order to obtain a BLER of 1 % on transmissions with MCS-1. When a scheduled UE does not have a high enough estimated SINR for its transmission to occur, it is considered to be allocated with MCS-0, i.e., rate zero, and the transmission for this UE is not considered.

In CoMP systems, the link adaptation selects a proper MCS for each link of UEs in \mathcal{G} based on the involved CoMP processing, the available CSI, and estimated inter-cluster interference \hat{z}_j^{inter} values [14]. It should be noted that the link adaptation can be affected by imperfections on the CSI \hat{H} as well as random variations on inter-cluster interference level z_j^{inter} perceived by each UE j . Thus, the selected MCS can be too conservative or too aggressive for the prevailing channel conditions at the time of transmission, resulting in waste of resources or too many errors. In either case, the system throughput will fall below what is achievable with perfect CSI z_j^{inter} and accurate inter-cluster interference estimate \hat{z}_j^{inter} .

In order to capture packet reception errors and their impact on the system throughput, the SINR and the BLER are employed as link quality measurements. Consider a transmission for the UE j , where the SINR $\hat{\gamma}_j$ estimated and used for link adaptation is determined using (2.5), such that it uses a certain MCS. First, by taking into account the estimated inter-cluster interference \hat{z}_j^{inter} , it is determined the $\text{BLER}(\hat{\gamma}_j, \text{MCS})$ for that transmission based on the curves of BLER presented in Figure 2.4(a). After that, a random test is performed in order to determine whether the transmitted data has been successfully received or not by the UE j .

2.10 System-level simulation

This section provides an initial performance assessment of downlink CoMP. Initially, it should be noted that the evaluations are done based on relatively ideal assumptions. The assessment should thus be seen as an indication of the potential of CoMP as a technological component of LTE-Advanced. Later, at the end of Chapter 4, performance evaluations are provided considering non-ideal conditions regarding CSI.

Computer simulation is taken as an important tool to analyze and assess the performance of complex systems such as CoMP. Thus, a system-level simulation tool based on the system model described in this chapter has been implemented. It is oriented to embrace

features aligned with the 3GPP LTE-Advanced architecture [2] and it is used to investigate the performance of RRA strategies. The models and assumptions are aligned with the 3GPP urban micro-cell environment and the SCM is used [47].

In the following, the most relevant simulation parameters and the performance metrics used to evaluate the performance achieved by the RRA strategies are introduced in Section 2.10.1.

2.10.1 Simulation parameters and performance metrics

The main parameters considered in the simulations are summarized in Table 2.2.

Table 2.2: Simulation parameters.

Parameter	Symbol	Value	Unit	Remark
Cellular scenario				
Number of clusters	C	7	–	w/ wrap-around [7, 10, 25]
Number of eNBs per cluster	B	7	–	three-sectorized cells
Number of sectors per cluster	–	21	–	3 sectors/cell
Number of antennas per eNB	N_{eNB}	1	–	–
Number of antennas per cluster	M	21	–	–
Number of antennas per UE	N_{UE}	1	–	–
Site-to-site distance	–	500	m	$3/2 \cdot$ radius of the sector
Minimum distance between eNB and UE	–	35	m	–
Average UEs speed	v	3	km/h	–
OFDMA				
Carrier frequency	f_c	2	GHz	–
System bandwidth	BW	1.92	MHz	–
Subcarrier spacing	Δf_c	15	kHz	–
Number of symbols per TTI	N_{SYM}	14	–	–
Number of subcarriers per PRB	N_{SUB}	12	–	180 kHz bandwidth
Number of PRBs	N_{PRB}	6	–	–
Transmit power per PRB	P_{PRB}	29.4	dBm	–
Required SNR at the sector border	–	-6.2	dB	–
Antenna pattern	$A(\theta^\circ)$	$-\min\left\{12\left[\frac{\theta^\circ}{70^\circ}\right]^2, 20\right\}$	dB	cf. [44]
Propagation				
Path loss model	–	$35.7 + 38 \log_{10}(d)$	dB	cf. [44]
Shadowing standard deviation	σ	8	dB	–
Spatial channel model	–	3GPP SCM	–	urban-micro scenario, NLOS
Algorithms				
Spatial precoding	–	ZF	–	cf. [50]
Power allocation	–	EPA	–	–
Link adaptation	–	–	–	Based on CSI and inter-cluster interference, MCSs according to [23]
Exponential filter constant	α	$[0, 0.1, \dots, 1]$	–	–
Simulation				
Number of snapshots	–	10	–	–
Snapshot duration	–	1	s	–
Effective TTI duration	–	1	ms	–
User distribution	–	Uniform	–	–
Traffic model	–	Full buffer	–	–
Offered load	–	2, 4, 6, and 8	UEs/sector	–

Basically, the simulation events are organized in snapshots, during which path loss and shadowing are assumed to remain constant for all the UEs while the time variations of fast fading are considered. The dynamics of fast fading can be captured by assuring that each snapshot takes at least 1 s, which is longer than 10 times the channel coherence time for the simulation parameters. In order to capture the impact of long term propagation effects on the system performance, several snapshots are simulated.

In the following, the metrics considered to evaluate the performance of the RRA strategies investigated in CoMP systems are described:

- System spectral efficiency measures the amount of bits per time-frequency resource and per sector. It does not take into account UEs left out on the scheduling;

- ▶ Offered load means the number of UEs physically present in a sector. Due to multi-user diversity, the larger the offered load, the larger the system spectral efficiency;
- ▶ Average inter-cluster interference power measures the amount of interference from external clusters. It allows to evaluate the efficiency of interference management;
- ▶ Cumulative Distribution Function (CDF) of the BLER observed by UEs in system;
- ▶ Probability Distribution Function (PDF) of the usage of the MCSs in all transmissions;
- ▶ PDF of the group size gives the distribution of the number of UEs in a cluster. It provides a general view of the dynamic adaptation of the group size.

UE spatial grouping

3.1 Introduction

For Long Term Evolution (LTE) systems, finding an optimum Physical Resource Block (PRB) reuse is a complex task because of the interdependencies between resource assignment and power allocation that arise when determining which User Equipments (UEs) should share a same PRB. Moreover, the high number of PRBs and UEs within a cluster gives high dimension to the Radio Resource Allocation (RRA) problem and makes prohibitively time-consuming finding its optimum solution. Therefore, one concentrates here on studying heuristics for solving the intra-cell resource reuse problem, which intend to be simple, effective, and to avoid excessive and non-linear operations.

In this chapter, the focus is more specifically on the RRA subproblem of determining a suitable set of UEs to spatially reuse a given PRB within a cluster having as objective the maximization of the total system throughput. Herein, UEs spatially compatible are those ones which can efficiently share the same PRB in space within each cluster using Space Division Multiple Access (SDMA) [6].

The Coordinated Scheduling (CS) and Joint Processing (JP) approaches introduced in Section 1.2.1 are considered here. In the CS case, one obtains an adaptive resource reuse scenario in which the interference is coordinated among the Antenna Ports (APs) from the same cluster. In the JP case, the multiple APs work as a distributed antenna array, so that the set of served UEs is considered as an SDMA group whose signals are separated in space using precoding, as it is usual in Multi-User (MU)-Multiple Input Multiple Output (MIMO) scenarios. For each Coordinated Multi-Point (CoMP) transmission approach, different Evolved Node Bs (eNBs) within a cluster cooperate with each other and exchange Channel State Information (CSI) through a fast backhaul in order to adjust their RRA strategies and mitigate the effects of intra-cluster interference.

The rest of this chapter is organized as follows. Section 3.2 presents a particular formulation of the UE grouping problem introduced in Section 1.4 for both CS and JP transmission approaches. RRA strategies employed to solve the UE spatial grouping problem observing the CS and JP transmission approaches are described in Sections 3.3 and 3.4, respectively. Finally, a brief summary of the chapter is provided in Section 3.5.

3.2 Problem statement

In this section, the RRA problem considered in this chapter is discussed. As stated before, the focus in this dissertation is on the RRA subproblem of spatially reusing PRBs within a

cluster as to maximize the system throughput such that the problem to be solved here is the choice of a set $\mathcal{G} \subset \{1, 2, \dots, J\}$ of UEs spatially compatible, i.e., which can efficiently share the same PRB in space. However, RRA in frequency, time, and space is a complex task in such systems due to the large number of degrees of freedom to be handled. Here, the assignment decisions in each PRB are taken independently, so that information about scheduling in some PRB is not used in each other. It makes the RRA problem less complex.

When observing the CS approach, UE scheduling decisions are made with coordination among cells within a cluster. This approach determines which PRBs should be used by which AP-UE links. Herein, each AP is assigned to only one UE such that $w_{j,m} = 1$ if the UE j is being served by AP m and $w_{j,m} = 0$ otherwise. So, a variable intra-cell resource reuse is implemented. In this approach, the power allocated to each UE j , as well as the power that the AP m will transmit, is the maximum transmit power allocated to each PRB, i.e., $p_j = P_{\text{PRB}}$.

In the CS approach, the general problem consists in maximizing the utility function $U(\mathcal{G}, \mathbf{U})$ for a given cluster regarding a certain RRA described by the UEs' group \mathcal{G} and precoding matrix \mathbf{U} . Here, the utility function represents the throughput of a cluster. This problem can be formulated as

$$\{\mathcal{G}^*, \mathbf{U}^*\} = \arg \max_{\{\mathcal{G}, \mathbf{U}\}} \{U(\mathcal{G}, \mathbf{U})\}, \quad (3.1a)$$

subject to

$$\mathcal{G} \subset \{1, 2, \dots, J\}, \quad (3.1b)$$

$$|\mathcal{G}| \leq M, \quad (3.1c)$$

$$\sum_{1 \leq m \leq M} w_{m,j} \leq 1, \quad 1 \leq j \leq J, \quad (3.1d)$$

$$\|\mathbf{U}_i\|_{\text{FRO}}^2 \leq P_{\text{PRB}}, \quad 1 \leq i \leq M. \quad (3.1e)$$

where constraint (3.1b) imposes that only UEs belonging to the cluster can be served by a RRA strategy. Constraint (3.1c) limits the total number of UEs selected to the number of APs in the cluster. Constraint (3.1d) limits the number of APs selected for coordinated transmission to a given UE. As it was introduced in Section 2.7, in the CS approach the precoding vector \mathbf{w}_j of the UE j becomes a sector selection vector, whose entries $w_{m,j}$, $\forall 1 \leq m \leq M$, are binary variables indicating whether sector m sends data to the UE j . Finally, per-sector power constraints in (3.1e) limit the total transmit power of each AP within the cluster.

When observing the JP transmission approach, multiple APs within a cluster cooperate in jointly transmitting precoded data symbols to multiple UEs such that desired signals overlap coherently and the intra-cluster interference is minimized. The CSI available is used to design individual transmit precoding vectors \mathbf{w}_j for each scheduled UE j . Therefore, the cluster of the CoMP scenario can be seen as a distributed MU-MIMO system using APs as elements of a distributed antenna array.

In the JP approach, the general problem consists in maximizing the utility function $U(\mathcal{G}, \mathbf{U})$ for a given cluster regarding a certain RRA described by the UEs group \mathcal{G} and precoding matrix \mathbf{U} . Here, the utility function also represents the throughput of a cluster. This problem can be formulated as

$$\{\mathcal{G}^*, \mathbf{U}^*\} = \arg \max_{\{\mathcal{G}, \mathbf{U}\}} \{U(\mathcal{G}, \mathbf{U})\}, \quad (3.2a)$$

subject to

$$\mathcal{G} \subset \{1, 2, \dots, J\}, \quad (3.2b)$$

$$|\mathcal{G}| \leq M, \quad (3.2c)$$

$$\|\mathbf{U}_i\|_{\text{FRO}}^2 \leq P_{\text{PRB}}, \quad 1 \leq i \leq M. \quad (3.2d)$$

where constraint (3.2c) limits the total number of UEs selected to the number of APs in cluster. For the JP approach, the power allocation is conducted for the whole cluster by considering a sum-power constraint on all sectors together as expressed in (2.13), however, the effective transmit power of each sector should be smaller than or equal to P_{PRB} . Thus, constraint (3.2d) limits the total transmit power of each AP within the cluster. As it can be noted, the formulation in (3.2) considers a precoding matrix \mathbf{U} such that it is quite general and can be extended straightforwardly to cases where RRA strategies perform separately precoding and power control. On the one hand, constraint (3.2d) on power usage might hinder finding the optimal RRA solution. On the other hand, it could be alleviated when regarding sub-optimal solutions.

As cooperation among different clusters was not assumed, both problems in (3.1) and (3.2) were formulated for a single cluster. From the CoMP system perspective, the individual maximization of utility function in a cluster still leads to a sub-optimal solution for the multi-objective problem of the overall multi-cell scenario, since the interactions among clusters are ignored. However, the complexity issues mentioned for both problems are expected to become even more significant for this multi-objective problem.

Even so, both problems (3.1) and (3.2) are hard-to-solve combinatorial problems and an optimum solution to these problems might be too complex for application in a practical CoMP system. Indeed, the general problem of allocating resources in a CoMP system to maximize the system throughput is a very complex optimization problem [51]. It involves subproblems like resource assignment, power allocation, antenna selection, resource reuse, UE spatial grouping, among others [6]. The optimum solution of some of these subproblems may also be quite complex, requiring the use of efficient suboptimal solutions. From now on, the study will be restricted to efficient suboptimal solutions.

3.3 Coordinated scheduling approach

Since the CSI is available among cooperating cells, in this approach the problem (3.1) can be seen as a dynamic channel allocation problem [5]. Having knowledge about all links associated with their controlled APs, each cluster can estimate the intra-cluster interference induced by the PRB reuse. Then, scheduling algorithms can be used to determine dynamically which AP-UE links can simultaneously use the same PRB. This scenario provides flexibility to decide if all APs within each cluster will be used or if some of them will be turned off to avoid the inter- and intra-cluster-interference and reduce the error probabilities.

Due to perfect knowledge of the intra-cluster interference, the CoMP system has an improved link adaptation in comparison to the conventional system. In the conventional system, the UE estimates the inter-cell interference due to the transmission of surrounding APs. In a CoMP system, the UE only estimates the inter-cluster interference while the interference caused by the APs within a same cluster is accurately determined. In this way, the information of interference used by link adaptation can be separated in two components: estimate for the inter-cluster interference, which is measured and reported by each UE, and knowledge of the intra-cluster interference, which is accurately determined.

In this approach, different amounts of information available for RRA in a cluster are considered. Initially, let a cluster in which each eNB performs individual RRA with perfect knowledge about the intra-cluster interference, while the UEs are able to estimate the inter-cluster interference. In this scenario, both interference-aware and interference-unaware schedulers are observed. While the former selects UEs without taking into account information on interference levels, the latter considers both channel quality and estimates for the inter-cluster interference. After that, the level of cooperation is then increased by performing joint multi-cell scheduling. Thus, two kinds of scheduling algorithms are classified: individual single-cell scheduling and joint multi-cell scheduling. The former assigns APs within a cluster individually one-by-one and uses the perfect knowledge about the intra-cluster interference to achieve an enhanced link adaptation. The latter performs decisions of scheduling with coordination among the transmissions of different APs within a cluster.

In the following, the single-cell scheduling and joint multi-cell scheduling are considered in Sections 3.3.1 and 3.3.2, respectively. The performance of RRA strategies in the conventional system is evaluated in Section 3.3.3. Finally, the performance of the CS approach for single-cell scheduling and multi-cell scheduling is analyzed in Section 3.3.4.

3.3.1 Individual single-cell scheduling

Single-cell schedulers assign each AP to a UE on each PRB and so lead to full resource reuse, assigning APs within a cluster individually, one-by-one, so that no actual information about other APs of the cluster is used for scheduling. For these schedulers, all PRBs are reused at all APs, unless no UE associated with the AP perceives a link quality high enough to support communication (see Section 2.9).

For comparison purposes, the single-cell schedulers are also employed in the conventional system, in which an estimate of the inter-cell interference perceived by each UE can or not be available. When it is available, it is important to highlight that the interference due to the cluster is viewed as a part of the estimate of total inter-cell interference. Although the knowledge about the transmissions is not fully available, the link adaptation will use a significant estimate for the inter-cell interference. Moreover, when it is not available, the link adaptation will be optimistic being based only on the Signal to Noise Ratio (SNR) and the system performance will be degraded. The operation of single-cell schedulers in the conventional system is similar to its operation in a CoMP system.

Three kinds of single-cell schedulers for the CS approach are considered:

- ▶ Random (RND) scheduler: this scheduler performs random scheduling;
- ▶ Maximum Gain (MaxGain) scheduler: this scheduler performs interference-unaware scheduling;
- ▶ Maximum SINR (MaxSINR) scheduler: it is based on interference-aware scheduling;

In the following, the RND, MaxGain and MaxSINR schedulers are described for the CoMP system, as well as an extension of each one for the conventional scenario is discussed.

3.3.1.1 Random

This scheduler selects UEs within the sector of a given AP in random manner, i.e., each UE within the sector has equal chance to be scheduled. It is important to highlight that due to random scheduling many UEs that don't contribute for the rate maximization will be selected.

For this scenario, an AP uses a PRB unless no UE associated with this AP perceives a link quality high enough to support communication (see Section 2.9).

In order to provide a better description of the RND scheduler, Algorithm 3.1 presents it in algorithmic form.

Algorithm 3.1 RND scheduler for CS.

```

for each PRB do
  for each cluster do
    for each AP do
      Selects a link within the sector at random with uniform distribution
    end for
    for each scheduled UE do
      Calculates the perceived intra-cluster interference
      Performs link adaptation
    end for
  end for
end for

```

As it can be observed, there is a loop over the PRBs and a loop over the APs in Algorithm 3.1, which are thus assigned one-by-one. In other words, for each resource allocation the RND scheduler selects a link at random on each PRB and AP and then performs link adaptation.

3.3.1.2 Maximum gain

It is well-known that, when no interference is considered, the system throughput is maximized by assigning each PRB at each AP m to the UE j^* with the highest channel gain [27]. For each PRB and AP, the MaxGain scheduler assigns the UE j with the highest channel gain according to

$$j^* = \arg \max_j \{ |h_{j,m}| \}. \quad (3.3)$$

As it can be seen in (3.3), this scheduler performs interference-unaware scheduling by always selecting the UE with the highest channel gain on each PRB and AP.

In order to provide a better description of the MaxGain scheduler, Algorithm 3.2 presents it in algorithmic form.

Algorithm 3.2 MaxGain scheduler for CS.

```

for each PRB do
  for each cluster do
    for each AP do
      Selects the link with the highest channel gain
    end for
    for each scheduled UE do
      Calculates the perceived intra-cluster interference
      Performs link adaptation
    end for
  end for
end for

```

As it can be observed in Algorithm 3.2, the MaxGain scheduler treats each cell as an independent cell (see Section 2.3) such that no information about other APs of the cluster is used. For each resource allocation, the MaxGain scheduler selects the link with the highest channel gain on each PRB and AP, and then performs link adaptation. The difference to the MaxGain scheduler applied in the conventional scenario relies on the usage of accurate information about intra-cluster interference for link adaptation. This additional information shall not change substantially the UEs scheduled on each PRB.

3.3.1.3 Maximum SINR

The MaxGain scheduler has no information about interference. When intra-cluster interference is considered, this solution is expected to provide higher system throughput,

since it still tends to select UEs close to the APs. For each PRB and AP, the MaxSINR scheduler assigns the UE j with the maximum Signal to Interference-plus-Noise Ratio (SINR) value according to

$$j^* = \arg \max_j \{\hat{\gamma}_j\}. \quad (3.4)$$

From (3.4), this interference-aware scheduler takes advantage of the CSI for scheduling UEs with high channel gains like the MaxGain scheduler, as well as it uses the estimate of intra-cluster interference for choosing the UEs with best link quality. However, even if the information about the CSI and estimate of the inter-cluster interference for all UEs within a cluster is available, determining the optimal scheduling would still be difficult because the number of APs transmitting on each PRB can change interference.

In order to provide a better description of the MaxSINR scheduler, Algorithm 3.3 presents it in algorithmic form.

Algorithm 3.3 MaxSINR scheduler for CS.

```

for each PRB do
  for each cluster do
    for each AP do
      Selects the link with the highest SINR
    end for
    for each scheduled UE do
      Calculates the perceived intra-cluster interference
      Performs link adaptation
    end for
  end for
end for

```

3.3.2 Joint multi-cell scheduling

The joint multi-cell scheduling makes use of the CSI to schedule a certain number of UEs while coordinating interference among AP-UE links, and therefore implements a dynamic RRA. For this approach, it is considered an interference-aware scheduler that adapts the number of APs transmitting in each PRB to provide a trade-off between cluster throughput and intra-cluster interference, which is termed here Best Rate Allocation (BRA).

The BRA scheduler sequentially increases the number of transmitting APs until the intra-cluster interference causes the cluster throughput to decrease. It is based on a greedy search-tree logic that tries to find a close to optimum solution without checking all the possible solutions [10]. The BRA scheduler starts by scheduling the AP-UE link with highest channel gain within the whole cluster. Then it calculates the throughput by scheduling each available AP-UE link on other APs together with the previously scheduled link. The scheduled link is the one which leads to the highest throughput and, in case of ties, the link with highest channel gain is chosen. This procedure continues adding new links whenever the cluster throughput increases. Otherwise, it finishes and goes to the next PRB. Algorithm 3.4 presents an algorithmic description of the BRA scheduler.

In Algorithm 3.4, for each PRB and cluster, the BRA scheduler selects the link with the highest channel gain and checks if the sum of the throughputs of all the scheduled links of the cluster decreased. After that, it selects the new link that maximizes the sum of the link throughputs by testing all possibilities. Then, it performs link adaptation and estimates the sum of the throughputs of scheduled links. Finally, the BRA scheduler removes the last scheduled link. This is necessary because the last scheduled link was the one that decreased the sum throughput. The solution provided by this algorithm should be close to optimal. But this good performance comes at the expense of a high number of iterations that make this

Algorithm 3.4 BRA scheduler for CS.

```

for each PRB do
  for each cluster do
    Selects the AP-UE link with highest channel gain
    Estimates cluster throughput
    while cluster throughput is increasing do
      Selects the AP-UE link with highest channel gain
      Estimates cluster throughput
      Performs link adaptation
    end while
    Removes last AP-UE link
  end for
end for

```

much slower than the MaxGain and MaxSINR schedulers.

3.3.3 Performance in the conventional scenario

In the following, the conventional scenario is simulated for comparison purposes. For calibration purposes, Section 3.3.3.1 presents the adjustment of the inter-cell interference estimation scheme described in Section 2.8, which will be used by other RRA strategies in the CoMP scenario, and Section 3.3.3.2 presents the performance of RRA strategies considered for rate maximization in the conventional scenario introduced in Section 3.3.1.

3.3.3.1 Inter-cell interference measurement scheme

In this section, the performance of the exponential filtering is evaluated over RRA strategies for the conventional scenario with different characteristics of UEs scheduling (see Section 2.8 for more details). For this purpose, the RND and MaxSINR schedulers are chosen. The former tends to schedule a varying set of UEs and the latter tends to choose the same UEs to receive data.

Figure 3.1 shows the Cumulative Distribution Function (CDF) of Block Error Rate (BLER) obtained by the RND and MaxSINR schedulers in the conventional scenario for a range of the parameter α , which is a factor that controls the oblivion of the exponential filter.

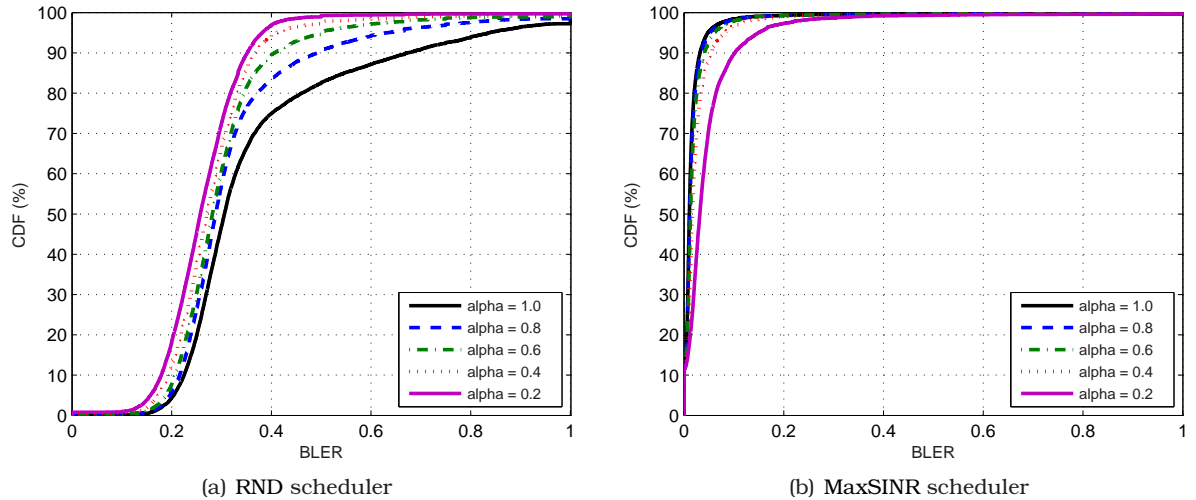


Figure 3.1: CDF of BLER varying the parameter α of the exponential filter.

From Figure 3.1(a) the RND scheduler has the lowest levels of BLER for $\alpha = 0.2$ while from Figure 3.1(b) the MaxSINR scheduler presents the best performance for $\alpha = 1$. The BLER of each algorithm has different behaviors when varying α . The RND scheduler has its best performance for a more conservative estimate of inter-cell interference, while the best performance of MaxSINR scheduler is for the more aggressive estimate of inter-cell interference, i.e., the last estimate. Being the inter-cell interference estimate predictable

it makes sense to believe that Maximum Rate (MR) algorithms like the MaxSINR scheduler select the same UEs for scheduling.

It was seen that the gains of using exponential filtering increased as the transmissions got less random being the last estimate of inter-cell interference adequate for MR algorithms. As the focus here is kept on RRA strategies for rate maximization, $\alpha = 1$ is adopted in the rest of this dissertation. Thus, regarding the knowledge assumed about the inter-cell interference in the CoMP scenario for a given UE and PRB, it is used the last measured interference value as the inter-cell interference estimate of the current Transmission Time Interval (TTI).

3.3.3.2 RRA in conventional scenario

In the following, the performance for the RRA strategies introduced in Section 3.3.1 are evaluated in a conventional system. The MaxGain and MaxSINR schedulers, which perform interference-unaware and interference-aware scheduling for rate maximization, respectively, and the RND scheduler as well as the MaxGain scheduler with interference-unaware link adaptation, which is termed by MaxGain-blind scheduler, are considered.

Figure 3.2 shows the system spectral efficiency of RRA strategies considered in the conventional scenario.

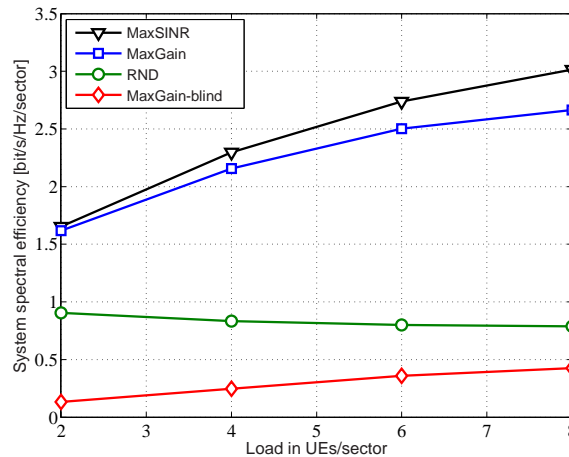


Figure 3.2: System spectral efficiency achieved by single-cell scheduling algorithms in the conventional scenario.

As it can be seen in Figure 3.2, the higher the load in UEs/sector is, the lower the system spectral efficiency of the RND scheduler is and the higher the system spectral efficiency of MR algorithms is. The performance of MaxGain-blind scheduler is compromised by the lack of an estimate of inter-cell interference for link adaptation, as it would happen to any of the other algorithms.

Besides that, the higher the load in UEs/sector is, the higher the performance gain of the MaxSINR scheduler becomes in comparison to MaxGain scheduler. However, a performance gain was only possible with high loads. At the lowest load in UEs/sector, both schedulers have the same performance.

Figure 3.3 presents the CDF of BLER and the Probability Distribution Function (PDF) of the usage of the Modulation and Coding Schemes (MCSs) for the MaxSINR and MaxGain schedulers.

As it can be seen in Figure 3.3, for high loads, the MaxSINR scheduler has lower BLER as well as higher usage of higher MCSs than the MaxGain scheduler. It happens because interference-aware scheduling, which is the case of the MaxSINR scheduler, takes advantage of availability of the estimate of the inter-cell interference to better map the link quality perceived by each UE.

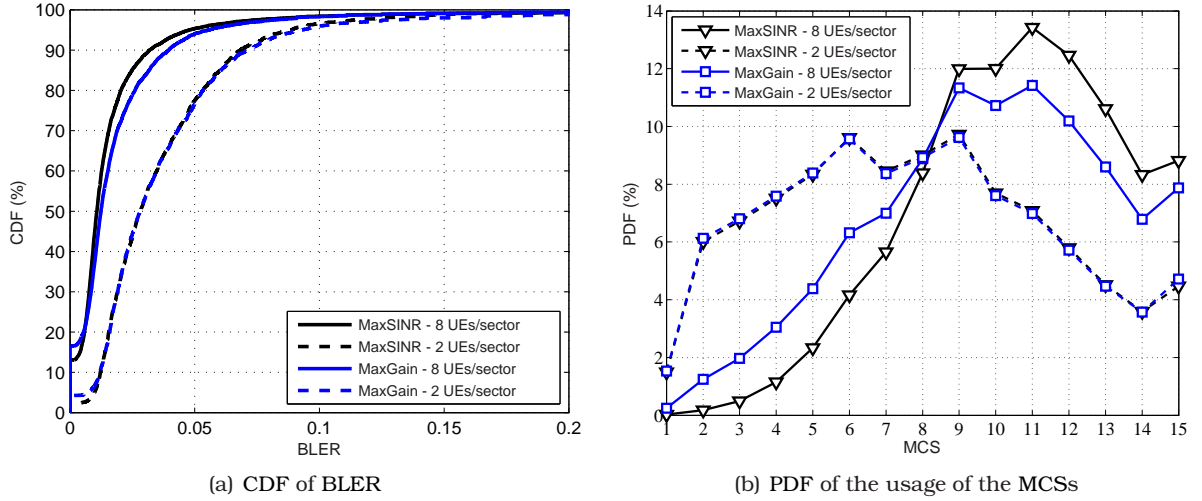


Figure 3.3: CDF of BLER and PDF of the usage of the MCSs presented by single-cell scheduling algorithms in the conventional scenario.

From Figure 3.3(a) and Figure 3.3(b), both MaxSINR and MaxGain schedulers have the same performance for low loads, as observed in Figure 3.2. From Figure 3.3(a) and Figure 3.3(b), it may be seen that it occurs because both algorithms have approximately the same curves of BLER and percentage of use of MCSs. As the MaxGain scheduler selects UEs with the highest channel gains and also with the lowest inter-cell interference estimates as the MaxSINR scheduler, for low UEs load both algorithms tend to select the same UEs.

3.3.4 Performance with coordinated scheduling

For CoMP schemes based on interference coordination, performance evaluation of RRA strategies introduced in Section 3.3 have been conducted considering different amounts of information. Initially, it is assumed a CoMP scenario which just considers the accurate knowledge of the intra-cluster interference to perform a better choice of MCSs. Afterwards, it is increased the level of coordination using the CSI to determine the intra-cluster interference and to perform adaptive UE spatial grouping.

RRA strategies for single-cell scheduling and multi-cell scheduling are presented in Section 3.3.4.2 and in Section 3.3.4.2, respectively.

3.3.4.1 Single-cell scheduling

In this section, RRA strategies for the CoMP scenario that perform scheduling independently by all sectors, as in the conventional scenario, are evaluated, but the inter-cluster interference that will occur during the associated data transmission is determined in a cooperative manner in order to improve the link adaptation process.

Figure 3.4 shows the system spectral efficiency achieved by RRA strategies considered for the CoMP scenario and the CDF of BLER for the MaxSINR scheduler in both CoMP and conventional scenarios.

As it can be seen in Figure 3.4(a), an enhanced link adaptation does not have a significant contribution to increase the spectral efficiency of the CoMP system when RRA strategies for rate maximization are considered. Spectral efficiency gains are only possible for the RND scheduler, which has its performance compromised due to the difficulty of interference estimation mechanisms when scheduled UEs change constantly.

From Figure 3.4(b), the majority of UEs experience lower BLER values in the CoMP scenario than in the conventional scenario, especially for low loads in UEs/sector. Therefore, even though the single-cell scheduling does not add significant gains in spectral efficiency to the

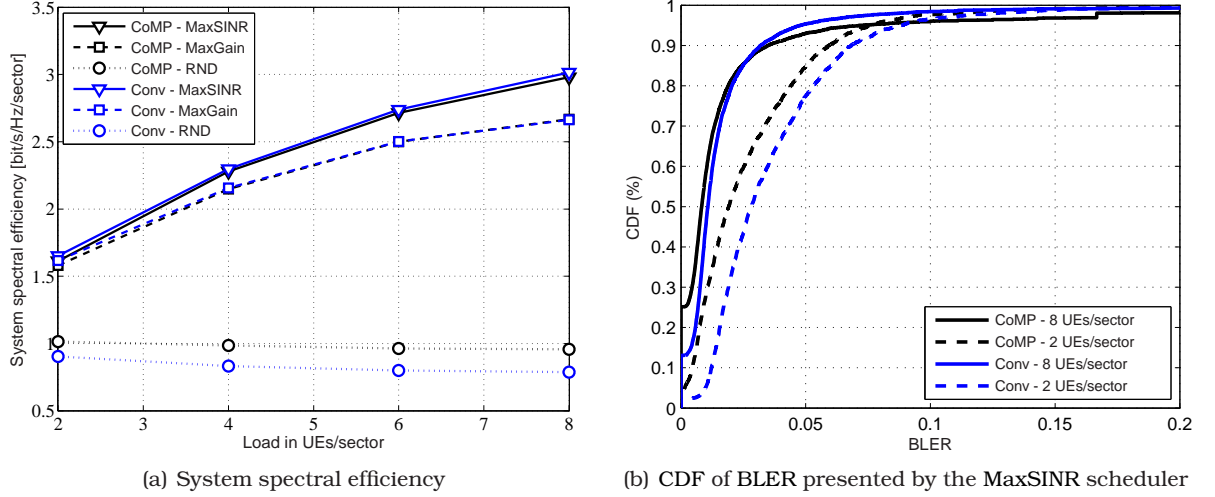


Figure 3.4: System spectral efficiency and CDF of BLER presented by single-cell scheduling algorithms in the both conventional and CoMP scenarios.

CoMP scenario it contributes to a better performance of link adaptation; in addition to not taking advantage of the availability of CSI for performing CS.

3.3.4.2 Joint multi-cell scheduling

In this section, the performance of the BRA scheduler, an interference-aware algorithm of joint multi-cell scheduling that effectively makes use of coordinated scheduling, is evaluated (see Section 3.3.2 for more details about this scheduler).

In the following, performance is evaluated for the best RRA strategy in the conventional scenario, i.e., MaxSINR scheduler, and the RRA strategy considered for joint multi-cell scheduling, i.e., BRA scheduler. Figure 3.5 shows the system spectral efficiency and the PDF of the usage of the MCSs for both RRA strategies and both scenarios.

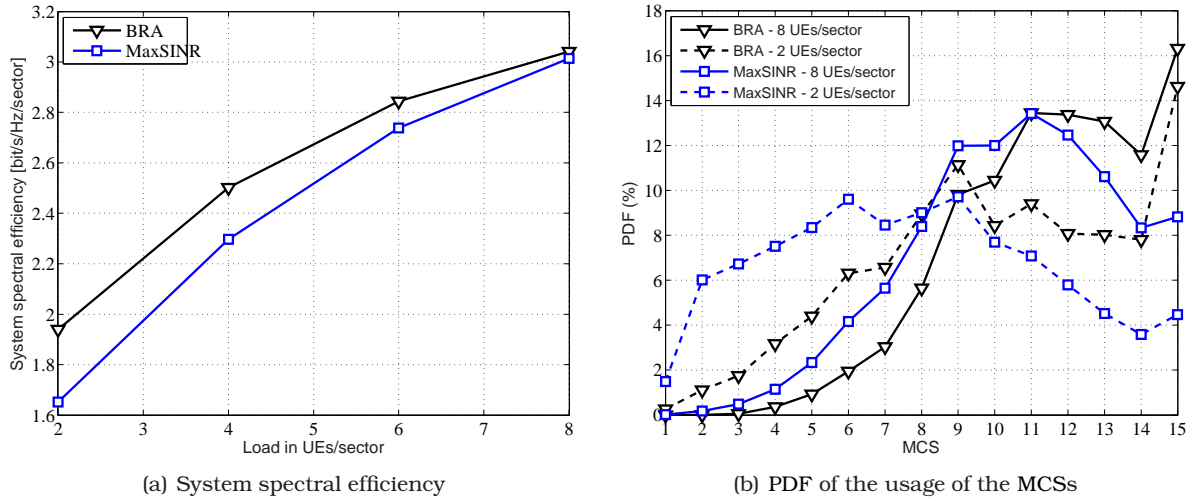


Figure 3.5: System spectral efficiency and PDF of the usage of the MCSs achieved by the joint multi-cell scheduling algorithm considered for the CoMP scenario.

It is shown in Figure 3.5(a) that the BRA scheduler has a gain in system spectral efficiency, especially for low loads in UEs/sector, clearly showing that not reusing all PRBs within a cluster can provide better results whenever inter-cluster interference can be estimated and employed to perform intelligent RRA. However, for high load in UEs/sector, the coordination was not able to provide a considerable gain.

From Figure 3.5(b), for both schedulers, the higher the load is, the higher the percentage of allocated high MCSs is and, for both loads, the BRA scheduler has higher usage of higher

MCSs than the MaxSINR scheduler. Due to the perfect knowledge about the intra-cluster interference, this scheduler determines more accurately the SINR and chooses better the MCS to be used on each link resulting in high spectral efficiency.

In order to try to understand the similar performance achieved by the BRA and MaxSINR schedulers for the highest load, the average inter-cluster interference power as well as the BLER presented by both schedulers is evaluated. Figure 3.6 shows the average inter-cluster interference power and the CDF of BLER for the BRA and MaxSINR schedulers.

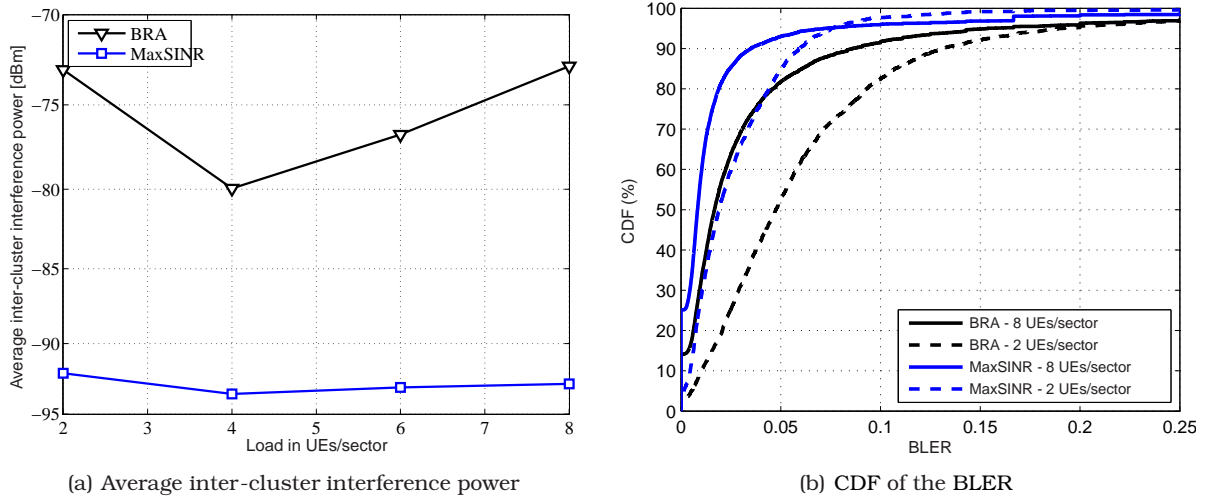


Figure 3.6: Average inter-cluster interference power and CDF of the BLER achieved by the joint multi-cell scheduling algorithm considered for the CoMP scenario.

As it is seen in Figure 3.6(a), BRA presents higher levels of average inter-cluster interference than the MaxSINR scheduler, indicating a greater number of transmissions in the CoMP system. The full reuse transmission achieved by the MaxSINR scheduler in the conventional scenario leads to higher interference and lower SINR values, resulting in a lower system spectral efficiency. Although the BRA scheduler decreases the inter-cluster interference levels, which is achieved with more transmissions, it makes a better management of interference and thus achieves a better use of higher MCSs.

From Figure 3.6(b), it can be seen that BRA has much higher BLER values than the MaxSINR scheduler, which is due to the link adaptation being more sensitive to variations of the inter-cluster interference with a joint multi-cell scheduling. Given that BRA forms groups of various sizes in subsequent TTIs, the inter-cluster interference estimation mechanism is not able to follow these variations, since it is based on the last estimate of the inter-cluster interference. Despite showing higher BLER values, BRA has a better performance than the MaxSINR scheduler.

3.4 Joint processing approach

This approach multiplexes in space several UEs on the same PRB, which in fact already happens in the CS approach. While the spatial multiplexing of signals intended to different UEs is done using space-domain precoding techniques [50], spectral efficiency gains are often obtained by transmitting to spatially compatible UEs, i.e., a given group of UEs whose channels are favorable for spatial separation [6]. When the JP transmission approach is considered, the problem (3.2) can be seen as an SDMA grouping problem [6].

To solve this problem, SDMA grouping algorithms which avoid placing UEs with highly correlated channels in the same SDMA group \mathcal{G} are usually employed [6]. Normally, SDMA grouping algorithms are heuristics composed by two elements: a **grouping metric** and a

grouping algorithm [6]. While the metric measures the spatial compatibility among the UEs in an SDMA group based on the CSI available at the cluster, the grouping algorithm, based on the grouping metric, builds and compares different SDMA groups. Once the SDMA group \mathcal{G} is determined, **spatial precoding**, **power allocation** and link adaptation can be realized. Additionally, performance gains can be achieved with dynamic adaptation of the SDMA group size.

Herein, particular SDMA algorithms which follow this model are considered. First, the grouping algorithm is discussed in Section 3.4.1. Next, the grouping metric is discussed in Section 3.4.2. Then, Section 3.4.3 describes dynamic adaptation of SDMA group size. After that, some information about the considered precoding is provided in Section 3.4.4. The power allocation is treated in Section 3.4.5 while respecting the per-sector power constraints, as introduced in Section 2.7. Finally, the performance of the JP approach is analyzed in Section 3.4.6.

3.4.1 Grouping algorithm

The task of the grouping algorithm is to arrange the UEs of the cluster in a spatially compatible SDMA group by using the grouping metric. Here, two algorithms for building SDMA groups are considered:

- ▶ Best Fit (BF) grouping algorithm: It is also a greedy algorithm similar to the one described in Section 3.3.2 for the CS transmission approach [10, 52–54];
- ▶ RND grouping algorithm: It just randomly builds an SDMA group of specific group size the same way the RND algorithm for the CS transmission approach described in Section 3.3.1 performs. It does not consider any grouping metric.

The grouping algorithm adds UEs to an SDMA group while a stop criterion is not satisfied. Here, two stop criteria are considered:

- ▶ Target Group Size (TGS) stop criterion: In this case, adding UEs is done until the group size G reaches the target SDMA group size G^* ;
- ▶ Maximum Grouping Metric (MGM) stop criterion: The stop happens when the grouping metric value is not increasing.

In the following, the BF and RND algorithms for the JP approach are described.

3.4.1.1 BF grouping algorithm

Starting from an SDMA group containing an initial UE j' , the BF algorithm extends the group by sequentially admitting the most spatially compatible UE with respect to the UEs already admitted to the SDMA group.

Let $\mathcal{G} = \{j'\}$ be the initial SDMA group containing only the UE j' , chosen as the UE with the highest channel norm, and let G be the size of the group \mathcal{G} . Then, the BF algorithm computes the grouping metric $\phi(\mathcal{G} \cup \{j\})$ for each UE $j \notin \mathcal{G}$. Next, the UE which leads to the highest value for the grouping metric $\phi(\cdot)$ is inserted into the group.

The same procedure is repeated with the remaining UEs and an additional UE is admitted to the group, and so on while the stop criterion (either TGS or MGM criterion) is not satisfied.

An algorithmic description of the BF grouping algorithm is given later for each grouping metric.

3.4.1.2 RND grouping algorithm

For comparison purposes, a random grouping algorithm is also considered, which selects UEs within a cluster in a random manner, like the RND algorithm presented in Algorithm 3.1 for the CS transmission approach. The only difference is that it selects UEs within a cluster while the RND algorithm for the CS approach selects UEs within a sector. By definition, the RND grouping algorithm considers TGS stop criterion.

The RND grouping-based algorithm under TGS criterion is sketched in the following.

Algorithm 3.5 RND grouping-based algorithm under TGS criterion.

```

for each PRB do
  for each cluster do
    while  $G \leq G^*$  do
      Selects a link within the sector at random with uniform distribution
    end while
    for each scheduled UE do
      Calculates the perceived intra-cluster interference
      Performs link adaptation
    end for
  end for
end for

```

3.4.2 Grouping metric

In general, the higher the channel gains are, the higher their achievable throughput. Therefore, UEs with high channel gains should be preferred. However, the effective gain of the channels of the UEs in an SDMA group are conditioned to the degree of spatial correlation among their channels [6, 15, 34, 35]. Because the higher the group throughput is, the more spatially compatible the UEs in an SDMA are, grouping metrics should favor SDMA groups whose UEs have high channel gain and whose UEs' channels are highly spatially uncorrelated.

The grouping metric is employed by the grouping algorithm to measure the spatial compatibility among UEs. In general, all grouping metrics make use of the CSI representing the channel matrix of the UEs available for CoMP processing.

In the following, three grouping metrics are:

- ▶ Capacity (CAP) grouping metric: It considers the capacity of an SDMA group as metric of spatial compatibility;
- ▶ Convex Combination (CC) grouping metric: It is a convex combination of the total spatial correlation and gain of the channels;
- ▶ Successive Projection (SP) grouping metric: It performs successive projections of the channel of the candidate UEs to an SDMA group onto the null space of the channels of previously selected UEs for an SDMA group.

In the following, each one of these grouping metrics is discussed.

3.4.2.1 CAP grouping metric

CAP grouping metric exactly reflects the estimated throughput of the SDMA group. The higher the group throughput is, the more spatially compatible the UEs in an SDMA group are. Therefore, the CAP grouping metric efficiently measures the spatial compatibility among the UEs. However, this grouping metric takes into account precoding, power allocation and link adaptation for each candidate UE to an SDMA group. Since precoding depends on complex operations, the good performance achieved by this metric comes at the expense of increased complexity [48].

This grouping metric resolves the problem of maximizing the utility function $U(\mathcal{G}, \mathbf{U})$, which represents the throughput of a given cluster, as stated in (3.2), and involves the determination of the UEs group \mathcal{G} and its precoding matrix \mathbf{U} . As the intra-cluster interference is totally cancelled by spatial precoding, the SINR estimate used to perform link adaptation only depends on the estimate of inter-cluster interference and, consequently, this solution is not necessarily optimal, since the inter-cluster interference might be unknown.

The BF grouping algorithm using the CAP metric under MGM stop criterion is sketched in the following.

Algorithm 3.6 BF grouping algorithm using the CAP metric under MGM stop criterion.

```

for each PRB do
  for each cluster do
     $j' \leftarrow \arg \max_{j \in \mathcal{J}} \{\|\mathbf{h}_j\|_2\}$ 
     $\mathcal{G} \leftarrow \{j'\}$ 
    while cluster throughput is increasing do
       $j^* \leftarrow \arg \max_{j \notin \mathcal{G}} \{\phi_{\text{CAP}}(\mathcal{G} \cup \{j\})\}$ 
       $\mathcal{G} \leftarrow \mathcal{G} \cup \{j^*\}$ 
    end while
     $\mathcal{G}^* \leftarrow \mathcal{G}$ 
  end for
end for

```

Since precoding involves complex operations such as matrix inversion, the complexity is expected to be high, specially for larger SDMA groups [48]. Therefore, this algorithm is only used for comparison purposes.

3.4.2.2 CC grouping metric

In the following, the CC grouping metric, which involves the convex combination of the spatial correlation and channel gains, is addressed [48]. First, an attenuation vector $\mathbf{a} \in \mathbb{R}_+^{J \times 1}$ containing the inverse of the channel gains of all UEs belonging to the cluster is defined as

$$\mathbf{a} = \left[\|\mathbf{h}_1\|_2^{-2} \ \|\mathbf{h}_2\|_2^{-2} \ \dots \ \|\mathbf{h}_J\|_2^{-2} \right]^T, \quad (3.5)$$

and a spatial correlation matrix $\mathbf{C} \in \mathbb{R}_+^{J \times J}$ is defined as

$$\mathbf{C} = \left| \sqrt{\text{diag}\{\mathbf{a}\}} (\mathbf{H}\mathbf{H}^H) \sqrt{\text{diag}\{\mathbf{a}\}} \right|. \quad (3.6)$$

Let the binary selection vector \mathbf{s} be defined as

$$\mathbf{s} = \left[s_1 \ s_2 \ \dots \ s_J \right]^T, \quad (3.7)$$

where s_j is a binary variable indicating whether the UE j belongs to the SDMA group \mathcal{G} , i.e., $s_j = 1, \forall j \in \mathcal{G}$, otherwise $s_j = 0$.

After that, when combining (3.5) and (3.6), the convex combination $\phi_{\text{CC}}(\mathcal{G}) \in \mathbb{R}_+^{1 \times J}$, which is composed by the spatial correlation and channel gains, is defined as

$$\phi_{\text{CC}}(\mathcal{G}) = \beta \frac{\mathbf{a}^T}{\|\mathbf{a}\|_2} \mathbf{s} + (1 - \beta) \mathbf{s}^T \frac{\mathbf{C}}{\|\mathbf{C}\|_{\text{FRO}}} \mathbf{s}, \quad (3.8)$$

where β is a parameter that controls the trade-off between spatial correlation and channel gain. Thus, the UE j^* to be added to group \mathcal{G} is given by [48]

$$j^* = \arg \min_j \{\phi_{\text{CC}}(\mathcal{G})_j\}, \quad 1 \leq j \leq K. \quad (3.9)$$

The BF grouping algorithm using the CC metric under TGS criterion is sketched in the following.

Algorithm 3.7 BF grouping algorithm using the CC metric under TGS criterion.

```

for each PRB do
  for each cluster do
     $j' \leftarrow \arg \max_{j \in \mathcal{J}} \{\|\mathbf{h}_j\|_2\}$ 
     $\mathcal{G} \leftarrow \{j'\}$ 
    while  $G \leq G^*$  do
       $j^* \leftarrow \arg \min_{j \notin \mathcal{G}} \{\phi_{\text{cc}}(\mathcal{G} \cup \{j\})\}$ 
       $\mathcal{G} \leftarrow \mathcal{G} \cup \{j^*\}$ 
    end while
     $G^* \leftarrow G$ 
  end for
end for

```

3.4.2.3 SP grouping metric

Here, the sum of channel gains with null space Successive Projections (SPs) is considered as grouping metric [6, 15, 34, 35]. For this metric, the channels of a set of UEs are successively projected onto the null space of the channels of previously selected UEs for the SDMA group.

In general, the higher the channel gain $\|\mathbf{h}_j\|_2^2$ of UE j , the higher its achievable throughput. However, considering null space projections, the effective gains of the channels of the UEs in an SDMA group are conditioned to the degree of spatial correlation among the channels [6, 15, 34, 35].

Let \mathcal{N}_1 and \mathcal{N}_2 denote the null spaces of the channels \mathbf{h}_1 and \mathbf{h}_2 , respectively, and consider that \mathbf{h}_1 is projected onto \mathcal{N}_2 and \mathbf{h}_2 is projected onto \mathcal{N}_1 . Then, if the channels \mathbf{h}_1 and \mathbf{h}_2 are highly spatially uncorrelated, much of the gains of the original channels are preserved in the equivalent channel after the projections. However, if the channels \mathbf{h}_1 and \mathbf{h}_2 are highly spatially correlated, a considerable part of the channel gains gets lost after the projection [6, 15, 34, 35].

This principle is also valid for an SDMA group \mathcal{G} with more than two UEs. However, in this case, the channel \mathbf{h}_j of each UE $j \in \mathcal{G}$ would have to be projected onto the joint null space of the UEs $j' \in \mathcal{G}, j' \neq j$. Using SPs, the channel \mathbf{h}_j of UE $j \in \mathcal{G}$ is projected only onto the null space of all UEs $j' \in \mathcal{G}, j' = 1, 2, \dots, j-1$ [34, 35]. Let \mathbf{I}_M denote an $M \times M$ identity matrix and $\mathbf{T}_j \in \mathbb{C}^{M \times M}$ denote the matrix that projects the channel \mathbf{h}_j of UE j onto the null space of the channels of UEs j' [34, 35]. Then, \mathbf{T}_j is written as

$$\mathbf{T}_j = \begin{cases} \mathbf{I}_M, & j = 1, \\ \mathbf{T}_{j-1} - \frac{\mathbf{T}_{j-1}^H \mathbf{h}_{j-1} \mathbf{h}_{j-1}^H \mathbf{T}_{j-1}}{\|\mathbf{h}_{j-1} \mathbf{T}_{j-1}\|_2^2}, & j = 2, \dots, G. \end{cases} \quad (3.10)$$

Using (3.10), the sum of the channel gains with null space SPs $\phi_{\text{SP}}(\mathcal{G})$ is written as

$$\phi_{\text{SP}}(\mathcal{G}) = \sum_{j=1}^G \|\mathbf{h}_j \mathbf{T}_j\|_2^2, \quad (3.11)$$

which will be used by the grouping algorithm to select a set of spatially compatible UEs for \mathcal{G} .

The BF grouping algorithm using the SP metric under TGS criterion is sketched in the following.

In the first loop, the first encoded UE is chosen to be the one with largest channel gain. In the second loop, considering the null space of the channel of the first encoded UE, the second

Algorithm 3.8 BF grouping algorithm using the SP metric under TGS criterion.

```

for each PRB do
  for each cluster do
     $j' \leftarrow \arg \max_{j \in \mathcal{J}} \{\|\mathbf{h}_j\|_2\}$ 
     $\mathcal{G} \leftarrow \{j'\}$ 
    while  $G \leq G^*$  do
       $j^* \leftarrow \arg \max_{j \notin \mathcal{G}} \{\phi_{\text{SP}}(\mathcal{G} \cup \{j\})\}$ 
       $\mathcal{G} \leftarrow \mathcal{G} \cup \{j^*\}$ 
    end while
     $G^* \leftarrow G$ 
  end for
end for

```

encoded UE is chosen to be the one that exhibits the largest gain in this subspace. At any step of the algorithm, the UE is selected that exhibits the largest gain within the subspace orthogonal to the channels of previously selected UEs.

3.4.3 Dynamic SDMA group size

The larger the SDMA group size G is, the higher the spatial multiplexing gains can be achieved [55] such that larger SDMA groups \mathcal{G} should be preferred. However, the previous steps may be insufficient to ensure a reliable transmission of all UEs in an SDMA group \mathcal{G} , mainly when the maximum group size is achieved, i.e., $G = M$. Besides that, often maximal spectral efficiency is achieved by transmitting to less UEs or using less beams than the available number of spatial dimensions [56].

Hence, the ideal SDMA group size G^* should be determined dynamically. Sequential Removal Algorithms (SRAs) remove UEs from an SDMA group \mathcal{G} while throughput gains are achieved. Thus, the power released after each removal can be redistributed among the remaining UEs in order to improve their performance.

It is important to mention again that the SRA removes UEs while throughput gains are achieved such that it is aware of the spatial precoding and power allocation. The grouping metrics considered in Section 3.4.2, that use grouping algorithm with TGS stop criterion, i.e., adding UEs until a fixed group size G is achieved, build SDMA groups unaware of the spatial precoding and power allocation. On the other hand, SRA is not employed when the MGM stop criterion is considered, since it has the same objective of the SRA, i.e., the group size G is dynamically determined while throughput gains are achieved. In this way, the SRA has a particular contribution for algorithms that consider fixed group size. Algorithm 3.9 presents an algorithmic description of the SRA.

Algorithm 3.9 SRA with a given removal criterion.

```

for each PRB do
  for each cluster do
    Removes a UE under a given removal criterion
    Estimates cluster throughput
    while cluster throughput is increasing do
      Removes a UE under a given removal criterion
      Estimates cluster throughput
      Performs link adaptation
    end while
    Adds the last UE
  end for
end for

```

In the following, three removal criteria are considered:

- MCS-0 removal criterion: It removes UEs allocated with MCS-0;

- ▶ Minimum Gain (MinGain) criterion: It removes the UE with the lowest channel gain;
- ▶ Minimum SINR (MinSINR) criterion: It removes the UE with the lowest estimated SINR.

In the following, each one of these criteria is described with more details.

3.4.3.1 MCS criterion

When UEs grouped in the SDMA group do not have a high enough estimated SINR so that its transmission can occur, it can be allocated with MCS-0 by the link adaptation. In this way, power resources among the APs cooperating will be unnecessarily allocated for them.

In this criterion, among the UEs with MCS-0 the UE j^* with the lowest estimated SINR $\hat{\gamma}_j$ is removed as defined below

$$j^* = \arg \min_j \{\hat{\gamma}_j\}, \quad \forall j \in \mathcal{G} \mid \text{MCS}_j = 0. \quad (3.12)$$

3.4.3.2 MinGain criterion

Since UEs whose channels are not spatially compatible affect the spatial separation of other UEs in the SDMA group, the effective channel gain will be affected. This criterion removes the UE with the lowest effective channel gain.

The UE j^* with the lowest effective channel gain is removed as defined below [48]

$$j^* = \arg \min_j \{|\mathbf{h}_j \mathbf{w}_j|^2\}, \quad \forall j \in \mathcal{G}. \quad (3.13)$$

This criterion is employed after the MCS-0 criterion, since it is necessary to assure that there are no UEs allocated with MCS-0 at the SDMA group after the removals.

3.4.3.3 MinSINR criterion

This criterion removes the UE with the lowest estimated SINR, like in the MCS-0 criterion, and it is employed after the MCS-0 criterion, like in the MinSINR criterion. The difference to both criteria previously presented relies on the removal of UEs with the lowest estimated SINRs among all UEs belonging to the SDMA group.

In this criterion, the UE j^* with the lowest estimated SINR $\hat{\gamma}_j$ is removed as defined below

$$j^* = \arg \min_j \{\hat{\gamma}_j\}, \quad \forall j \in \mathcal{G}. \quad (3.14)$$

3.4.4 Spatial precoding

The CSI can be used to mitigate the intra-cell interference $z_{j,c}^{intra}$ and efficiently separate streams intended to different UEs. This task is accomplished, e.g., by employing precoding techniques [50] which adaptively weight the symbols transmitted from each antenna in the cluster. The precoding is often used for obtaining orthogonal transmissions among UEs.

There exist different spatial precoding techniques that allow to separate signals intended to the UEs belonging to the SDMA group \mathcal{G} . Among them, linear precoding techniques are often considered by future wireless systems due to their simplicity and good performance [6, 34].

Linear precoding, in case of spatial multiplexing, implies linear processing by means of $M \times G$ precoding matrix \mathbf{W} that is applied at the transmitter side. In the general case, G is smaller or equal than M , implying that G signals are spatially multiplexed and transmitted using M transmit antennas.

In this dissertation, Zero-Forcing (ZF) precoding is considered, which steers a beam towards UE j direction and nulls in the direction of the UEs $j' \neq j$, thus eliminating intra-cluster interference [50]. For the SDMA group \mathcal{G} with channel matrix \mathbf{H} , the precoding matrix \mathbf{W} is given by

$$\mathbf{W} = \mathbf{H}^\dagger, \quad (3.15)$$

where \mathbf{H}^\dagger represents the pseudo-inverse $\mathbf{H}^\dagger = \mathbf{H}\mathbf{H}^{\text{H}}(\mathbf{H}\mathbf{H}^{\text{H}})^{-1}$ of the group channel matrix \mathbf{H} of SDMA group \mathcal{G} .

The precoding vectors \mathbf{w}_j , with $j \in \mathcal{G}$, do not have unit norm initially. However, per-UE normalization under the precoding vectors \mathbf{w}_j building the ZF precoding matrix \mathbf{W} can be performed by

$$\mathbf{w}_j = \frac{\mathbf{w}_j}{\|\mathbf{w}_j\|_2}, \quad \forall j \in \mathcal{G}, \quad (3.16)$$

where \mathbf{w}_j represents the j^{th} column of the precoding matrix \mathbf{W} of SDMA group \mathcal{G} .

For ZF precoding, the interference suppression comes at the cost of a reduction in the effective channel gains, which might lead to large performance losses if UEs with spatially correlated channels belong to the SDMA group \mathcal{G} .

3.4.5 Power allocation

In this section, the power allocation is addressed. To each UE $j \in \mathcal{G}$, power is allocated afterwards while respecting the constraint on the maximum power per PRB P_{PRB} available at each AP. Since the RRA strategies employed for the JP approach consider a total power constraint in all antennas together of a cluster with M transmission antennas given by P_{SUM} (see Section 2.7). It is initially done Equal Power Allocation (EPA) among the G UEs belonging to the SDMA group \mathcal{G} as follows

$$p_j = \frac{P_{\text{SUM}}}{G}, \quad \forall j \in \mathcal{G}. \quad (3.17)$$

Because the power ratio among elements of each column of the matrix \mathbf{U} cannot be changed in order to preserve the properties of the spatial precoding and because no AP can use more power than P_{PRB} , the per-sector power constraints are respected by scaling the whole precoding matrix \mathbf{U} so that the squared norm of the row with highest norm becomes equal to P_{PRB} .

Considering the precoding matrix $\mathbf{U} \in \mathbb{C}^{M \times G}$, the power scaling can be easily handled as follows. First, the sector i^* which consumes the highest power is chosen as

$$i^* = \arg \max_{1 \leq i \leq N_{\text{SEC}}} \{P_{\text{SEC}, i}\}, \quad (3.18a)$$

where

$$P_{\text{SEC}, i} = \|\mathbf{U}_i\|_2^2. \quad (3.18b)$$

As it can be seen in (3.18), the total power spent by a sector i corresponds to the sum of the squared absolute value of the weights it employs to each transmit signal. Hence, the transmit power of AP i corresponds to the squared norm of the i^{th} row of precoding matrix \mathbf{U} .

After that, the power scaling must be performed by scaling the whole \mathbf{U} matrix so that the squared norm of the row \mathbf{u}_{i^*} with highest norm becomes equal to P_{PRB} , i.e.,

$$\mathbf{U} = \frac{\mathbf{U}}{\sqrt{P_{\text{SEC}, i^*}}}. \quad (3.19)$$

3.4.6 Performance with SDMA grouping

In this section, the performance obtained by SDMA grouping algorithms is investigated. The performance of the CAP-based SDMA grouping algorithm, which performs interference-aware grouping, is investigated in Section 3.4.6.1. Section 3.4.6.2 provides a performance assessment of some interference-unaware SDMA grouping algorithms, namely, RND, CC and SP algorithms. Finally, Section 3.4.6.3 deals with the performance evaluation of interference-unaware SDMA grouping combined with SRAs.

3.4.6.1 Interference-aware grouping

In this section, the performance obtained by the CAP algorithm is presented comparing its performance with the BRA's performance. For the grouping performed by the CAP algorithm, the group size is dynamically adjusted. Thus, the distribution of the group size provides a general view of the behavior of UE spatial grouping, which allows us to analyze the efficiency of the CAP algorithm.

Figure 3.7 presents the system spectral efficiency achieved by the CAP algorithm with and without precoding normalization in comparison to system spectral efficiency achieved by the BRA scheduler. The same figure also presents the PDF of the group size for the CAP algorithm with and without precoding normalization and the BRA scheduler.

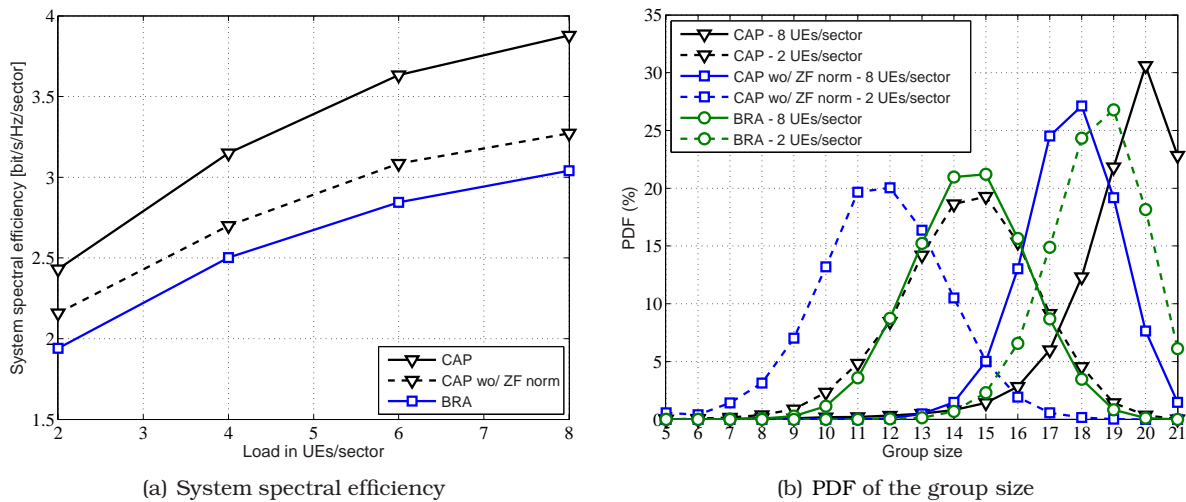


Figure 3.7: System spectral efficiency and PDF of the group size achieved by the CAP grouping algorithm.

As it can be seen in Figure 3.7(a), the CAP algorithm without precoding normalization presents a gain of spectral efficiency with respect to the BRA algorithm. This gain represents a shift that occurs in practically all loads, being around 11% for the lowest load and around 7% for the highest load. Now, observing the CAP algorithm with precoding normalization in comparison to BRA, the higher the load in UEs/sector is, the higher the comparative gain is. Here, the gain achieves almost 30% for the highest load.

From Figure 3.7(b), for both loads the CAP algorithm achieves higher SDMA group sizes G than the CAP algorithm without precoding normalization. When BRA and CAP algorithms are compared, it is shown that, for the lowest load, the behavior of group size for the CAP algorithm is almost kept in relation to BRA. For the highest load, there is a small difference. The average group size achieved by the CAP algorithm is between 19 and 20 UEs while it for the BRA algorithm is between 18 and 19 UEs. Thus, dynamics of the UE spatial grouping with JP transmission is maintained in comparison to CS transmission.

Figure 3.8 presents the CDF of BLER and the PDF of the usage of the MCSs for the BRA

and CAP algorithms.

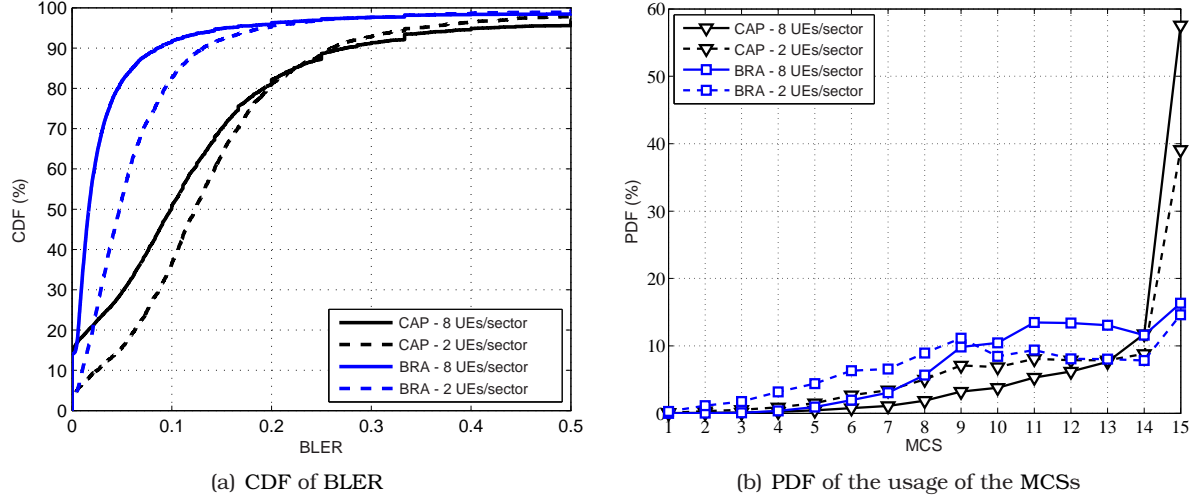


Figure 3.8: CDF of BLER and PDF of the usage of the MCSs presented by the CAP grouping algorithm.

Even though the CAP algorithm has a better spectral efficiency than the BRA scheduler, it shows high BLER values for any value of load in UEs/sector, as it is shown in Figure 3.8(a). The CAP algorithm, like the BRA scheduler, uses the CSI to iteratively build a group of UEs that achieves high joint throughput. Since this approach compares achievable cluster throughputs when building a given set of UEs, it indirectly chooses UEs that have high channel gain, receive little interference from other clusters and are more spatially compatible. Since the grouping performed by the CAP algorithm is based on estimates for the inter-cluster interference, the SDMA groups are much diversified in subsequent TTIs, like the BRA scheduler. Figure 3.8(a) allows to infer that the link adaptation performed for dynamic UE spatial grouping under the JP approach is more sensitive to variations of the inter-cluster interference than under the CS approach.

From Figure 3.8(b), for both loads the CAP algorithm has higher percentage of use of the highest MCS than the BRA scheduler. For the highest load, it is shown that with the CAP algorithm almost 60% of the transmissions achieve the highest MCS while with the BRA algorithm the highest MCS is achieved by less of 20% of transmissions. This happens because the SDMA grouping algorithm performs spatial precoding in order to mitigate the intra-cluster interference, which is totally canceled by using the ZF precoder. Since the intra-cluster interference is canceled, the UEs are able to be serviced with higher MCSs. Besides that, due to the power scaling performed for the JP approach because no AP can use more power than P_{PRB} , only one AP transmits with the maximum power per PRB P_{PRB} while the other APs transmit with power below P_{PRB} . This strategy reduces the power consumption on the system and consequently reduces the levels of inter-cluster interference in comparison to the conventional scenario and CS approach, also favoring the use of higher MCSs.

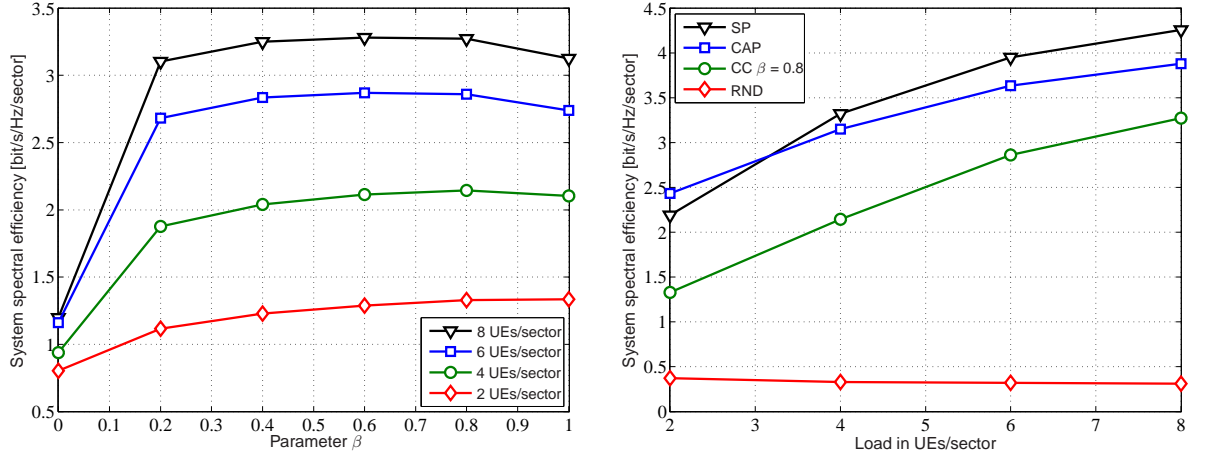
3.4.6.2 Interference-unaware grouping

As observed in Section 3.4.6.1, the CAP algorithm has a gain in system spectral efficiency in comparison to the BRA algorithm, the main algorithm considered for the CS approach. However, as stated in Section 3.4.2.1, the computation of the CAP-based metric involves computing precoding vectors for each UE to be added in the SDMA group such that this algorithm is only used for comparison purposes. Besides that, interference-aware grouping algorithms, like the BRA and CAP algorithms, have shown high levels of BLER.

In the following, the performance of algorithms described in Section 3.4.2 that

perform interference-unaware grouping is presented. The first algorithm considered is the RND algorithm, which is considered only for comparison purposes, being it described in Section 3.4.1. Next, the second algorithm considered is the CC algorithm, which is composed by a more simple metric that involves the convex combination of the spatial correlation and channel gains, being it described in Section 3.4.2.2. After that, the SP algorithm is considered, which deals with user orthogonalization based on successive projections onto null space (see Section 3.4.2.3 for more details).

Figure 3.9 presents the system spectral efficiency for the RND, CC, CAP and SP algorithms.



(a) System spectral efficiency achieved by the CC grouping algorithm for a range of the parameter β (b) System spectral efficiency achieved by the RND, CC, CAP and SP grouping algorithms

Figure 3.9: System spectral efficiency achieved by the RND, CC, CAP and SP grouping algorithms.

As it can be seen in Figure 3.9(a), the CC algorithm has the worst performance for $\beta = 0$, i.e., when only spatial correlation is considered for grouping. The best performance is achieved introducing a small amount of correlation in combination with channel gains of the UEs, which is given by β around 0.8 for almost all loads.

From Figure 3.9(b), it can be seen from the performance of the RND algorithm that grouping UEs not spatially compatible affects very much the spatial separation achieved by the ZF precoding, reducing the spectral efficiency of the system. Similarly, the CC algorithm was also not appropriate to the task of grouping spatially compatible UEs, since this performance was far below the CAP's performance.

It was shown that the SP algorithm performed very well and obtained performance gains for almost all loads. However, for the lowest load the performance of the SP algorithm was worse than the performance achieved by the CAP algorithm.

In order to try to understand the worse performance achieved by the SP algorithm in comparison to CAP for the lowest load, the distribution of the percentage of use of the MCSs as well as the BLER presented by both algorithms are evaluated. Figure 3.10 presents the CDF of BLER and the PDF of the usage of the MCSs for the CAP and SP algorithms.

From Figure 3.10(a), for the highest load, both SP and CAP algorithms have the same performance. However, it is shown that for the lowest load the SP algorithm has lower percentage of use of the highest MCS and higher percentage of use of other MCSs than the CAP algorithm. Due to low load in UEs/sector the SP algorithm with fixed group size is forced to group UEs whose channels are not spatially compatible, which affects very much the spatial separation achieved by the ZF precoding reducing the spectral efficiency of the system, as shown in Figure 3.9(b).

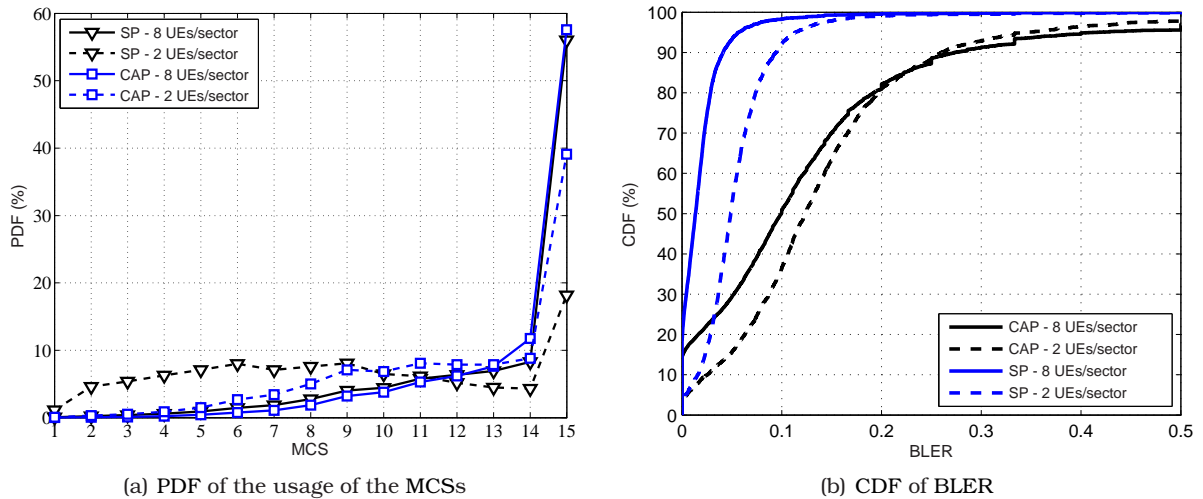


Figure 3.10: PDF of the usage of the MCSs and CDF of BLER presented by the SP and CAP grouping algorithms with fixed group size.

As it can be seen in Figure 3.10(b), the performance in terms of BLER was worse with the CAP algorithm than with the SP algorithm, which allows to infer that the link adaptation is much more sensitive to variations on the inter-cluster interference when estimates for the inter-cluster interference are used for grouping. Unlike the CAP algorithm, the SP algorithm tends to select the same UEs, which contributes to reduce the levels of BLER. Indeed, since the SP algorithm performs an interference-unaware grouping it chooses the most spatially compatible UEs without considering the estimates for inter-cluster interference to building the SDMA group and thus it is more stable.

In order to obtain more gains with the SP algorithm, the performance regarding several fixed group sizes less than $G = 21$ is evaluated. Figure 3.11 presents the system spectral efficiency achieved by the SP algorithm regarding several fixed group sizes.

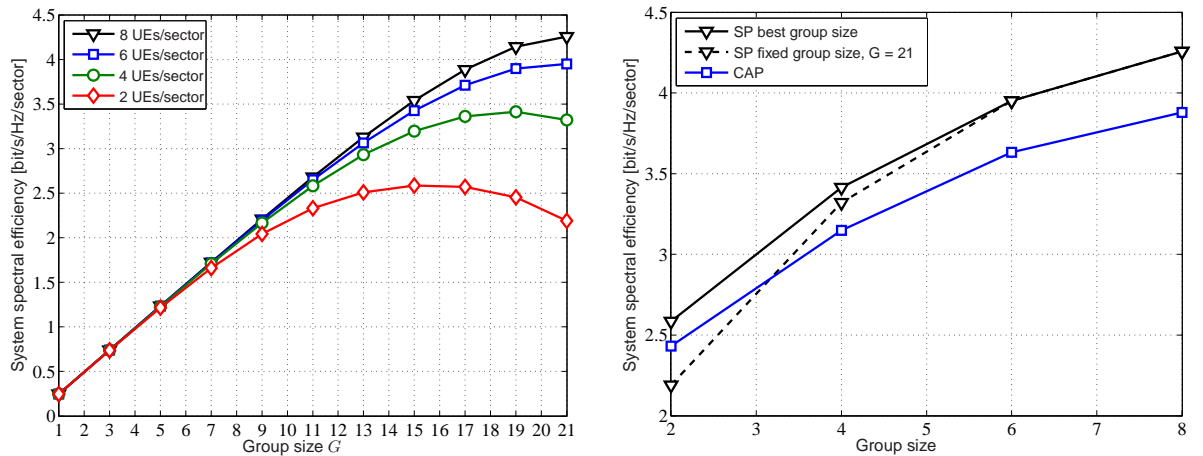


Figure 3.11: System spectral efficiency achieved by the SP grouping algorithm regarding several fixed group sizes.

By Figure 3.11(a), for the lowest load, the maximum spectral efficiency is achieved by SDMA group sizes G smaller than the maximum SDMA group size $G = 21$, while for the highest load, the maximum spectral efficiency value is reached for $G = 21$.

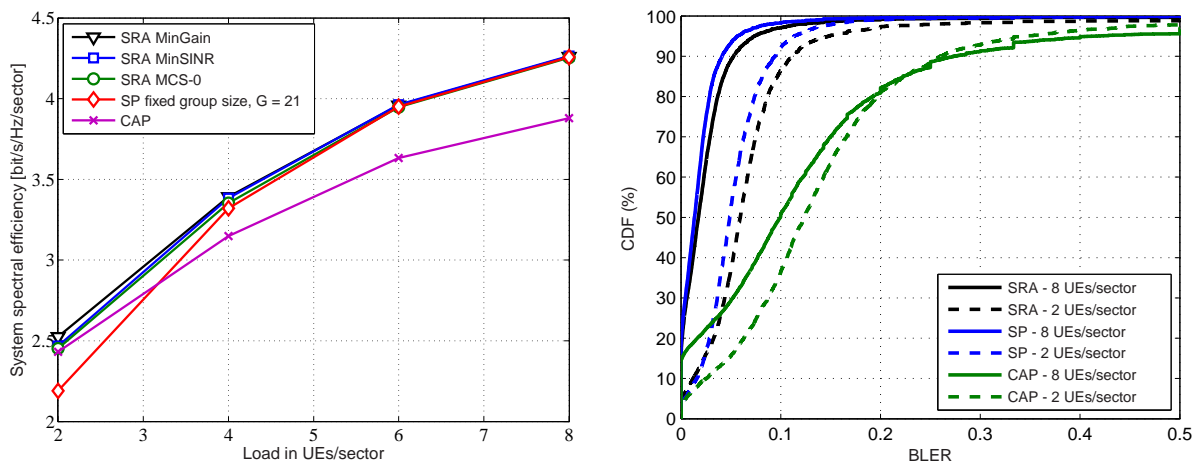
From Figure 3.11(b), the SP algorithm with fixed group size was not appropriate to the task of grouping UEs spatially compatible for low load in UEs/sector, since this

performance was far below the CAP's performance, but by properly selecting the best group sizes given in Figure 3.11(a), the SP algorithm achieved better performance than the CAP algorithm. This result indicates that SDMA grouping with dynamic group size should achieve better performance than the interference-unaware grouping algorithms under TGS stopping criterion considered in this section.

3.4.6.3 SDMA grouping with dynamic group size

In order to obtain more gains, the SDMA group size can be dynamically adapted according to channel conditions and the load by employing sequential removals of UEs of the SDMA group, which is possible by the use of SRAs. The SRAs introduced in Section 3.4.3 are employed in order to obtain an adaptive size of the SDMA group and so higher system spectral efficiency. Here, the removal criteria defined in Section 3.12, which remove UEs by MCS-0, MinGain and MinSINR criteria, are considered.

Figure 3.12 presents the system spectral efficiency achieved by the SP algorithm combined with SRAs comparing its performance with the CAP's performance.



(a) System spectral efficiency achieved by several SRAs (b) System spectral efficiency achieved by the SRA MinGain

Figure 3.12: System spectral efficiency achieved by several SRAs.

As it can be seen in Figure 3.12(a), for low loads, significant gains in spectral efficiency can be achieved with use of SRAs. For high loads the SDMA grouping is better capable of choosing spatially uncorrelated UEs, due to the multi-user diversity, reducing the need for UE removal. Further, removing UEs with MCS-0 is responsible for most of the gain. Between the MinGain and MinSINR criteria, removing UEs by the MinGain criterion proved to be more efficient than removing UEs by the MinSINR criterion. Besides that, SRAs are able to provide gains in spectral efficiency compared to the performance achieved by the CAP algorithm for the lowest load, which was not possible with the use of the SP algorithm with fixed group size.

From Figure 3.12(b), the performance in terms of BLER was worse with the SRA than with the SP algorithm under fixed group size although it has better performance in terms of system spectral efficiency. Since the removals are based on increasing the cluster throughput and so based on computation of the SINR estimates for each UE belonging to the SDMA group, this strategy tends to choose a diversified number of UEs, which contributes to increase the levels of BLER, like the CAP algorithm. Although the SRA shows high BLER values, it has a better performance than the SP algorithm.

In the following, the PDF of the usage of the MCSs and the PDF of the group size achieved by the SRA-MinGain and CAP algorithms are presented in Figure 3.13.

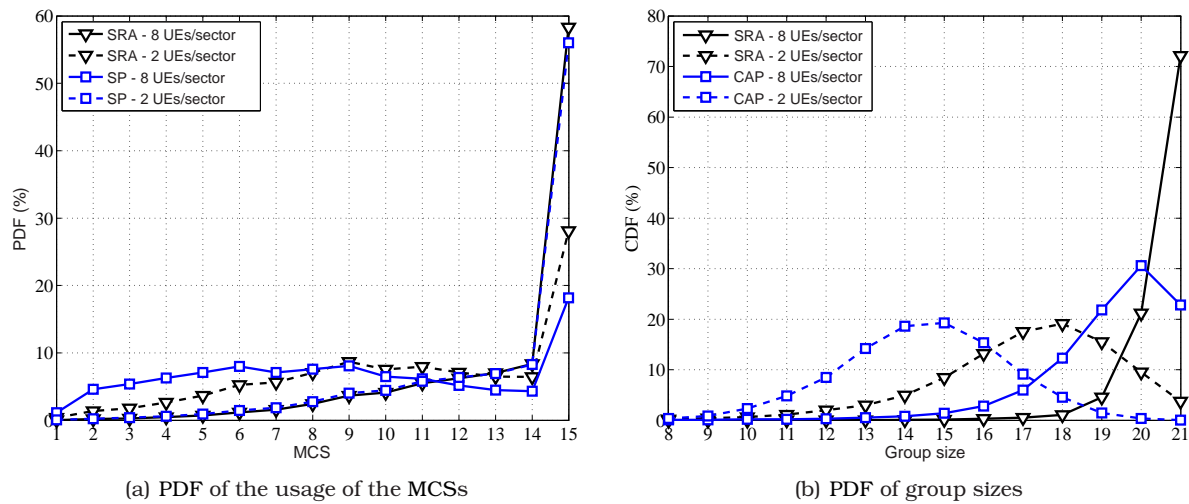


Figure 3.13: PDFs of the usage of the MCSs and group sizes achieved by the SP grouping algorithm combined with SRA MinGain.

As it can be seen in Figure 3.13(a), the effect observed in Figure 3.10(a) for low loads does not happen with SRA. Here, the SRA removes the UEs whose channels are not spatially compatible and that were forcibly grouped into the SDMA group by the SP algorithm with fixed group size, $G = 21$.

From Figure 3.13(b), it has been verified that the most frequent group size is not always the one that provides maximum spectral efficiency. This implies that the performance of the SP algorithm for a fixed group size is somehow degraded, especially for $G = 21$. For example, for the lowest load the best performance of the SP algorithm with fixed group size is achieved for $G = 15$ (see Figure 3.11(a)), while the most frequent group size with the use of SRA is $G = 18$. When the SRA and CAP algorithms are compared, it is shown that, for both loads the SRA achieves higher SDMA group sizes G than the CAP algorithm. It is also seen that, for the highest load, the average group size achieved by the SRA is given between 20 and 21 UEs, thus being close to the maximum allowed value of 21. This result indicates that the SRA performs almost full reuse within a cluster for high loads.

3.5 Summary

This chapter provided system-level analyses for strategies of RRA in CoMP systems considering UE spatial grouping observing both CS and JP transmission approaches. This chapter has shown the performance gains of using interference knowledge and spatial processing in the scheduling of a CoMP system in terms of system spectral efficiency as a function of the number of UEs/sector.

Initially, the MaxGain algorithm was simulated in the conventional scenario with interference-unaware link adaptation and it has been shown to have the worst performance. This happens because the link adaptation uses a very optimistic estimate of the UEs channel quality resulting in high levels of BLER. This result shows clearly that the inter-cell interference is an important issue to be considered by efficient link adaptation schemes that have as objective the maximization of the throughput. The single-cell schedulers simulated in the CoMP scenario with an enhanced link adaptation presented similar performance than the same algorithms simulated in the conventional scenario. This result showed that the estimates of inter-cell interference used for link adaptation were very accurate when single-cell rate maximization strategies performed full reuse of the PRBs in the conventional scenario.

Taking advantage of the availability of CSI for performing interference coordination, the BRA scheduler, which indeed models the CS transmission approach, provided considerable gains compared to the conventional schedulers. The CS approach uses the CSI available to iteratively build a group of UEs that achieves high joint throughput. Because this approach compares achievable cluster throughputs when building a given set of UEs, it indirectly chooses UEs that have high channel gain and receive little interference from other APs. Differently from what happened in the conventional scenario, in which full reuse of PRBs in all sectors has been used, the BRA performs adaptive multi-cell scheduling. It has been seen that the BRA scheduler outperformed the MaxGain and MaxSINR schedulers, clearly showing that not reusing all PRBs can provide better results whenever inter-cluster interference can be estimated and employed to perform intelligent RRA.

Additionally, the RND, CC, CAP and SP algorithms considered for the JP transmission approach were simulated. It was shown that the SP algorithm achieves the best performance when compared to the other algorithms previously presented for high loads in UEs/sector. However, for low loads in UEs/sector the algorithms under fixed group size have worse performance than the dynamic algorithms such that the best group size G^* should vary from load to load and shall depend on the channel conditions. It has been shown that the performance of the SP algorithm for a fixed group size is somehow degraded, mainly for low loads in UEs/sector. In particular, the SP algorithm combined with SRA-MinGain algorithm has achieved the best performance for all considered loads.

SINR balancing

4.1 Introduction

In order to provide a more reliable communication to the User Equipments (UEs) grouped in the SDMA group \mathcal{G} , it is desirable to support a certain level of link quality. As it is known, the link quality mainly depends on the Signal to Interference-plus-Noise Ratio (SINR). Hence, the quality of UEs' links might be assured if individual target SINRs values $\gamma_j^t, \forall j \in \mathcal{G}$, are met [39].

The target SINRs represent minimum values of quality defined for a given service type. According to each service class, there might exist a relation between a target SINR and the required SINR for a given Modulation and Coding Scheme (MCS) in order to be possible to achieve a necessary rate required by the service class. This way, the SINR balancing has the objective of providing a minimum quality to the downlink Coordinated Multi-Point (CoMP) transmissions of the grouped UEs. In this dissertation, the target SINR values are considered as the SINR thresholds of the MCS defined by the link adaptation for each UE $j \in \mathcal{G}$.

The SINR balancing problem introduced in Section 1.4 is investigated in a multiuser CoMP scenario, in which UEs are subject to an SINR constraint and strong inter-cell interference, and there is a power limitation per antenna [37]. Therefore, the considered solution in this dissertation extends the algorithm in [39], which is based on the single-cell scenario and a sum power constraint.

It is important to account for the possibility that the SINR constraints may be infeasible, i.e., that they cannot be jointly supported. If the constraints are infeasible, the initial conditions must be relaxed, e.g., by reducing the target SINR values or number of UEs grouped. Given that the constraints are feasible, power minimization can be performed after the SINR balancing in order to reduce the power used in excess and thus the inter-cluster interference [39].

The remainder of this chapter is organized as follows: The formulation of SINR balancing problem with joint beamforming and power control is treated in Section 4.2. In Section 4.3, the SINR balancing solution under sum-power constraint is presented. In Section 4.4, the feasibility of the SINR balancing algorithm is established through Sequential Removal Algorithms (SRAs). Power minimization after SINR balancing is treated in Section 4.5. In Section 4.6, simulation results are presented and discussed. Finally, a brief summary of the chapter is provided in Section 3.5.

4.2 Problem statement

In order to state the problem of balancing the SINR among several co-channel UEs, a total power constraint on the power allocation vector \mathbf{p} , defined as P_{SUM} in Section 2.7, is considered for each cluster. Consider the target SINRs values $\gamma_j^t, \forall j \in \mathcal{G}$, as above defined. Using the power allocation vector \mathbf{p} and the precoding matrix \mathbf{W} , both defined in Section 2.7, and considering the downlink SINR $\gamma_j(\mathbf{W}, \mathbf{p})$, defined in (2.5), the downlink SINR balancing problem can be written as

$$C^{DL}(P_{\text{SUM}}) = \max_{\mathbf{W}, \mathbf{p}} \min \frac{\gamma_j(\mathbf{W}, \mathbf{p})}{\gamma_j^t}, \quad \forall j \in \mathcal{G}, \quad (4.1a)$$

subject to

$$\|\mathbf{w}_j\|_2 = 1, \quad (4.1b)$$

$$\|\mathbf{p}\|_1 \leq P_{\text{SUM}}. \quad (4.1c)$$

As it was shown in (2.5), the downlink SINR values γ_j of all UEs j are coupled by the intra-cell interference z_j^{intra} , which depends on both precoding vectors $\mathbf{w}_{j'}$ and transmission powers $p_{j'}$. Therefore, the power allocation vector \mathbf{p} and the precoding matrix \mathbf{W} cannot be optimized separately. Thus, the downlink problem (4.1) is hard to solve, but its uplink dual can be more easily solved by an iterative uplink beamformer and power update algorithm [39].

The uplink SINR $\gamma_j^{UL}(\mathbf{w}_j, \mathbf{q})$ is given by

$$\gamma_j^{UL}(\mathbf{w}_j, \mathbf{q}) = \frac{q_j \mathbf{w}_j^H \mathbf{R}_j \mathbf{w}_j}{\mathbf{w}_j^H \left(\sum_{\substack{j'=1 \\ j' \neq j}}^G q_{j'} \mathbf{R}_{j'} + (z_j^{\text{inter}} + \sigma_\eta^2) \mathbf{I} \right) \mathbf{w}_j}, \quad \forall j \in \mathcal{G}. \quad (4.2)$$

As it can be observed in (4.2), the uplink SINRs $\gamma_j^{UL}(\mathbf{w}_j, \mathbf{q}), \forall j \in \mathcal{G}$ are coupled only by the transmission powers $q_{j'}$ but not by the beamformers \mathbf{w}_j . This makes the uplink case much easier to solve than the downlink case. Indeed, in [39] the authors showed that the downlink SINR balancing problem (4.1) can be more easily solved by solving its uplink dual. Assuming equal receiver noise and exploiting duality between uplink and downlink, it can be shown that if a set of target SINR values $\gamma_j^t, \forall j \in \mathcal{G}$, may be achieved in the uplink using a set of beamformers \mathbf{w}_j , then the same target SINR values can be achieved in the downlink with the same beamformers \mathbf{w}_j and an adequate power allocation.

However, in [39], only a single-cell case is considered, i.e., one sector, and inter-cell interference is not included in the model. This solution is investigated with some modifications in a CoMP scenario, in which there is a power limitation per sector and UEs are subject to strong inter-site-cell interference. In order to achieve similar conditions to the single-cell case, the effect of inter-cell interference is incorporated into the effect of noise. Initially, it is assumed that the inter-cluster interference is Gaussian distributed in the same way that the noise, which allows us to simply add the interfering power estimate \hat{z}_j^{inter} directly to the noise power σ_η^2 to take the SINR measurements. Now, considering unequal noise, the matrices $\tilde{\mathbf{R}}_j = \mathbf{R}_j / (z_j^{\text{inter}} + \sigma_\eta^2)$ and interferences plus noise variances $z_j^{\text{inter}} + \sigma_\eta^2 = 1, 1 \leq j \leq K$ are scaled.

Let \mathbf{q} be the power allocation vector in the uplink. Therewith, the uplink SINR becomes

$$\gamma_j^{UL}(\mathbf{w}_j, \mathbf{q}) = \frac{q_j \mathbf{w}_j^H \tilde{\mathbf{R}}_j \mathbf{w}_j}{\underbrace{\sum_{\substack{k=1 \\ k \neq j}}^K q_k \mathbf{w}_j^H \tilde{\mathbf{R}}_k \mathbf{w}_j}_{z_j^{intra}} + 1}, \quad \forall j \in \mathcal{G}. \quad (4.3)$$

Considering the uplink SINR $\gamma_j^{UL}(\mathbf{w}, \mathbf{q})$ defined above, the uplink SINR balancing problem can be written as

$$C^{UL}(P_{\text{SUM}}) = \max_{\mathbf{w}, \mathbf{q}} \min_{\gamma_j^t} \frac{\gamma_j^{UL}(\mathbf{w}_j, \mathbf{q})}{\gamma_j^t}, \quad \forall j \in \mathcal{G}, \quad (4.4a)$$

subject to

$$\|\mathbf{w}_j\|_2 = 1, \quad (4.4b)$$

$$\|\mathbf{q}\|_1 \leq P_{\text{SUM}}. \quad (4.4c)$$

4.3 SINR balancing under sum-power constraint

The downlink beamforming problem (4.1) under SINR constraints can be solved efficiently by an iterative uplink beamformer and power update algorithm [39]. The solution achieved by [39] for the SINR balancing problem (4.1) is presented here in a CoMP scenario under sum-power constraint.

In the following, the power assignment and the beamforming algorithms are separately performed in Sections 4.3.1 and 4.3.2, respectively.

4.3.1 Power assignment

For fixed beamformers $\tilde{\mathbf{W}}$, the downlink problem (4.1) reduces to a pure power assignment. The authors in [39] give the proof that the optimum downlink power assignment is achieved for $P_{\text{SUM}} = \|\mathbf{p}\|_1$. In the following, the power assignment is presented. First, consider a coupling matrix $\Psi(\tilde{\mathbf{W}})$

$$[\Psi(\tilde{\mathbf{W}})]_{j,j'} = \begin{cases} \tilde{\mathbf{w}}_{j'}^H \tilde{\mathbf{R}}_j \tilde{\mathbf{w}}_{j'}, & j' \neq j, \\ 0 & j' = j. \end{cases} \quad (4.5)$$

Consider also a noise vector $\boldsymbol{\sigma} = [1 \ 1 \ \dots \ 1_G]^T$ and a weight matrix \mathbf{D} defined as

$$\mathbf{D} = \text{diag} \left\{ \frac{\gamma_1^t}{\tilde{\mathbf{w}}_1^H \tilde{\mathbf{R}}_1 \tilde{\mathbf{w}}_1}, \frac{\gamma_2^t}{\tilde{\mathbf{w}}_2^H \tilde{\mathbf{R}}_2 \tilde{\mathbf{w}}_2}, \dots, \frac{\gamma_G^t}{\tilde{\mathbf{w}}_G^H \tilde{\mathbf{R}}_G \tilde{\mathbf{w}}_G} \right\}. \quad (4.6)$$

In the downlink scenario, consider an extended power vector $\mathbf{p}_{ext} = \begin{pmatrix} \mathbf{p} \\ 1 \end{pmatrix}$ and an extended downlink coupling matrix $\Upsilon(\tilde{\mathbf{W}}, P_{\text{SUM}})$

$$\Upsilon(\tilde{\mathbf{W}}, P_{\text{SUM}}) = \begin{bmatrix} \mathbf{D}\Psi(\tilde{\mathbf{W}}) & \mathbf{D}\boldsymbol{\sigma} \\ \frac{1}{P_{\text{SUM}}}\mathbf{1}^T \mathbf{D}\Psi(\tilde{\mathbf{W}}) & \frac{1}{P_{\text{SUM}}}\mathbf{1}^T \mathbf{D}\boldsymbol{\sigma} \end{bmatrix}. \quad (4.7)$$

An eigensystem can be formulated for problem (4.1) such that the optimal downlink power vector \mathbf{p} is obtained by the dominant eigenvector associated to the maximal eigenvalue [39].

Let the eigensystem be organized in the following

$$\Upsilon(\tilde{\mathbf{W}}, P_{\text{SUM}})\mathbf{p}_{ext} = \frac{1}{C^{DL}(\tilde{\mathbf{W}}, P_{\text{SUM}})}\mathbf{p}_{ext} \quad \text{with } [\mathbf{p}_{ext}]_{K+1} = 1. \quad (4.8)$$

The dominant eigenvector \mathbf{p}_{ext} of the extended downlink coupling matrix $\Upsilon(\tilde{\mathbf{W}}, P_{\text{SUM}})$, associated to the maximal eigenvalue $\lambda_{max} = 1/C^{DL}(\tilde{\mathbf{W}}, P_{\text{SUM}})$, is scaled so that the last component be one. This way, the extended power vector \mathbf{p}_{ext} provides the optimal downlink power vector \mathbf{p} [39].

Now, in the uplink scenario, consider an extended power vector $\mathbf{q}_{ext} = \begin{pmatrix} \mathbf{q} \\ 1 \end{pmatrix}$ and an extended uplink coupling matrix $\Lambda(\tilde{\mathbf{W}}, P_{\text{SUM}})$

$$\Lambda(\tilde{\mathbf{W}}, P_{\text{SUM}}) = \begin{bmatrix} \mathbf{D}\Psi^T(\tilde{\mathbf{W}}) & \mathbf{D}\sigma \\ \frac{1}{P_{\text{SUM}}}\mathbf{1}^T\mathbf{D}\Psi^T(\tilde{\mathbf{W}}) & \frac{1}{P_{\text{SUM}}}\mathbf{1}^T\mathbf{D}\sigma \end{bmatrix}. \quad (4.9)$$

Thus, considering fixed beamformers $\tilde{\mathbf{W}}$, the downlink problem (4.1) reduces to a pure power assignment problem and an eigensystem can be formulated for this problem as follows

$$\Lambda(\tilde{\mathbf{W}}, P_{\text{SUM}})\mathbf{q}_{ext} = \lambda_{max} \left(\Lambda(\tilde{\mathbf{W}}, P_{\text{SUM}}) \right) \mathbf{q}_{ext}. \quad (4.10)$$

The dominant eigenvector \mathbf{q}_{ext} of the extended uplink coupling matrix $\Lambda(\tilde{\mathbf{W}}, P_{\text{SUM}})$, associated to the maximal eigenvalue λ_{max} , is scaled so that the last component be one. This way, the extended power vector \mathbf{q}_{ext} provides the optimal uplink power vector \mathbf{q} [39].

4.3.2 Beamforming

For a given power allocation vector $\tilde{\mathbf{q}}$, the beamformers $\tilde{\mathbf{w}}_j, \forall j \in \mathcal{G}$, which maximize (4.3), are obtained by G decoupled problems. The optimal beamformer of each UE is the solution of a generalized eigenvector problem [39] as seen below

$$\hat{\mathbf{w}}_j = \arg \max_{\mathbf{w}_j} \frac{\mathbf{w}_j^H \tilde{\mathbf{R}}_j \mathbf{w}_j}{\mathbf{w}_j^H \mathbf{Q}_j(\tilde{\mathbf{q}}_{ext}) \mathbf{w}_j}, \quad \forall j \in \mathcal{G}, \quad (4.11a)$$

subject to

$$\|\mathbf{w}_j\|_2 = 1. \quad (4.11b)$$

So, the optimal beamformer $\hat{\mathbf{w}}_j$ of the UE j is the solution of the generalized eigenvector problem $(\tilde{\mathbf{R}}_j, \mathbf{Q}_j(\tilde{\mathbf{q}}_{ext}))$, $\forall j \in \mathcal{G}$, where

$$\mathbf{Q}_j(\tilde{\mathbf{q}}_{ext}) = \sum_{\substack{j'=1 \\ j' \neq j}}^G [\tilde{\mathbf{q}}_{ext}]_{j'} \tilde{\mathbf{R}}_{j'} + \mathbf{I}. \quad (4.12)$$

Thus, the iterative algorithm proposed by [39] can be summarized in Algorithm 4.1 (see [39] for more details).

4.4 Target SINR feasibility and SRAs

The problem (4.1) is only feasible if the target SINRs can be simultaneously achieved. In other words, the target SINRs $\gamma_1^t, \gamma_2^t, \dots, \gamma_G^t$ are jointly feasible if and only if $C^{DL}(P_{\text{SUM}}) > 1$. When the SINR constraints cannot be fulfilled, it is necessary to relax some of the constraints until the problem becomes feasible.

Algorithm 4.1 SINR balancing algorithm.

```

for each Physical Resource Block (PRB) do
  for each cluster do
     $n \leftarrow 0$ 
     $\mathbf{q}^{(0)} \leftarrow [1, 1, \dots, 1]^T$ 
     $\mathbf{R}_j \leftarrow \mathbf{R}_j / (z_j^{inter} + \sigma_\eta^2), \quad 1 \leq j \leq K$ 
     $\sigma_\eta^2 \leftarrow 1, \quad 1 \leq j \leq K$ 
    repeat
       $n \leftarrow n + 1$ 
      solve  $(\hat{\mathbf{R}}_j, \mathbf{Q}_j(\mathbf{q}_{ext})), 1 \leq j \leq K$ 
       $\mathbf{w}_j^{(n)} \leftarrow \mathbf{w}_j^{(n)} / \|\mathbf{w}_j^{(n)}\|_2, \quad 1 \leq j \leq K$ 
      solve  $\Lambda(\mathbf{W}^{(n)}, P_{SUM})[\mathbf{q}_1^{(n)}] = \lambda_{max}(n)[\mathbf{q}_1^{(n)}]$ 
    until  $\lambda_{max}(n-1) - \lambda_{max}(n) < \epsilon$ 
    solve  $\Upsilon(\mathbf{W}^{(n)}, P_{SUM})[\mathbf{p}_1^{(n)}] = \lambda_{max}(n)[\mathbf{p}_1^{(n)}]$ 
  end for
end for

```

This can be done by relaxing the target SINRs $\gamma_1^t, \gamma_2^t, \dots, \gamma_G^t$ until the SINR balancing problem becomes feasible. However, this strategy can hide the problem of the significant efficiency loss due to spatial separation of correlated UEs when these are jointly grouped in a same group \mathcal{G} .

Alternatively, removal of UEs can also make the SINR balancing problem become feasible. In each removal, the released resources can be allocated to the remaining UEs, so that various removal strategies could be adopted. SRAs remove UEs from the system until the SINR targets of the remaining UEs are achieved.

In the following, two criteria for UEs removal when the SINR feasibility is not achieved by the SINR balancing algorithm are presented. The first criterion is only based on power, while the second is based on both power and correlation.

Due to the potential energy to be released to the remaining UEs, intuitively, the best metric to verify which UE should be removed is the maximum power criterion. The UE j^* which demands the highest amount of power is removed as defined below [48]

$$j^* = \arg \max_j \{p_j\}, \quad \forall j \in \mathcal{G}. \quad (4.13)$$

Indeed, the maximum power criterion is one of the most commonly used criteria to determine which UEs should be removed [48]. Nevertheless, due to the power penalty achieved with the spatial separation of correlated UEs channels, the removal of UEs that consume much power and that are highly correlated with other UEs may result in large gains.

Furthermore, a removal metric based on the power and on the spatial correlation is developed. First, combining (2.13) and (3.6), the removal metric is defined as

$$\phi = \mathbf{p}^T (\mathbf{1} - \mathbf{C}), \quad (4.14)$$

and the UE j^* to be removed is given by

$$j^* = \arg \min_j \{\phi_j\}, \quad \forall j \in \mathcal{G}. \quad (4.15)$$

Each element ϕ_j in the vector ϕ is obtained by the product of the power vector \mathbf{p}^T with the j^{th} column of the matrix of inverse correlation $(\mathbf{1} - \mathbf{C})$. Since the main diagonal of $(\mathbf{1} - \mathbf{C})$ is null, the power p_j of all UE j does not make up the element ϕ_j . Thus, UEs j with high

power p_j contribute to increase the elements $\phi_{j'}$ of UEs j' , $\forall j' \neq j$, but the high power p_j is not considered in ϕ_j . Besides, UEs j that consume low power and that are highly correlated with UEs j' , $\forall j' \neq j$, contribute to decrease the element $\phi_{j'}$ because the matrix of inverse correlation provides low values for high correlations. Furthermore, minimizing the removal metric ϕ tends to select the UE j^* that both consumes much power and is very correlated to other UEs that consume little power. This strategy distributes better the power among the remaining UEs.

4.5 Power minimization under SINR constraints

It is known that the total transmission power achieved with the SINR balancing can be minimized while the SINR feasibility is kept, i.e., $C^{DL}(P_{\text{SUM}}) > 1$ [39]. When applied in a CoMP system, this strategy minimizes the interference and improves the power efficiency of the system. Clearly, the minimum transmit power is achieved to $C^{DL}(P_{\text{SUM}}) = 1$, i.e., $\gamma_{j(dB)} = \gamma_{j(dB)}^t, \forall j \in \mathcal{G}$.

In order to improve the SINRs, it is possible to establish a safety margin under the target SINR $\gamma_{j(dB)}^t$, denoted here by SINR gap $\Delta_{\gamma_{j(dB)}^t}$. Whenever $\gamma_{j(dB)} > \gamma_{j(dB)}^t + \Delta_{\gamma_{j(dB)}^t}, \forall j \in \mathcal{G}$, the power vector \mathbf{p} is scaled to ensure a minimum safety margin for all UEs.

This strategy adds power to the CoMP system in comparison to the previous strategy, but it improves the SINR levels. In this way, increasing the SINR gap $\Delta_{\gamma_{j(dB)}^t}$ means to make the SINR more robust against possible imprecisions that can affect the performance of the SINR balancing algorithm. Hence, it possibly reduces the Block Error Rate (BLER) and it may achieve an additional improvement on system throughput.

4.6 Results

In this section, the Radio Resource Allocation (RRA) strategies introduced in this chapter are used to balance the SINR of the UEs grouped by a Space Division Multiple Access (SDMA) grouping algorithm and the performance evaluation of the SINR balancing strategies is performed considering the same parameters defined in Section 2.10.1. In this section, the improvement in the performance achieved by the SINR balancing algorithm is investigated in comparison to the performance obtained by an SDMA grouping algorithm combined with Zero-Forcing (ZF) precoding.

The strategies for SINR balancing treated in previous sections are summarized in Section 4.6.1. The performance metrics used to evaluate the performance achieved by the SINR balancing algorithm are introduced in Section 4.6.2. In Section 4.6.3, the performance achieved by the SINR balancing algorithm is investigated. Finally, Section 4.6.4 shows the effect of imperfect Channel State Information (CSI) on the performance of RRA strategies for the SINR balancing studied in this chapter and the RRA strategies for UE spatial grouping defined in Chapter 3.

4.6.1 SINR balancing strategies definition

In this section, the definition of SINR balancing strategies is presented. Before this, it is important to mention that the SINR balancing is combined with the best SDMA grouping so far, i.e., the Successive Projection (SP) algorithm combined with SRA and using the Minimum Gain (MinGain) criterion. This algorithm is referred in this chapter simply as *SDMA grouping algorithm* (see Section 3.4.2.3 and Section 3.4.3 for more details).

The RRA strategies considered in this chapter and their names are listed in Table 4.1.

It is important to highlight that the use of estimates of the inter-cluster interference in the

Table 4.1: SINR balancing strategies definition.

SDMA grouping		SINR balancing		
Metric	SRA	SRA	Power minimization	Definition
SP	MinGain	-	-	SINR balancing
SP	MinGain	Power-based	-	SINR balancing w/ SRA power
SP	MinGain	Power & correlation-based	-	SINR balancing w/ SRA power & corr.
SP	MinGain	-	Power scaling	SINR balancing w/ power min.

SINR balancing algorithm (introduced in Section 4.2) is considered usual so that a statement indicating its use is omitted. On the other hand, the non-usage of estimates of inter-cluster interference is followed by a statement on the name of the SINR balancing algorithm.

The improvement in the system spectral efficiency achieved by the SINR balancing algorithm is compared to the SDMA grouping's performance. Moreover, in order to get more gains compared to the performance of the SINR balancing algorithm, removal of UEs and power minimization are considered for several SINR target values.

When power minimization and SRA are considered, it is possible to establish a safety margin for the target SINR γ_j^t , denoted in Section 4.5 by SINR gap $\Delta_{\gamma_j^t}$, in order to improve the SINRs perceived by the grouped UEs.

4.6.2 Performance metrics

In the following, performance metrics considered to evaluate the performance of the SINR balancing algorithm are described:

- ▶ Cumulative Distribution Function (CDF) of the SINR means the cumulative distribution of the SINR observed by the UEs in the system;
- ▶ SINR gap $\Delta_{\gamma_j^t}$ represents a safety margin, which is provided by the SINR balancing algorithm, under the target SINR $\gamma_{j(dB)}^t$, which is achieved by the SDMA grouping algorithm, such that the balanced SINR for each UE j is given by $\gamma_{j(dB)} = \gamma_{j(dB)}^t + \Delta_{\gamma_j^t(dB)}$;
- ▶ Power economy represents the percentual gain in power consumption achieved with power minimization.

4.6.3 Performance with SINR balancing

In the following, the performance obtained with the SINR balancing algorithm is investigated by analyzing the system spectral efficiency, power consumption and group size achieved with the SRAs. The power consumption is an important variable to be evaluated because of the power distribution performed by the SINR balancing algorithm. In its turn, the distribution of group sizes provides a general view of the behavior of removals, allowing us to evaluate the efficiency of each SRA. Finally, the BLER is another important variable, since the SINR balancing algorithm provides guarantees of SINR levels.

The analyses are organized as follows. Performance evaluation of the SINR balancing under SDMA grouping is shown in Section 4.6.3.1. Section 4.6.3.2 presents the SINR feasibility analysis and the power minimization analysis is presented in Section 4.6.3.3.

4.6.3.1 SINR balancing under SDMA grouping

In the following, the performance gains achieved by the SINR balancing algorithm are evaluated. Figure 4.1 presents the spectral efficiency of the SINR balancing with and without inter-cluster interference knowledge and the CDF of the BLER of the SINR balancing with inter-cluster interference knowledge in comparison to the SDMA grouping algorithm.

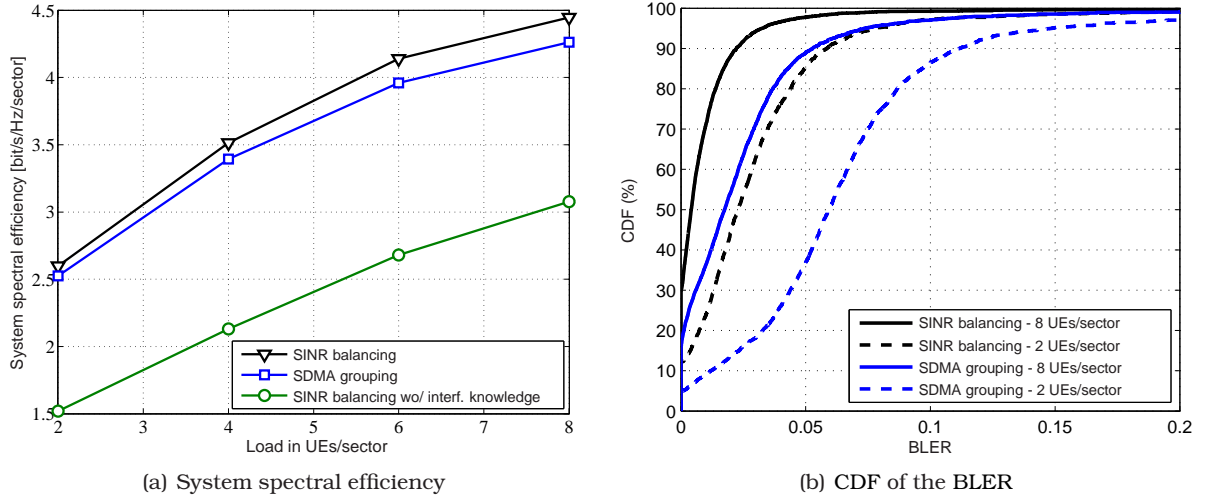


Figure 4.1: System spectral efficiency achieved by the SINR balancing with and without inter-cluster interference knowledge and CDF of the BLER presented by the SINR balancing algorithm.

It may be seen in Figure 4.1(a) that incorporating the effect of inter-CoMP-cell interference into the effect of noise provides satisfactory gains to SINR balancing. It is also seen that the SINR balancing provides significant gains in relation to SDMA grouping, since it performs a better power distribution. From Figure 4.1(b), it is seen that the improvement of system throughput achieved by the SINR balancing algorithm is due to reduced levels of BLER.

Figure 4.2 presents the CDF of the SINR obtained with the SDMA grouping and SINR balancing algorithms.

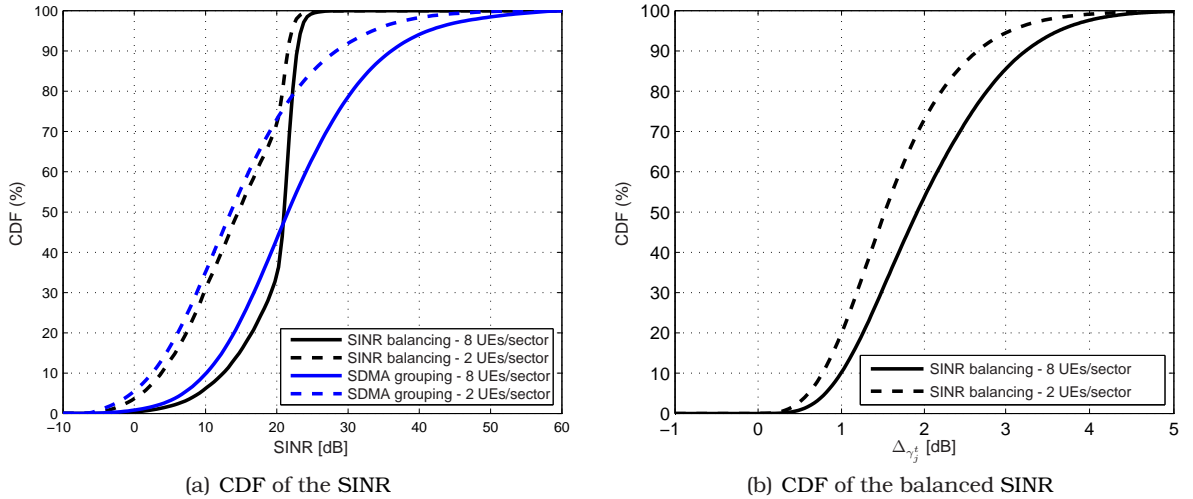


Figure 4.2: CDFs of the SINR and balanced SINR presented by the SINR balancing algorithm.

As it can be seen in Figure 4.2(a), the better power distribution presented by the SINR balancing algorithm reduces the levels of high SINR in order to establish a safety margin of SINR mainly for those UEs that have estimated SINR close to the SINR target level given by the MCS used on the transmission. From Figure 4.2(b), it is seen that the SINR balancing always achieves SINR feasibility.

4.6.3.2 SINR feasibility analysis

As shown in Section 4.6.3.1, the SINR balancing always achieves SINR feasibility. In this section, the SINR feasibility is evaluated with the most aggressive SINR targets γ_j^t by increasing the SINR gap $\Delta\gamma_j^t$. When the SINR feasibility is not achieved by the SINR balancing algorithm removal of UEs is performed according to the criteria introduced in Section 4.4.

Figure 4.3 presents the system spectral efficiency of the SINR balancing algorithm without

and with removal of UEs considering the criterion of maximal power and the criterion based on power and correlation.

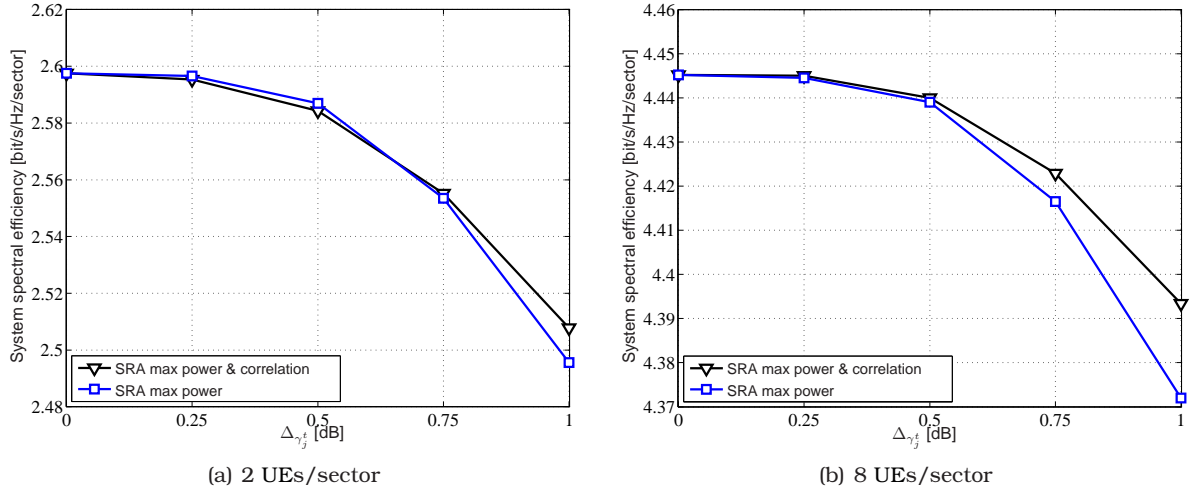


Figure 4.3: System spectral efficiency achieved by SRAs for several SINR gaps $\Delta\gamma_j^t$.

As it can be seen in Figure 4.3(a) and Figure 4.3(b), both SRAs combined with more aggressive SINR gap $\Delta\gamma_j^t$ have performed worse than the SINR balancing algorithm for $\Delta\gamma_j^t = 0$ dB. It is seen that introducing a safety margin $\Delta\gamma_j^t$ does not contribute for increasing the system spectral efficiency.

Besides that, the SINR balancing algorithm with removal of UEs does not provide considerable performance gains in the system spectral efficiency even for $\Delta\gamma_j^t = 0$ dB. It occurs because the SDMA grouping algorithm already selects a suitable set of UEs which does not need removing UEs in order to achieve feasibility for SINR values, as shown in Figure 4.2(b).

4.6.3.3 Power minimization analysis

In order to get more gains on the performance of the SINR balancing algorithm, power minimization is considered for several SINR target values. In the following, the performance gains achieved with power minimization is evaluated for 2 and 8 UEs/sector.

Figure 4.4 presents the spectral efficiency of the SINR balancing with power minimization for various SINR gaps $\Delta\gamma_j^t$ and for two loads in UEs/sector.

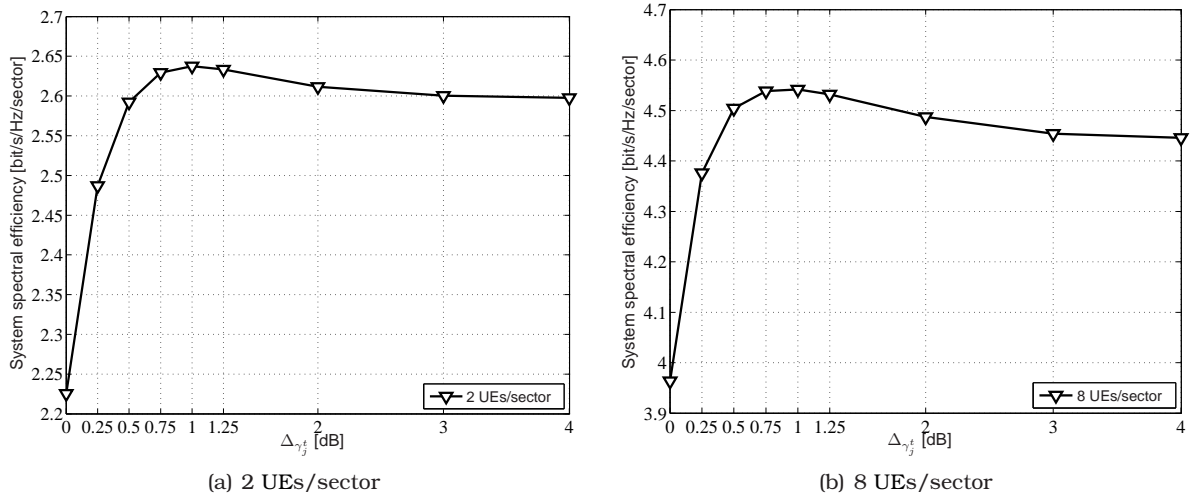


Figure 4.4: System spectral efficiency achieved by the power minimization algorithm for several SINR gaps $\Delta\gamma_j^t$ [dB].

It can be seen in Figure 4.4 that the power minimization algorithm with an SINR gap $\Delta\gamma_j^t = 0$ dB has the worst performance on both loads. This happens because this algorithm

balances the lowest SINRs γ_j at the SINR target level γ_j^t , i.e., $C^{DL}(\mathbf{W}, P_{max}) = 1$, which leaves no safety margin for eventual errors and, consequently, the system performance is slightly degraded. However, the maximum gain achieved with the power minimization occurs for an SINR gap $\Delta_{\gamma_j^t} = 1$ dB and has value around 2% for 8 UEs/sector, which is negligible.

Figure 4.5 presents the CDF of the balanced SINR and the CDF of the BLER of the SINR balancing algorithm with power minimization for SINR gap $\Delta_{\gamma_j^t} = 0$ dB and $\Delta_{\gamma_j^t} = 1$ dB. As

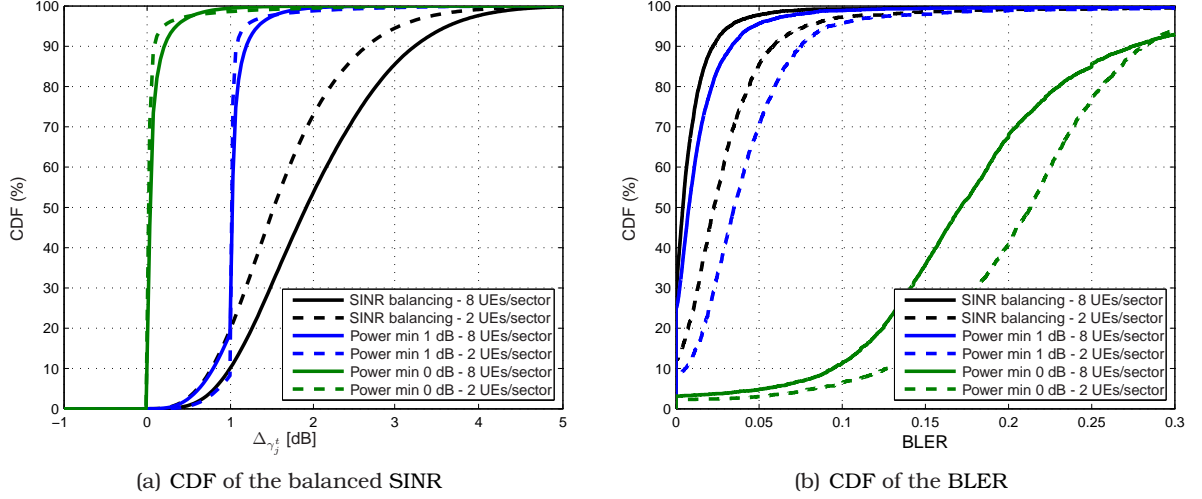


Figure 4.5: CDFs of the balanced SINR and BLER presented by the power minimization algorithm.

it can be seen in Figure 4.5(a), for both loads the power minimization leads almost 80% of the transmissions to the SINR target γ_j^t , i.e., SINR gap $\Delta_{\gamma_j^t} = 0$ dB. From Figure 4.5(b), the power minimization for SINR gap $\Delta_{\gamma_j^t} = 0$ dB presents higher BLER than the SDMA grouping algorithm.

On the other hand, when the power minimization is performed for all transmissions with SINR higher than $\gamma_j^t + \Delta_{\gamma_j^t}$, it is seen in Figure 4.5(a) that less than 20% of the transmissions have SINR values below $\gamma_j^t + \Delta_{\gamma_j^t}$ for the lowest load, and less than 10% of the transmissions have SINR below $\gamma_j^t + \Delta_{\gamma_j^t}$ for the highest load. However, from Figure 4.5(b), the performance in terms of BLER was worse with the power minimization for $\Delta_{\gamma_j^t} = 1$ dB than with the SINR balancing algorithm without power minimization although it has better performance in terms of system spectral efficiency.

Although the power minimization does not add significant spectral efficiency gains to SINR balancing for both loads, it still minimizes the power consumption, thus being more energy-efficient. Figure 4.6 presents the spectral efficiency of the SINR balancing with power minimization for SINR gaps $\Delta_{\gamma_j^t} = 0$ dB and $\Delta_{\gamma_j^t} = 1$ and the power economy achieved by the SINR balancing algorithm with and without power minimization in relation to SDMA grouping for an SINR gap $\Delta_{\gamma_j^t} = 1$ dB.

As it can be seen in Figure 4.6(a), the power minimization algorithm with an SINR gap $\Delta_{\gamma_j^t} = 1$ dB does not provide significant spectral efficiency gains but it considerably reduces power consumption.

Figure 4.6(b) shows that, for the highest load, the SINR balancing saves up to 33% of the power, while the SINR balancing with power minimization saves up to 48% in the power consumption of SDMA grouping, which are substantial amounts of power. At the same time, it preserves the same spectral efficiency. This strategy is also motivated by the low complexity of the power scaling and is more energy-efficient than the other studied strategies.

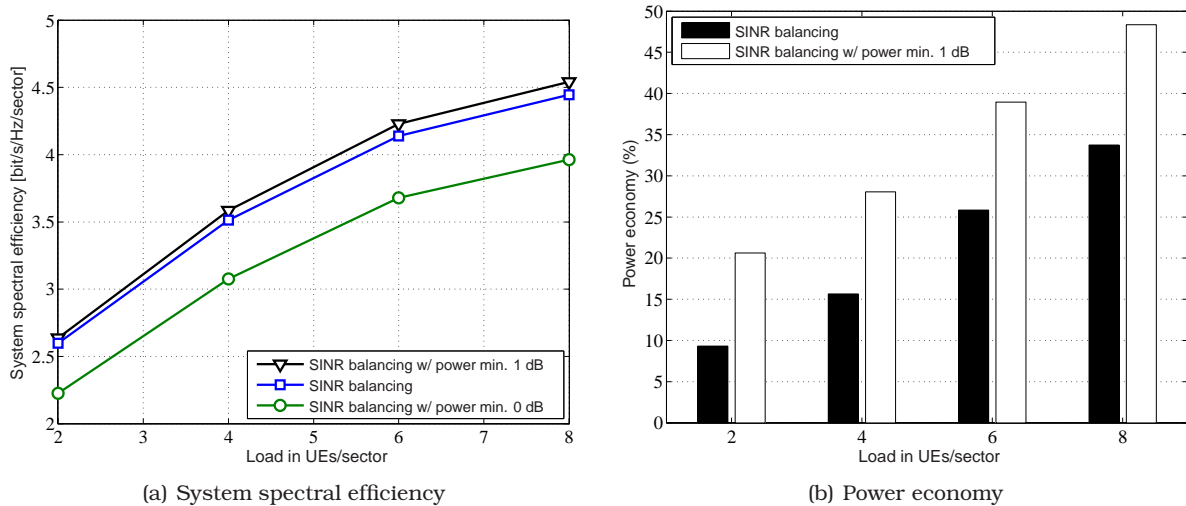


Figure 4.6: System spectral efficiency and power economy achieved by the power minimization algorithm.

4.6.4 Impact of imperfect CSI on the CoMP performance

So far the implementations have assumed an instantaneous and error-free CSI feedback to simplify the analysis. However, imperfect CSI should be addressed to achieve results closer to the ones expected in real-world implementations.

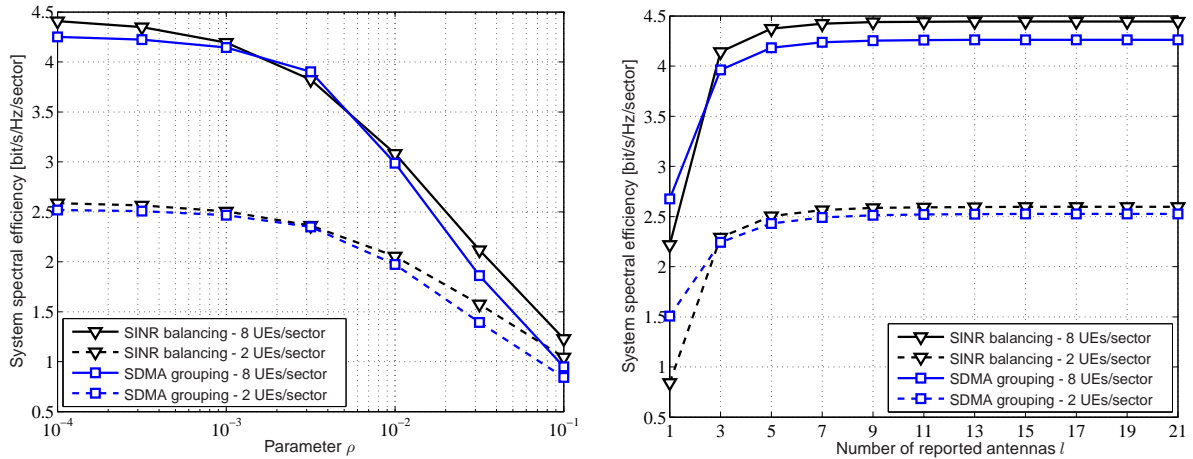
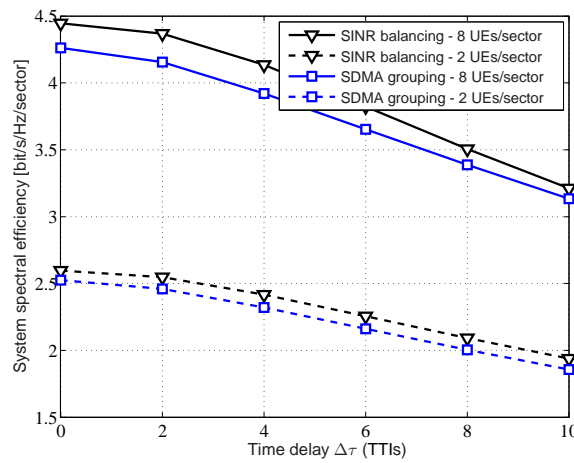
In the following, the impact of imperfect CSI is investigated on the performance of the RRA strategies described in this chapter and in Chapter 3. This issue has been addressed in Section 2.6 and modeled by channel estimation errors, partial feedback and outdated channel knowledge. The performance achieved with perfect CSI will be compared with that achieved with the different CSI imperfections in terms of system spectral efficiency.

Figure 4.7 shows the effect of channel estimation errors, partial CSI feedback and feedback delay on the system spectral efficiency achieved by the SINR balancing and SDMA grouping algorithms.

As it can be seen in Figure 4.7(a), when the channel estimation errors are quite significant, the SINR balancing is less sensitive to imperfections on channel estimation than the SDMA grouping. The SINR balancing provides significant gains in relation to SDMA grouping for both loads, because it performs a better power distribution as well as adapts precoding vectors. The losses in the spectral efficiency are apparent just from a given value of ρ . It is observed that for 8 UEs/sector and $\rho = 10^{-2}$ the spectral efficiency decreases significantly for both algorithms. Note that $\rho = 10^{-2}$ represents the introduction of estimation errors in the estimated channel vector $\hat{\mathbf{h}}_j$ with 10% of magnitude of the error vector \mathbf{e}_j .

It is shown in Figure 4.7(b) that just a small part of the CSI of all available Antenna Ports (APs) in a CoMP system is necessary for maintaining the performance achieved with complete CSI. When complete CSI is considered, each UE reports the CSI relative to APs. On its turn, partial CSI feedback requires just a small part of the CSI. Note also that the reduction of overhead is much more significant than the performance loss due to partial CSI feedback. It is important to mention that the amount of signaling reported by each UE varies depending on the UE's location.

As it is shown in Figure 4.7(c), the system spectral efficiency decreases almost linearly with the feedback delay such that its effect could not be neglected when considering CoMP systems.

(a) Channel estimation errors for $l = 21$ antennas and $\Delta\tau = 0$ TTIs(b) Partial CSI feedback for $\rho = 0$ and $\Delta\tau = 0$ TTIs(c) Outdated channel knowledge for $\rho = 0$ and $l = 21$ antennas**Figure 4.7:** Effect of channel estimation errors, partial CSI feedback and feedback delay on the system spectral efficiency.

4.7 Summary

In general, this chapter evaluated the performance of RRA strategies over models for perfect and imperfect CSI. An SINR balancing algorithm [39] has been studied as a Joint Processing (JP) transmission approach for the downlink of CoMP systems. For this purpose, the SINR balancing algorithm presented in [39] for the single-cell scenario has been investigated with some small modifications in a Multi-User (MU) CoMP scenario, in which UEs are subject to an SINR constraint and strong inter-cluster interference, and there is a power limitation per antenna [37].

From the results presented in Section 4.6.3, it was observed an increase in system spectral efficiency with the balancing of the SINR values perceived by the UEs. The SINR balancing also provides a considerable gain in terms of BLER. On the other hand, the SINR balancing with power minimization does not provide reasonable additional gains in the system spectral efficiency, but provides an expressive gain in power economy.

When channel estimation errors, partial CSI feedback and outdated CSI were assumed in an imperfect CSI model, the results presented in Section 4.6.4 showed that there was a very large decrease in performance in terms of system spectral efficiency, due to imperfect CSI, when compared to the ideal situation.

Results about channel estimation errors corroborated that it is a very critical point on

the performance of CoMP systems. It is known that a large amount of signaling is required to ensure the complete CSI to be available at each Evolved Node B (eNB). Indeed, it has been shown that there is a trade-off between the potential performance gains of cooperation versus the increased signaling overhead. It has been verified that just a considerably smaller amount of signaling is required to ensure a reliable cooperative transmission compared to full CSI. Results about outdated channel knowledge showed that it deserves attention, specially if some feedback delay constraint is assumed.

From the results, it is possible to verify that the performance loss due to imperfect CSI is inherent to CoMP systems. Thus, practical aspects such as channel estimation errors, limited feedback and feedback delay can not be neglected by RRA strategies for CoMP systems. It was also seen that the performance of the SINR balancing outperformed the SDMA grouping algorithm for both perfect and imperfect CSI.

Conclusions

5.1 Summary of the dissertation

The main objective of this dissertation was to study Radio Resource Allocation (RRA) strategies that aim at maximizing the throughput of a Coordinated Multi-Point (CoMP) system. The RRA subproblem of determining a suitable set of User Equipments (UEs) to spatially reuse a given radio resource considering the multiple geographically separated transmission points was investigated. The UE spatial grouping problem was studied in different scenarios.

Initially, an interference-unaware link adaptation was simulated in the conventional scenario. It has been shown to achieve the worst performance, clearly showing that the inter-cell interference is an important variable to be considered by efficient link adaptation schemes that have as objective the maximization of the throughput. After that, an interference-aware scheduler was shown to achieve improvements in the system spectral efficiency, specially for high diversity in UEs/sector, in comparison to an interference-unaware scheduler.

In the CoMP scenario, the single-cell schedulers use the perfect knowledge about the intra-cluster interference to enhance the link adaptation. However, single-cell schedulers presented similar performance in both conventional and CoMP scenarios. Thus, the estimates of inter-cell interference used for link adaptation in the conventional scenario were shown to be sufficiently accurate. After that, the Channel State Information (CSI) was also used to implement a dynamic joint multi-cell scheduling and thus coordinate the transmissions. This strategy indeed models a coordinated scheduling.

Next, different Space Division Multiple Access (SDMA) grouping algorithms with fixed and dynamic group sizes were employed to determine an efficient group of UEs that efficiently shares the same resource in space; while the spatial multiplexing of signals conveyed through them was done using precoding. Since the intra-cluster interference is totally canceled by using Zero-Forcing (ZF) spatial precoding, the UEs are able to achieve higher throughput.

In order to obtain more performance gains in the system spectral efficiency and to provide a more reliable communication for the UEs selected by SDMA grouping algorithms, a well-known Signal to Interference-plus-Noise Ratio (SINR) balancing algorithm was analyzed. This algorithm was simulated in order to solve both precoding and power control problems by alternating them in a novel scenario, in which there was a power limitation per Antenna Port (AP) and UEs were subject to strong inter-cluster interference. In order to guarantee the feasibility of the solution achieved by the SINR balancing algorithm, Sequential Removal Algorithms (SRAs) were developed to remove UEs in an SDMA group until the remaining UEs

reach their SINR targets.

Finally, the SDMA grouping and SINR balancing algorithms were evaluated over models for imperfect CSI in order to have performance results somewhat closer to those expected in the real-world implementations.

5.2 Conclusions about RRA for CoMP systems

This master thesis provided system-level analyses for RRA strategies that exploit coordination in the downlink of CoMP systems to implement adaptive frequency reuse and so improve system throughput. The results showed that quite high throughput gains are achieved through intelligent RRA. However, it is also shown a critical degradation on performance of these RRA strategies due to imperfect CSI. In the following, the main conclusions regarding the RRA strategies studied in this dissertation are discussed.

System-level analyses were provided considering UE spatial grouping observing both Coordinated Scheduling (CS) and Joint Processing (JP) approaches. The interference-aware grouping algorithms — Best Rate Allocation (BRA) and Capacity (CAP) algorithms — take advantage of the availability of CSI in order to perform adaptive multi-cell scheduling. Both algorithms iteratively build a group of UEs that achieves high joint throughput. Because these algorithms choose UEs based on their intra and/or inter-cluster interference estimate the UEs groups are much diversified in subsequent Transmission Time Intervals (TTIs). It was seen that interference-aware grouping algorithms have much higher Block Error Rate (BLER) values than interference-unaware grouping algorithms, as the Successive Projection (SP) algorithm, which is due to the fact of the link adaptation being more sensitive to fast variations of the inter-cluster interference. From this, it can be concluded that to take advantage of availability of the CSI, the inter-cluster interference should be efficiently predicted or the link adaptation should be less sensitive to variations on the inter-cluster interference estimate.

In addition, the SP algorithm with fixed group size was observed to lead to better performance for high loads than the above mentioned algorithms with dynamic group size. Besides the interference cancellation, this gain is obtained also due to the null space successive projections which keep a significant similarity with the projection performed by a ZF precoder and so effectively capture the spatial compatibility among the UEs. However, for low diversity in UEs/sector the algorithms under fixed group size have worse performance than the dynamic algorithms such that the best group size G^* should vary from load to load and shall depend on the channel conditions. It was shown that the SP algorithm combined with the SRA-Minimum Gain (MinGain) algorithm outperformed all the other algorithms for any load. It was also shown that SRAs achieved performance gains in low load situations. For higher loads, the SDMA grouping is better capable of choosing spatially uncorrelated UEs, due to the multi-user diversity, reducing the need for UE removal.

As for the SINR balancing, even though it does not aim at rate maximization, slight throughput gains were achieved, given that by reaching the SINR targets the BLER is reduced. According to the results of balanced SINR, it can be concluded that the SDMA grouping already selects a suitable set of UEs, which achieves suitable SINR feasibility when considering SINR balancing. It is also seen that the SINR balancing provides power reduction in relation to the SDMA grouping, since it performs a better power distribution. Despite the power minimization not providing significant spectral efficiency gains, it still minimizes power consumption thus being more energy-efficient.

The SINR balancing has outperformed the SDMA grouping algorithm even when imperfect CSI is assumed. However, compared to the SINR balancing, the SDMA grouping has shown a

slightly worse degradation due to imperfect CSI. From the results presented in Section 4.6.4, it could be seen that the performance loss due to imperfect CSI is inherent to CoMP systems. Results about channel estimation errors corroborated that it is a critical point on the performance of CoMP systems. It is known that a large amount of signaling is required to ensure that the complete CSI will be available at the Evolved Node B (eNB). However, it runs into the trade-off between the potential performance gains of cooperation versus the increased signaling overhead. It was verified that just a substantially smaller amount of signaling is required to ensure a reliable cooperative transmission. Results about outdated channel knowledge showed that it deserves attention specially if some feedback delay constraint is assumed. Thus, practical aspects such as channel estimation errors, limited feedback and feedback delay can not be neglected by the cooperative transmission techniques of CoMP systems.

The performance evaluation of the RRA strategies has shown promising results regarding the provision of high spectral efficiency values in CoMP systems, as it is expected from Long Term Evolution (LTE)-Advanced systems.

5.3 Perspectives of future works

This section points out perspectives that look promising for the RRA in CoMP systems. The solution derived in this dissertation opens up many ways for the design of new system-level techniques. In the following, some interesting topics as an extension to the work carried out in this dissertation are presented:

- ▶ Higher number of antennas per cluster: Since the system throughput for the SDMA is much higher than any other algorithms, other scenarios with a higher number of antennas per cluster (e.g., multi-antenna eNBs) could result on even better throughputs for the system.
- ▶ Link adaptation: Rapid and significant variations in the instantaneous channel conditions due to propagation effects present in mobile radio communication, which are mentioned in Section 2.4, as well as the interference level due to transmissions in other cells and by other UEs will impact the experienced quality of each radio-link. Therefore, in order to take advantage of availability of the CSI, variations of the radio-link quality must be taken into account and preferably exploited such that the inter-cluster interference should be efficiently predicted or the link adaptation should be less sensitive to variations on the inter-cluster interference estimate. However, due to imperfect CSI and random nature of interference, perfect adaptation to the instantaneous radio-link quality is never possible.
- ▶ Multiple Input Multiple Output (MIMO)-like schemes: In the MIMO scenario, UEs can also perform spatial processing to mitigate the effects of the intra-cluster interference [56]. Multiple antennas for both transmitting and receiving ends and the use of cooperative transmission/reception techniques may allow to achieve higher capacity and link reliability.
- ▶ Multi-group SDMA: By now, it has been considered the single-SDMA group case. However, the system performance might be eventually enhanced by clustering groups of antennas within the cluster and allocating them to different SDMA groups. In this case, intra-cell/inter-group interference could be mitigated using spatial processing. For example, each group of UEs might be seen as a single user and beamforming

techniques can be applied to guarantee that the data streams sent to different groups will not interfere with each other. Besides, in practice, only a limited number of eNBs can cooperate in order to keep the overhead manageable.

- ▶ **Quality of Service (QoS)-aware scheduling:** This dissertation focused on maximizing the system throughput, but CoMP is also compromised with the throughput of cell-edge UEs. The impact of the solutions on the QoS and fairness are still open for analysis, which aroused the interest of many researchers, as shown in the literature review. The RRA becomes more complex when QoS constraints are considered, due to the existing trade-off between system throughput and UE satisfaction. Simulating other traffic model such as File Transfer Protocol (FTP) and Voice over Internet Protocol (VoIP) traffics in order to investigate the behavior of the algorithms can be of interest.

Bibliography

- [1] ITU, "Background on IMT-Advanced," ITU, Tech. Rep. Doc. IMT-ADV/1, march 2008.
- [2] 3GPP, "Requirements for further advancements for E-UTRA (LTE Advanced)," 3GPP, Tech. Rep. TR 36.913 V10.0.0, march 2011.
- [3] Parkvall, S. and Dahlman, E. and Furuskär, A. and Jading, Y. and Olsson, M. and Wänstedt, S. and Zangi, K., "LTE-Advanced - Evolving LTE towards IMT-Advanced," in *Proceedings of the IEEE Vehicular Technology Conference (VTC)*, sept. 2008, pp. 1–5.
- [4] J. Zhang, M. Kountouris, J. Andrews, and R. Heath, "Multi-mode transmission for the MIMO broadcast channel with imperfect channel state information," *IEEE Transactions on Communications*, vol. 59, no. 3, pp. 803–814, march 2011.
- [5] 3GPP, "Further advancements for E-UTRA physical layer aspects," 3GPP, Tech. Rep. TR 36.814 V9.0.0, march 2010.
- [6] T. Maciel and A. Klein, "On the performance, complexity, and fairness of suboptimal resource allocation for multi-user MIMO-OFDMA systems," *IEEE Transactions on Vehicular Technology*, vol. 59, no. 1, pp. 406–419, jan. 2010.
- [7] L. H. Zheng Feng, Wu Muqing, "Coordinated Multi-Point Transmission and Reception for LTE-Advanced," in *Proceedings of the IEEE Wireless Communications, Networking and Mobile Computing*, sept. 2009, pp. 1–4.
- [8] X. Shang-hui and Z. Zhong-pei, "Coordinated multipoint transmission systems with the clustered super-cell structure configuration," sept. 2009, pp. 1–4.
- [9] Gesbert, D. and Hanly, S. and Huang, H. and Shamaï Shitz, S. and Simeone, O. and Wei Yu, "Multi-cell MIMO cooperative networks: A new look at interference," *IEEE Journal on Selected Areas in Communications*, vol. 28, no. 9, pp. 1380–1408, december 2010.
- [10] R. Batista, R. dos Santos, T. Maciel, W. Freitas, and F. Cavalcanti, "Performance evaluation for resource allocation algorithms in CoMP systems," in *Proceedings of the IEEE Vehicular Technology Conference (VTC)*, sept. 2010, pp. 1–5.
- [11] B. Hassibi and B. Hochwald, "How much training is needed in multiple-antenna wireless links?" *IEEE Transactions on Information Theory*, vol. 49, no. 4, pp. 951–963, april 2003.

- [12] R. D. Wetherington, E. Donaldson, and R. Moss, "Interference Predictions - Philosophies, Objectives, and Future Directions," in *Electromagnetic Compatibility Symposium Record, 1969 IEEE*, 1969, pp. 80–84.
- [13] R. Zhang and L. Hanzo, "Joint and distributed linear precoding for centralised and decentralised multicell processing," in *Proceedings of the IEEE Vehicular Technology Conference (VTC)*, sept. 2010, pp. 1–5.
- [14] C. A. Ariyaratne, "Link Adaptation improvements for Long Term Evolution (LTE)," Master's thesis, Blekinge Institute of Technology, Sweden, nov. 2009.
- [15] M. Fuchs, G. Del Galdo, and M. Haardt, "Low-complexity space-time-frequency scheduling for MIMO systems with SDMA," *IEEE Transactions on Vehicular Technology*, vol. 56, no. 5, pp. 2775–2784, sept. 2007.
- [16] T. Yoo, N. Jindal, and A. Goldsmith, "Finite-rate feedback MIMO broadcast channels with a large number of users," in *IEEE International Symposium on Information Theory*, july 2006, pp. 1214–1218.
- [17] A. Kühne and A. Klein, "Adaptive subcarrier allocation with imperfect channel knowledge versus diversity techniques in a multi-user OFDM-system," in *Proceedings of the IEEE Personal, Indoor and Mobile Radio Communications (PIMRC)*, sept. 2007, pp. 1–5.
- [18] V. Correia, F. Cavalcanti, and Y. Silva, "Analysis of MIMO precoding with base station cooperation and imperfect channel estimation," in *Anais do Simpósio Brasileiro de Telecomunicações (SBrT)*, Rio de Janeiro, Brazil, sept. 2008, pp. 1–5.
- [19] J. Zhang, R. Chen, J. Andrews, A. Ghosh, and R. Heath, "Networked mimo with clustered linear precoding," *IEEE Transactions on Wireless Communications*, vol. 8, no. 4, pp. 1910–1921, april 2009.
- [20] S. Han, C. Yang, M. Bengtsson, and A. Perez-Neira, "Channel norm-based user scheduler in coordinated multi-point systems," in *Proceedings of the IEEE Global Telecommunications Conference*, dec. 2009, pp. 1–5.
- [21] R. Zakhour and D. Gesbert, "A two-stage approach to feedback design in multi-user mimo channels with limited channel state information," in *Proceedings of the IEEE Personal, Indoor and Mobile Radio Communications (PIMRC)*, sept. 2007, pp. 1–5.
- [22] A. Kuhne and A. Klein, "An analytical consideration of imperfect CQI feedback on the performance of a multi-user OFDM-system," august 2007.
- [23] 3GPP, "Physical layer procedures," 3GPP, Tech. Rep. TR 36.213 V10.0.1, dec. 2010.
- [24] A. Papadogiannis, D. Gesbert, and E. Hardouin, "A dynamic clustering approach in wireless networks with multi-cell cooperative processing," in *Proceedings of the IEEE International Conference on Communications (ICC)*, may 2008, pp. 4033–4037.
- [25] J. Jin, Q. Wang, G. Liu, H. Yang, Y. Wang, and X. Zhang, "A novel cooperative multi-cell MIMO scheme for the downlink of LTE-advanced system," in *Proceedings of the IEEE International Conference on Communications (ICC)*, june 2009, pp. 1–5.
- [26] Q. Wang, D. Jiang, G. Liu, and Z. Yan, "Coordinated Multiple Points Transmission for LTE-Advanced Systems," in *Proceedings of the IEEE Wireless Communications, Networking and Mobile Computing*, sept. 2009, pp. 1–4.

- [27] E. Rodrigues and F. Casadevall, "Adaptive Radio Resource Allocation Framework for Multi-User OFDM," in *Proceedings of the IEEE Vehicular Technology Conference (VTC)*, april 2009, pp. 1–6.
- [28] S. Kaneko, M. Fushiki, M. Nakano, and Y. Kishi, "BS-cooperative scheduler for a multi-site single-user MIMO cellular system," in *Proceedings of the IEEE Vehicular Technology Conference (VTC)*, sept. 2010, pp. 1–5.
- [29] J. Jang and K. B. Lee, "Transmit Power Adaptation for Multiuser OFDM Systems," *IEEE Journal on Selected Areas in Communications*, vol. 21, no. 2, pp. 171–178, jan. 2003.
- [30] Y. J. Zhang and K. B. Letaief, "Multiuser adaptive subcarrier-and-bit allocation with adaptive cell selection for OFDM systems," *IEEE Transactions on Wireless Communications*, vol. 3, no. 5, pp. 1566–1575, sept. 2004.
- [31] D. Tse and P. Viswanath, *Fundamentals of wireless communications*, 1st ed. Cambridge University Press, 2005.
- [32] D. P. Palomar and J. R. Fonollosa, "Practical algorithms for a family of waterfilling solutions," *IEEE Transactions on Signal Processing*, vol. 53, no. 2, pp. 687–695, Feb. 2005.
- [33] Q. Spencer and A. Swindlehurst, "Channel allocation in multi-user MIMO wireless communications systems," in *Proceedings of the IEEE International Conference on Communications (ICC)*, vol. 5, june 2004, pp. 3035 – 3039 Vol.5.
- [34] T. Yoo and A. Goldsmith, "Optimality of Zero-Forcing Beamforming with Multiuser Diversity," in *Proceedings of the IEEE International Conference on Communications (ICC)*, vol. 1, may 2005, pp. 542–546 Vol. 1.
- [35] P. Tejera, W. Utschick, G. Bauch, and J. Nossék, "Subchannel Allocation in Multiuser Multiple-Input Multiple-Output Systems," *IEEE Transactions on Information Theory*, vol. 52, no. 10, pp. 4721–4733, oct. 2006.
- [36] S. Sigdel and W. Krzymien, "User scheduling for network MIMO systems with successive zero-forcing precoding," in *Proceedings of the IEEE Vehicular Technology Conference (VTC)*, sept. 2010, pp. 1–6.
- [37] R. Batista, T. Maciel, Y. Silva, and F. Cavalcanti, "SINR balancing combined with SDMA grouping in CoMP systems," in *Proceedings of the IEEE Vehicular Technology Conference (VTC)*, sept. 2011, pp. 1–5.
- [38] —, "Impact evaluation of imperfect CSI on the performance of downlink CoMP systems," in *Anais do Simpósio Brasileiro de Telecomunicações (SBRT)*, Curitiba, Brazil, sept. 2011, pp. 1–5.
- [39] M. Schubert and H. Boche, "Solution of the multiuser downlink beamforming problem with individual SINR constraints," *IEEE Transactions on Vehicular Technology*, vol. 53, no. 1, pp. 18 – 28, jan. 2004.
- [40] W. Yu and T. Lan, "Transmitter Optimization for the Multi-Antenna Downlink With Per-Antenna Power Constraints," *IEEE Transactions on Signal Processing*, vol. 55, no. 6, pp. 2646–2660, june 2007.

- [41] A. Tolli, H. Pennanen, and P. Komulainen, "SINR balancing with coordinated multi-cell transmission," in *Proceedings of the IEEE Wireless Communications and Networking Conference (WCNC)*, april 2009, pp. 1–6.
- [42] Balamurali, "A low complexity resource scheduler for cooperative cellular networks," dec. 2009, pp. 1–6.
- [43] E. Dahlman, S. Parkvall, J. Sköld, and P. Beming, *3G Evolution: HSPA and LTE for Mobile Broadband*, 2nd ed. Academic Press, 2008.
- [44] 3GPP, "Spatial channel model for MIMO simulations," 3GPP, Tech. Rep. TR 25.996 V6.1.0, sept. 2003.
- [45] —, "Physical layer aspects for evolved UTRA," 3GPP, Tech. Rep. TR 25.814 V7.1.0, sept. 2006.
- [46] R. Ertel, P. Cardieri, K. Sowerby, T. Rappaport, and J. Reed, "Overview of spatial channel models for antenna array communication systems," *IEEE Transactions on Professional Communication*, vol. 5, no. 1, pp. 10–22, feb. 1998.
- [47] J. Salo, G. D. Galdo, J. Salmi, P. Kyösti, M. Milojevic, D. Laselva, and C. Schneider, "MATLAB implementation of the 3GPP Spatial Channel Model (3GPP TR 25.996)," Tech. Rep., jan. 2005.
- [48] T. Maciel, "Suboptimal resource allocation for multi-user MIMO-OFDMA systems," Ph.D. dissertation, TU Darmstadt, 2008.
- [49] J. C. Ikuno, M. Wrulich, and M. Rupp, "System level simulation of LTE networks," in *Proc. 2010 IEEE 71st Vehicular Technology Conference*, Taipei, Taiwan, May 2010.
- [50] V. Stankovic, "Multi-user MIMO wireless communications," Ph.D. dissertation, Technische Universität Ilmenau, Germany, nov. 2006.
- [51] G. Nemhauser and L. Wosley, *Integer and combinatorial optimization*. John Wiley & Sons, 1999.
- [52] F. Shad, T. D. Todd, V. Kezys, and J. Litva, "Dynamic Slot Allocation (DSA) in indoor SDMA/TDMA using a smart antenna basestation," *IEEE/ACM Transactions on Networking*, vol. 9, no. 1, pp. 69–81, Feb. 2001.
- [53] G. Dimic and N. D. Sidiropoulos, "On downlink beamforming with greedy user selection: performance analysis and a simple new algorithm," *IEEE Transactions on Signal Processing*, vol. 53, no. 10, pp. 3857–3868, Oct. 2005.
- [54] D. B. Calvo, "Fairness analysis of wireless beamforming schedulers," Ph.D. dissertation, Technical University of Catalonia, Spain, nov. 2004.
- [55] M. Fuchs, G. Del Galdo, and M. Haardt, "A novel tree-based scheduling algorithm for the downlink of multi-user MIMO systems with ZF beamforming," in *Proceedings of the IEEE International Conference on Acoustics, Speech, and Signal Processing (ICASSP)*, vol. 3, March 2005, pp. iii/1121–iii/1124 Vol. 3.
- [56] A. Tolli and M. Juntti, "Scheduling for multiuser MIMO downlink with linear processing," in *Proceedings of the IEEE Personal, Indoor and Mobile Radio Communications (PIMRC)*, vol. 1, Sept. 2005, pp. 156–160.